

Dlk1 Membrane-to-Nuclear Signalling During Motor Neuron Functional Diversification

Dissertation

In partial fulfilment of the requirements for the degree

“Doctor rerum naturalium”

In the IMPRS Neuroscience Program

At the

Georg August University Göttingen, Faculty of Biology

Submitted by

Nidhi Subhashini

Born in

Darbhanga, India

Göttingen, October 10, 2016

Members of the Thesis Committee:

Prof. Dr. Till Marquardt, Reviewer

Interfaculty Chair for Neurobiological Research

RWTH Aachen University, Medical Faculty (UKA) & Faculty for Mathematics, Computer
and Natural Sciences

c/o European Neuroscience Institute, Göttingen

Prof. Dr. Andre Fischer, Reviewer

Speaker

German Centre for Neurodegenerative Diseases (DZNE), Göttingen

Dep. for Psychiatry and Psychotherapy, University Medical Centre

Dr. Judith Stegmüller

University Clinical Centre Aachen

Clinic for Neurology

Date of oral examination: November 21, 2016

Affidavit

I hereby, declare that this PhD thesis “Dlk1 Membrane-to-Nuclear Signalling During Motor Neuron Functional Diversification” has been written independently with no other aids or sources than quoted.

Nidhi Subhashini
10th October, 2016
Göttingen, Germany

Contents

Acknowledgements	i
List of Abbreviations	iii
List of Illustrations	vi
I Abstract	1
II Introduction	2
2.1 Specification of Spinal Neurons	2
2.2 Ventral Patterning of Spinal Cord and Motor Neuron Development	6
2.3 Functional Diversification of Motor Neurons	9
2.4 Dlk1 as a Determinant of Motor Neuron Functional Diversification	12
2.5 Notch Signalling and Dlk1 as a Ligand of Notch	14
2.6 Notch Signalling During Spinal Neuron Diversification	18
2.7 NFAT Proteins as Interesting Signal Carriers from Cytosol to Nucleus	20
2.8 NFAT Signalling During Development of Central Nervous System	23
2.9 NFAT Regulates Transcription of K ⁺ Channels	25
2.10 Dlk1 and NFAT Linked Together in Several Different Cellular Systems	27
2.11 Goals of the Present Study	28
III Materials	29
3.1 Laboratory consumables and plastic wares	29
3.2 Antibodies	29
3.3 Enzymes	30
3.4 Chemicals and reagents	31
3.5 Plasmids	35

3.6 Kits	35
3.7 Primers	36
3.8 Software	36
3.9 Animal Models for Experiments	37
3.10 Equipment	38
IV Methods	39
4.1 Molecular Cloning	39
4.2 Cell Culture	48
4.3 Co-immunoprecipitation	53
4.4 SDS-PAGE	54
4.5 Western Blot	55
4.6 Chick Experiments	57
4.7 Mouse Experiments	63
4.8 Embedding tissue in Cryo-moulds and Cryo-sectioning	67
4.9 Immunohistochemistry (IHC)	68
4.10 Image Acquisition	69
4.11 Luciferase Reporter Assay	69
4.12 Statistical Analysis	70
V Results	71
PART-1: Dlk1 Extracellular Interaction	
5.1 Generation of Dlk1 Variants with Specific Deletions	71
5.2 Generation of Notch Variants with Specific Deletions	73
5.3 Dlk1 Extracellular Segment Interacts with Notch Like a Canonical Notch Ligand	76
5.4 What Luciferase Assay Reveals About Notch-Dll1 and Notch-Dlk1 Interaction, Activation and Inhibition	79

5.5 Ectopic expression of Dlk1 Inhibits Notch and Promotes Early Cell Cycle Exit	81
PART-2 Dlk1 Intracellular Signalling	
5.6 Dlk1 Processing and Release of its Intracellular Segment (DLK1-ICD)	83
5.7 Generation of NFAT Constitutively Nuclear and NFAT Dominant Negative Versions of NFAT	85
5.8 Localisation of NFAT Variants in Cell culture and in Chick Embryos	86
5.9 Direct Physical Interaction of the Dlk1-ICD with the C-terminal Portion of NFATc4	88
5.10 NFAT-cn Interacts with <i>KCNG4</i> Cis-Regulatory Module	89
5.11 NFAT-cn Overexpressing Cells Exit from Chick Motor Column	90
5.12 Overexpressing NFAT-dn in MNs Induces Hyperexcitability	91
5.13 NFAT-dn overexpressing MNs fail to acquire Fast MN properties	93
5.14 Generation of Conditional NFAT-dominant Negative Mouse Line	94
VI Discussion	97
6.1 Dlk1 Interacts with Notch and Inhibits Notch	98
6.2 Is Inhibition of Notch Sufficient for fast MN properties?	99
6.3 Dlk1 is Cleaved Intracellularly and the Cleaved Intracellular Segment is Stable	100
6.4 Dlk1 Interacts with the Transcription Factor NFATc4	101
6.5 NFATc4 Regulates Transcription of <i>KCNG4</i>	101
6.6 Inhibition of NFAT Induces Hyperexcitability in MNs During Chick Spinal Cord Development	102
6.7 Does Dlk1 Function Mediate via Activation of NFAT?	103
6.8 A Model for the Novel Notch-Dlk1- NFATc4 Signalling Pathway	103
6.9 Impact of Cis-inhibition of Notch by Dlk1 on the MN Diversification Process	105

6.10 Dlk1-NFATc4 a Novel Interaction or Different Flavour of NFAT Signalling	106
6.11 Transcriptional Regulation by NFAT Signalling	107
VII Summary	108
VIII Outlook	110
IX References	111
CURRICULUM VITAE	127

Acknowledgements

I would like to thank Prof. Till Marquardt for his years of mentorship and for giving me the opportunity to perform this work in his laboratory. His enthusiasm for science and unique ideas in his field is remarkable and will inspire me throughout my future career.

I am grateful to the members of my thesis committee Prof. Andre Fischer and Dr. Judith Stegmüller for all the productive meetings we've had over the years. Their advice has been conducive in guiding the direction of my thesis project. I also wish to express my gratitude to Dr. Kristine Hennigfeld for collaborative luciferase reporter assays and Dr. Oliver Valerius for LCMS analysis.

I am extremely thankful to Prof. Michael Hörner, Sandra Drube and Mirja, the coordination team of IMPRS Neuroscience program, for taking care of me right from the beginning of my arrival to Germany and helping me to survive the pressures of pursuing a PhD. Additionally, I am also thankful to the whole IMPRS Neuroscience batch 2011 to be so joyous, friendly and helpful throughout our studies.

I am indebted to all the past and present members of the Developmental Neurobiology laboratory who not only created a helpful work environment but also shared their work and knowledge. I would like to specially thank, Dr. Piotr Fabrowski and Dr. Daniel Müller for reading my thesis and giving important inputs. Alex, Beate, and Yehan were the ladies of the lab who were kind and ready to help whenever I needed.

I thank Mummy and Papa for being wonderful parents, for being there for me even when I was 4000 miles away and continuously reminding me of having healthy food rather than lazy junk food. I thank my brother Sanchit for coming up with instant solutions to any kind of problem I faced due to living away from home. I would also like to express my gratitude to Göttingen, the city of science. Göttingen has given me unexpected happiness, experiences, independence, love of my life and even my first salary. Göttingen will remain one of the most beautiful places of my life.

I thank my seniors Mayur Vadhvani, Pitachaiah Ishwar Cherukuri, Aniket Ghosh to share their experiences with me which helped a lot in important decision making.

I wish to thank my close friends Dragomir Milovanovic, Kanika Vanshylla, Manho Wong with whom I celebrated every other day in Göttingen, and discussed every other topic than Science.

Most importantly, I thank Sabin Prajapati for his love, support, kindness and patience. He has been a constant source of calmness when I was stressed, a source of motivation when I felt low, a source of smile when I cried and an unlimited source of friendship. Without his warm words and great cooking skills this thesis could not have been completed.

List of Abbreviations:

pg	Picograms
AHP	Afterhyperpolarization
ATPase	Class of enzymes (phosphatases) that decompose ATP into ADP
BMP	Bone morphogenetic protein
BSA	Bovine serum albumin
cDNA	Complementary DNA
ChAT	Choline acetyltransferase
CNS	Central nervous system
DEPC	Diethylpyrocarbonate
Dlk1	Delta like homolog 1
DMSO	Dimethyl sulfoxide
DNA	Deoxyribonucleic acid
DSL	Delta/Serrate/lag
eGFP	Enhanced green fluorescent protein
Err3	Oestrogen-related receptor gamma
Fig.	Figure
FMNT	Functional motor neuron type
g	Gram
GFP	Green fluorescent protein
Hb9	Motor neuron and pancreas homeobox 1
Hox	Homeobox
IRES	Internal ribosome entry site
Isl1	Islet 1 transcription factor

Lhx	LIM homeobox protein
LIM	Acronym of Lin11, Islet1 and MEC 3
LMC	Lateral motor column
LMCI	Lateral LMC
LMCm	Medial LMC
MAP	Mitogen-activated protein
MHC	Myosin heavy chain
mM	Millimolar
MMC	Medial motor column
MN	Motor Neuron
mRNA	Messenger RNA
NeuN	Neuronal nuclei
NFAT	Nuclear factor of activated T-cells
Nkx6.1	NK6 homeobox 1
NLS	Nuclear localization signal/sequence
OCT	Optimal Cutting Temperature
Oligo2	Oligodendrocyte transcription factor 2
OPN	Osteopontin
PBS	Phosphate Buffered Saline
pMN	Motor neuron progenitors
RNA	Ribonucleic acid
rpm	Revolutions per minute
Shh	Sonic hedgehog
vAChT	Vesicular acetylcholine transporter
w/v	Weight per volume

Wnt Amalgam of Wingless (drosophila) and int-1 (mouse)

μl Microlitre

List of Illustrations

Fig.2.1a Simplified Rostrocaudal and Dorsoventral signalling system in spinal cord	3
Fig.2.1b Segmentation of mouse spinal cord by various Hox genes	4
Fig.2.2a Ventral patterning in the spinal cord	7
Fig.2.2b Positions of Motor Columns Along the Spinal Cord	8
Fig.2.3 Functional Subclasses of MNs	10
Table 2.3. Properties and Molecular Markers of MNs Subtypes	11
Fig.2.4. Dlk1 Transmembrane Protein Alters Motor Neuron Properties	13
Fig.2.5a Canonical Notch Signalling	15
Fig.2.5b Canonical Notch Ligands	16
Figure.2:5c Dlk1 as a Non-Canonical Notch Ligands Compared with Canonical Ligands	17
Fig.2.7 Illustration of NFAT Signalling Pathway	21
Fig.4.1.1 Phase separation and RNA isolation	40
Table 4.1.2.a: Pipetting Protocol	41
Table 4.1.2.b: Cycling Protocol	42
Table 4.2.3 Seeding Densities for Hela Cells	49
Fig.4.4 Apparatus used for SDS-PAGE	54
Fig.4.5.1 Sandwich for Western Blot	55
Figure 4.6.1 Stable Expression Vector Outline (tol2-pCAGEN)	57
Fig.4.6.2 In-ovo Electroporation of Chick Neural Tube	58
Fig.4.6.4 A Chronological Outline of Patch-Clamp Recordings from Chick Spinal Cord	62
Fig.5.1 Mouse Dlk1 wild type and truncated versions cloned with FLAG tag.	72
Fig.5.2a Generation of Notch1 Truncations Lacking Putative Activating or Inhibitory Regions or Both.	74

Fig.5.2b Western blot analysis of Notch1WT and truncated versions.	75
Fig.5.3a Interaction of Canonical Notch Ligand Dll1 with Native and Truncated Versions of Notch1	76
Fig.5.3b Interaction of the Non-Canonical Notch Ligand Dlk1 extracellular segment with Native and Truncated Versions of Notch1	78
Fig.5.4 Dlk1 is a Potent Suppressor of Notch Signalling	80
Fig.5.5 Dlk1 Induces Early Cell Cycle Exit in Chick Neural Tube	82
Fig.5.6 Cleavage and Release of Dlk1 Intracellular Segment in HeLa cells	84
Fig.5.7 Construction and expression of native, constitutively-active and dominant-negative NFATc4	85
Fig.5.8a Localisation of native, dominant negative and constitutively nuclear NFATc4 in HeLa cells	86
Fig.5.8b Localisation of native, dominant negative and constitutively nuclear NFATc4 in the chick neural tube.	87
Fig.5.9 Dlk1-ICD Physically Interacts with the C-terminal Portion of NFATc4	88
Fig.5.10 Effect of NFAT-cn on the <i>KCNG4</i> Cis-Regulatory Module	89
Fig.5.11 Mouse NFAT-cn Overexpression is Incompatible with Motor	90
Fig.5.12 NFAT-dn Overexpression Induces Hyperexcitability in MNs	92
Fig.5.13 NFAT-dn overexpression leads to reduction of fast MN population	93
Fig.5.14a The Transgene Introduced in Mice by Random Insertion	94
Fig.5.14b Selective Expression of NFAT-dn in mouse MN/oligodendrocyte lineage	95
Fig.5.14c Targeted Expression of NFAT-dn-IRES-GFP Driven by ChAT-Cre in Post-mitotic MNs	96
Fig.6.8 A novel Notch-Dlk-NFATc4 signalling Pathway	104
Fig.7 A Summary of the Study	109

I Abstract

Motor neurons of the spinal cord and hindbrain are responsible for translating neural commands into movements. For the execution of smooth movements, it is necessary that motor neuronal impulses are in turn translated into the gradual build-up of muscle force. This task is achieved by the diversification of motor neurons into a range of 'slow' to 'fast' types that are recruited by presynaptic activity according to the amount and manner of force they generate in the muscle. During embryonic development motor neurons are generated from neural progenitor cells residing in the ventral neural tube. A lot of information has become available in recent years about how the motor neuron progenitors are specified and how motor neurons differentiate into different 'positional identities' according to the specific muscles or muscle groups they supply. However, very little is known about how the motor neurons diversify into the different slow and fast types required for the automated gradation and task-dependent application of muscle force.

Dlk1, a type1 transmembrane protein, was recently identified as a determinant of motor neuron functional diversification by promoting fast motor neuron properties. However, the signalling mechanisms that allow Dlk1 to alter gene expression and promote fast motor neuron properties still remained unresolved. The present thesis attempted to dissect the signalling mechanism in a stepwise fashion starting from the plasma membrane, where the Dlk1 protein resides, to the nucleus where it affects gene expression. As a starting point, the supervisor's laboratory had identified the Notch and NFATc4 as interacting partners of Dlk1. Knowing that Notch is a principal player in generation of cellular diversity throughout development while NFATc4 is a transcription factor that shuttles between cytosol and nucleus, I divided my study into two parts. In the first part of the thesis, I used biochemical and immunohistochemical assays to resolve the physical interaction between the Dlk1 extracellular segment with Notch, its impact on Notch activation by canonical ligands and its influence on motor-neurogenesis. In the second part of my study, I show that Dlk1 is cleaved intracellularly and that the resulting Dlk1 intracellular segment interacts with NFATc4. My study also indicates the transcriptional regulation of Dlk1 target genes by NFAT. With the help of electrophysiological recordings in genetically manipulated chick spinal cord, I further found that suppressing NFAT activity alters the physiological properties of motor neurons. The result of my studies thus give rise to a model according to which Dlk1, by physically connecting Notch and NFAT signalling pathways, directly connects neurogenesis to motor neuron functional diversification.

II Introduction

2.1 Specification of Spinal Neurons

Neurons in the spinal cord (spinal neurons) have two important roles: the neurons in dorsal spinal cord relay sensory information to the brain while the ventral spinal neurons integrate descending and proprioceptive sensory input and generate motor outputs (Jessell 2000). The specification of these spinal neurons, after neural induction, depends on two basic signalling systems along the rostrocaudal and dorsoventral axes of the neural tube (Fig.2.1a). A rostrocaudal signalling gradient generates the main subdivisions of central nervous system (CNS) from rostral forebrain to caudal spinal cord. On the other hand, dorsoventral signalling gradient generates cell type diversity within each rostrocaudal subdivision. In addition, local signals among developing neurons are thought to establish the complete set of neuronal subtypes.

The rostrocaudal signalling axis originates from the primitive streak during the gastrula stage of embryo and from the posterior paraxial mesoderm. Among these signals, increasing levels and convergent actions of fibroblast growth factors (FGFs), bone morphogenetic proteins (BMPs), retinoids and Wnts promote increasingly caudal neural characteristics. High levels of these proteins are therefore found in the region of the neural plate giving rise to the spinal cord (Stern 2005). Studies in chick has shown that at initial stages of gastrulation (stage 3: 10-12 hours after incubation of eggs), prospective neural cells need exposure to paraxial mesoderm caudalizing (PMC) activity and FGFs for generic caudal character. Later at stage 4 of chick embryonic development, retinoids become important to specify the progenitor cells into caudal spinal characteristics (Durstun, van der Wees et al. 1998, Muhr, Graziano et al. 1999).

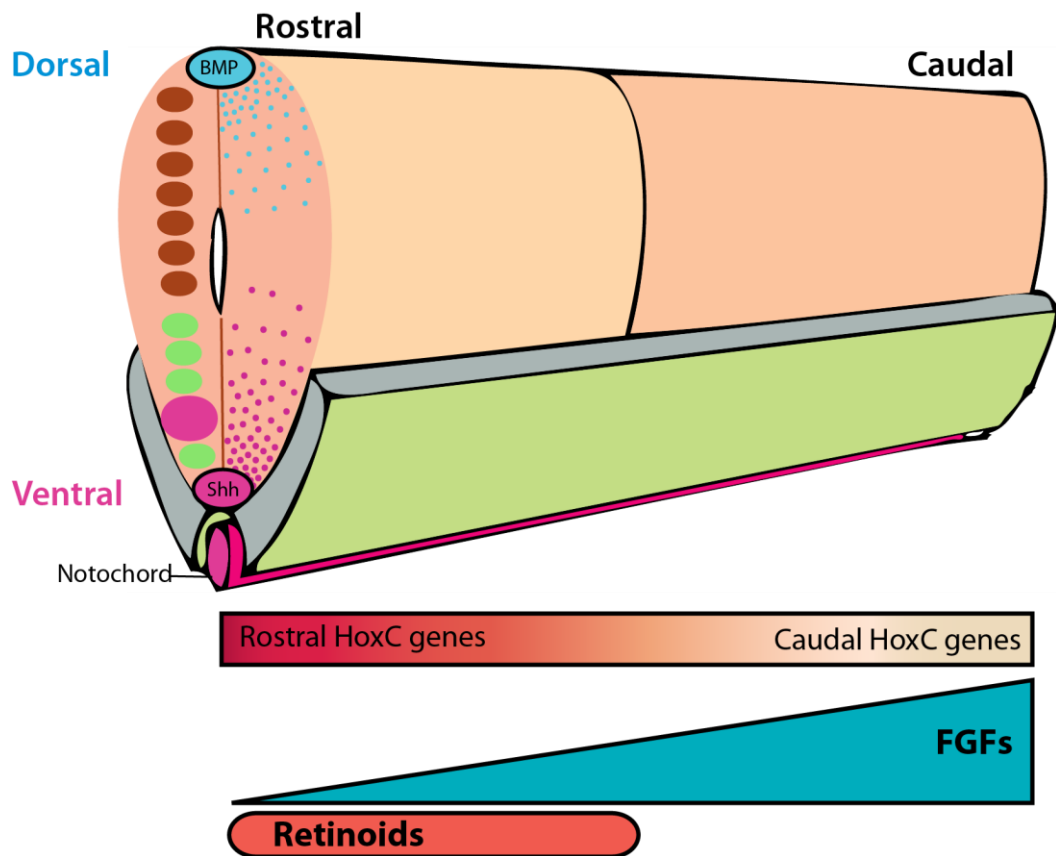


Fig.2.1a Simplified Rostrocaudal and Dorsoventral signalling system in spinal cord

After spinal cord formation, the combinatorial actions of Retinoids and FGFs (originating from paraxial mesoderm) gradient activate different HoxC genes and thus several segments of spinal cord from rostral end to caudal end are formed. Each of those segments is exposed to Shh (purple) and BMP (blue) gradients along dorsoventral axis. The gradient of Shh and BMP define the positioning of 12 neuronal progenitor domains (green, pink and brown).

As a result of chronological exposure to these signalling mechanisms with combinatorial actions of homeodomain proteins (Hox-proteins), the spinal cord eventually becomes subdivided into four broad segments: Cervical, Brachial, Thoracic and Lumbar (Fig. 2.1b). These spinal segments are defined by the combinatorial expression of Hox transcriptions factors, the boundaries of which become further sharpened by cross-repressive actions among different Hox protein classes (Dasen, Tice et al. 2005, Jung, Lacombe et al. 2010).

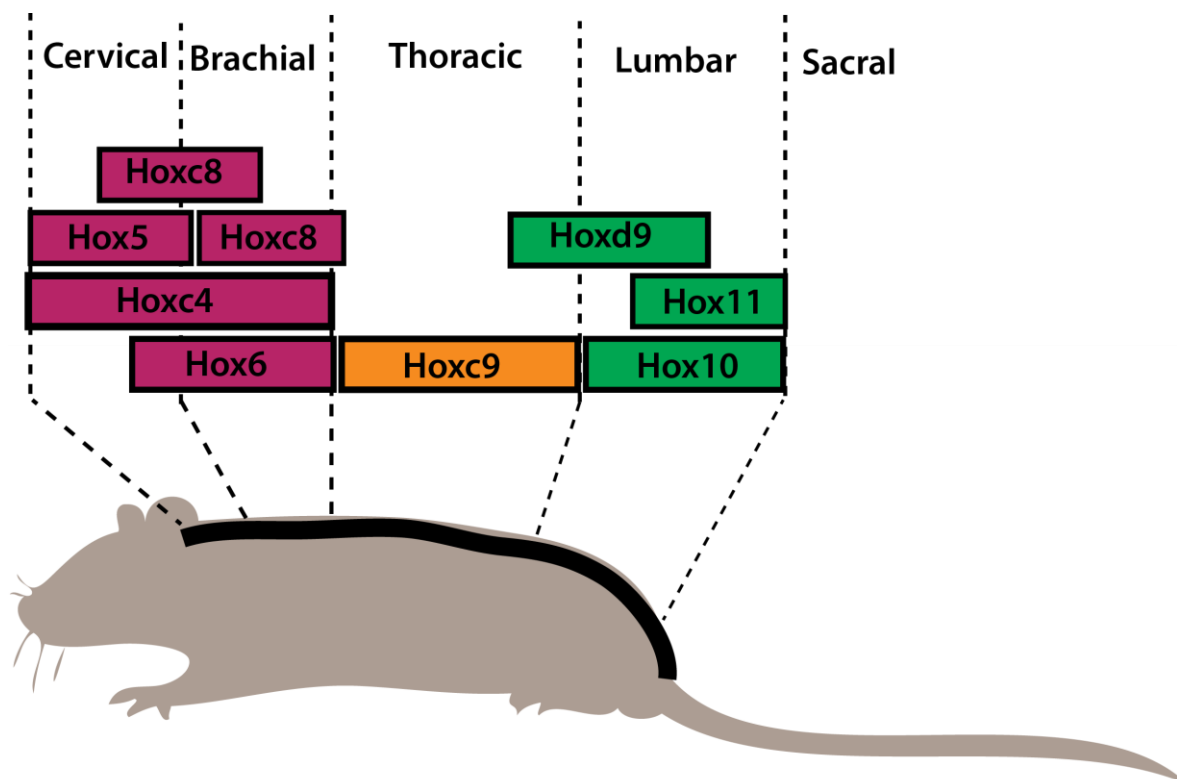


Fig.2.1b Segmentation of mouse spinal cord by various Hox genes

Spinal cord segments are broadly classified into five different levels based on anatomical location. Spinal segments in neck region are called as Cervical. Around the level of forelimbs, spinal cord is thicker and is termed as Brachial, while the segments at hind limb level are referred to as Lumbar (also thicker). In between Brachial and Lumbar lies the thinner spinal cord segments called as Thoracic segments.

Spinal neurons differentiate into several neuronal subtypes along dorsoventral axis. During the neural tube stage of embryonic development, commissural and association neurons differentiate in the dorsal half of the caudal neural tube while in ventral half, motor neurons (MNs) and interneurons differentiate. The differentiation of ventral neuronal subtypes depends on signals from the axial mesoderm, the notochord which lies beneath the ventral neural tube. Later on these signals are provided by floor plate cells which are located at extreme ventral midline within the spinal cord (Placzek 1995). Sonic hedgehog (Shh) is the principal morphogenetic signal secreted by notochord and floor plate cells and is the main determinant of ventral neural patterning (Patten and Placzek 2000). Shh is a diffusible molecule that forms a concentration gradient and affects differently on the cells of the developing embryo depending on its concentration. However, Shh signalling does not contribute in dorsal neuronal subtype generation. Dorsal identities are set by bone morphogenic proteins (BMP) signalling from the epidermis, which then promotes the

formation of the roof plate (Liem, Jessell et al. 2000). Retinoic acid (RA) produced by somites also controls dorsoventral cell identity (Pierani, Brenner-Morton et al. 1999). These morphogen gradients establish 12 progenitor domains giving rise to seven dorsal interneuron progenitor domains, four ventral interneuron progenitor domains (p0, p1, p2 and p3) and one motor neuron progenitor domain (pMN).

2.2 Ventral Patterning of Spinal Cord and Motor Neuron development

MNs are clustered into motor columns in ventral spinal cord and are most diverse neuronal subclass in the spinal cord. The concentration of Shh protein within the ventral-to-dorsal gradient defines the position in which ventral neuron types are generated. The gradient of Shh signalling is interpreted by two classes of homeodomain proteins: class I and class II (Briscoe, Pierani et al. 2000). Depending on its concentration, Shh signalling suppresses class I homeodomain proteins (Pax7, Dbx1, Dbx2, Irx3 and Pax6) (Lu, Shashikant et al. 1996, Shoji, Ito et al. 1996, Mastick, Davis et al. 1997, Mansouri and Gruss 1998, Pierani, Moran-Rivard et al. 2001) while activating class II proteins (Nkx6.1 and Nkx2.2) (Briscoe, Sussel et al. 1999, Sander, Paydar et al. 2000) expression, thus creating a grid of cells exposed to different levels of Shh and homeodomain proteins. Different combinations of homeodomain proteins, induced or repressed by Shh, thereby define boundaries of the five-neural progenitor (p) domains (p0, p1, p2, pMN and p3) and corresponding post-mitotic neurons (V0, V1, V2, MN and V3). Out of five subtypes of ventral neurons generated V0-V3 represent different ventral interneurons and MN represent motor neurons. Apart from the homeodomain proteins, basic helix-loop-helix (bHLH) proteins also play important role in ventral patterning but their expression is thought to be under the regulation of Shh-controlled homeodomain proteins.

Generation of the motor neurons is restricted to pMN progenitor domain by combinatorial action of Pax6 and Nkx6.1 which inhibit Nkx2.2, and Dbx2 respectively and together activate expression of the basic helix-loop-helix (bHLH) protein, Olig2 (Marquardt and Pfaff 2001, Novitch, Chen et al. 2001). Olig2 in turn co-ordinately activates expression of the proneural bHLH transcription factor Neurogenin2 (Ngn2) (Lee, Lee et al. 2005). As Ngn2 accumulates in some of the pMNs it drives them from the progenitor state towards post-mitotic MNs by promoting cell cycle exit, while suppressing Notch signalling and glial fates. Later Olig2 and Ngn2 expressions are downregulated after initiating the expression of the LIM homeodomain proteins Hb9 and Isl1 that promote MN specification. Hb9 stimulates its own expression and implements an MN-specific gene expression program by inducing expression of Islet1, Islet2, Lhx3 and ChAT which provide MNs independence from the Shh and retinoid signalling (Tanabe, William et al. 1998). The pMN domain remains active after an initial phase of MN generation, but switches to the generation of oligodendrocytes (Richardson, Smith et al. 2000, Lu, Sun et al. 2002).

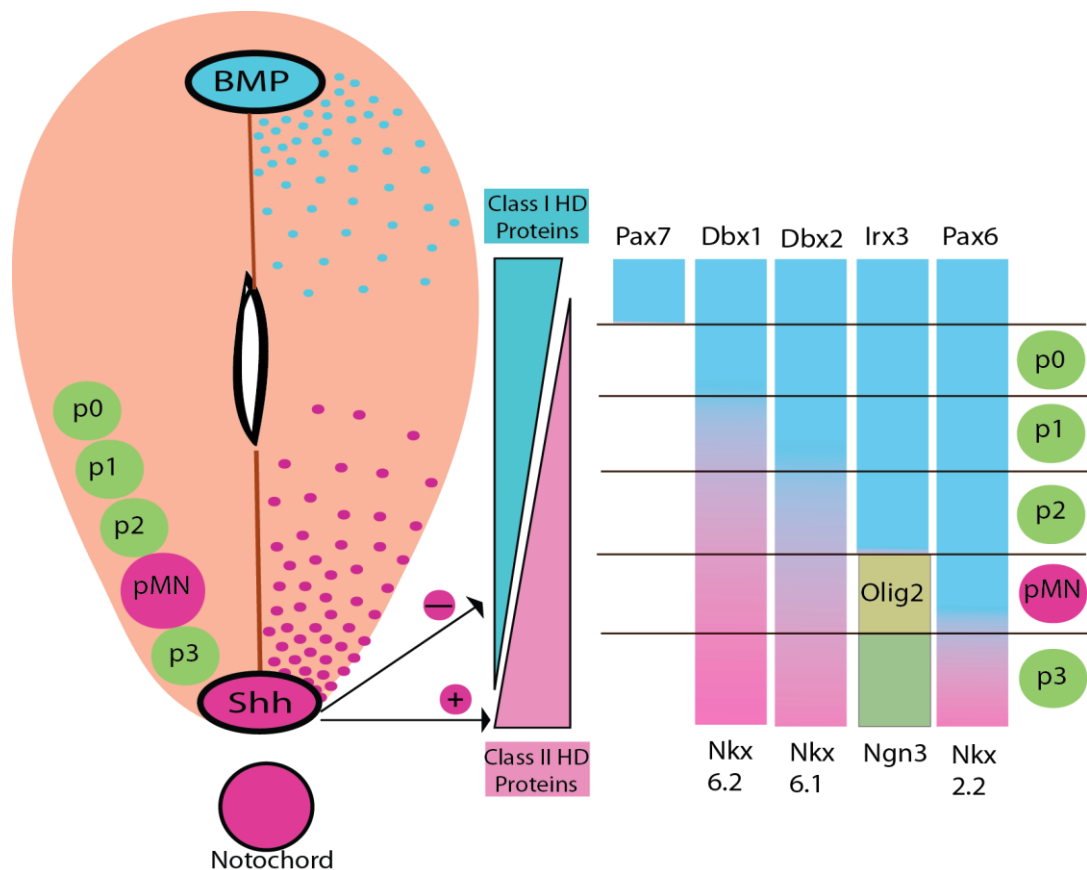


Fig.2.2a Ventral Patterning in the Spinal cord

Scheme illustrating the generation of ventral spinal progenitor domains. Shh secreted from the notochord and the floor plate make a ventral-high, dorsal-low gradient within ventral spinal cord (purple dots). Shh represses the Class-I homeodomain proteins (blue) (Pax7, Dbx1, Dbx2, Irx3, Pax6) and induces the Class-II homeodomain proteins (green) (Nkx6.2, Nkx6.1, Nkx2.2) and later bHLH protein Olig2 (light green). The cross-repressive activity of Class I and II proteins give rise to 5 progenitor domains (p0, p1, p2, p3 and pMN).

All spinal motor neurons originate from single progenitor domain but with further development, they acquire many subtype identities. The motor neuron subtypes can be categorised on basis of anatomical positions or based on functional and physiological differences. Anatomically motor neurons are divided into four motor columns along the rostrocaudal axis as shown in figure 2.2b. The medial motor column (MMC) present throughout the spinal cord innervates axial musculature. The lumbar motor columns (LMCs) are present only at brachial and lumbar levels of spinal cord and innervate limbs. The other two motor columns, the hypaxial motor column (HMC) and the preganglionic chain (PGC)

are present only at thoracic level of spinal cord and innervate body wall and sympathetic ganglia respectively.

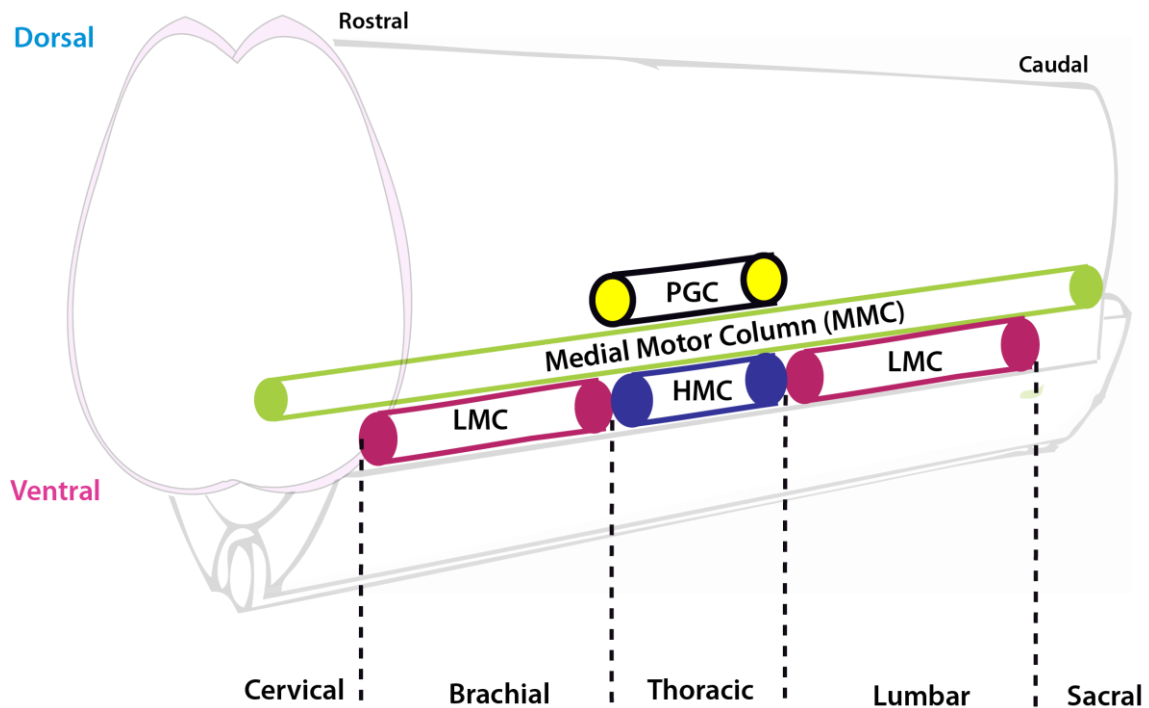


Fig.2.2b Positions of Motor Columns Along the Spinal Cord

Relative representation of different motor columns along the axis of spinal cord. Only one side of motor columns are shown, same amount of motor columns also exists in other half of spinal cord. The medial motor column (green) is present throughout the spinal cord at all levels. The Preganglionic Chain (yellow) and Hypaxial Motor Column (blue) are present only at thoracic levels while the lateral motor columns (red) are present only at brachial and lumbar levels where limbs are connected.

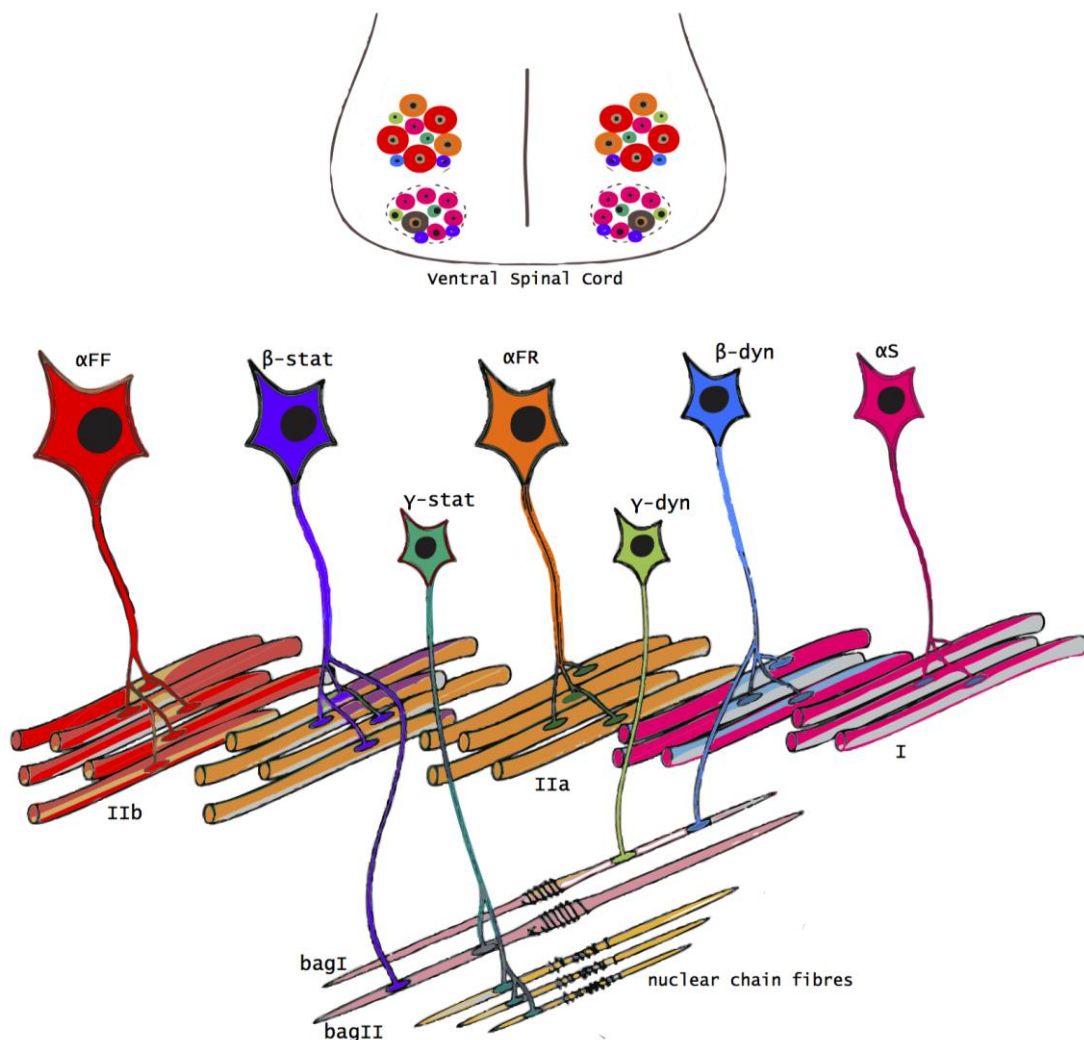
2.3 Functional Diversification of Motor Neurons

Motor neuron diversity is a functional necessity for precise control over muscle contraction during complex movements, therefore all MNs are not functionally equal. MNs are not only diverse but also segregated and grouped into different muscle specific motor pools. Based on different axonal conduction velocities and firing patterns, MNs are classified as alpha (α), gamma (γ) and beta (β) MNs (Burke, Levine et al. 1973). While alpha MNs innervate only extrafusal muscle fibres and receive direct Ia (sensory fibre) inputs from proprioceptive neurons, the gamma MNs innervate only intrafusal muscle fibres in muscle spindles and lack Ia inputs. The beta MNs innervate both intrafusal and extrafusal muscle fibres but very little is known about their physiological properties. The electrophysiological difference between alpha and gamma MNs lies in axonal conducting velocities which also led to their nomenclature. The alpha MNs have faster conducting axons and are responsible for force generation in muscles during movement while gamma MNs have slower conducting axons and instead of contributing in force generation, they modulate the sensitivity of the muscle spindle stretch receptors by controlling intrafusal fibre contractility. Since there are several kinds of extrafusal and intrafusal muscle fibres known, it is intuitive to consider that a corresponding number of functional types of MNs exist.

Muscle spindles have two major kinds of intrafusal fibres i.e. nuclear bag fibres (with relatively greater length and larger diameter) and nuclear chain fibres (with relatively shorter length and smaller diameter). Nuclear bag fibres are further classified into bag1 fibre contracting slowly and bag2 fibres which contracts faster. The two functional subtypes of gamma MNs are the gamma dynamic neurons that innervate only bag1 fibres and the gamma static innervate bag2 fibres and chain fibres. However, neither anatomically nor electro-physiologically or even at the molecular level, the gamma subtypes can be differentiated from each other.

Extrafusal muscle fibres are categorised into three types based on their ATPase reactivity pattern i.e. type IIB, IIA and I and they can also be differentiated by Myosin heavy chain isoform expression. These three fibre types have contrasting physiological properties in terms of mitochondrial content, fatigue resistance and force generation. A given alpha MN only innervates muscle fibres of a single type and hence alpha MNs are categorised into

three types corresponding to the kind of extrafusal fibres they innervate i.e. 'slow', 'intermediate' and 'fast' (Burke, Levine et al. 1973).



modified from (Manuel and Zytnicki 2011)

Fig.2.3 Functional Subclasses of MNs

Cartoon of location of MNs (MNs) in transverse section of spinal cord (top) and different kinds of MNs innervating their target muscle fibres (below). FF-type α -MNs innervate IIB fibres. FR α -MNs innervate IIA fibres. S-type α -MNs innervate type I muscle fibres. β -MNs innervate both extra- and intrafusal muscle fibres. β -static MNs innervate either type IIA or IIB extrafusal fibres and the intrafusal bag2 fibre. β -dynamic MNs innervate type I extrafusal muscle fibres and the intrafusal bag1 fibre. γ -MNs are smallest in size and innervate exclusively intrafusal muscle fibres. γ -static MNs innervate the intrafusal bag2 fibre and/or the nuclear chain fibres. γ -dynamic MNs innervate the intrafusal bag1 fibre.

Also, the electrophysiological properties of the alpha MN types precisely match to the contractile properties of their muscle fibre target (Fig.2.3). Slow contracting type I fibres are innervated by slow alpha (α S) MNs with relatively lower rheobases and lower firing frequencies. The fastest alpha (α FF) MNs, in contrast, possess higher rheobase and highest firing frequencies among the alpha MN types and supply to the fast contracting fatigable type IIB fibres. Similarly, the alpha MNs innervating the fast fatigue resistant type IIA fibres are thought to show intermediate electrophysiological properties.

The innervation pattern of the different MNs and the expression of combinations of membrane receptors and ion channels that together determine membrane electrical properties of MNs likely depend on well-regulated developmental pathways involving complex molecular signals. However, only a few of these signals are known so far (Table 2.3). Certain proteins like α 3 subunit of the Na⁺, K⁺ ATPase (Dobretsov, Hastings et al. 2003), Err3 (Friesse, Kaltschmidt et al. 2009), Gfra1 (Shneider, Brown et al. 2009) and Wnt7a (Ashrafi, Lalancette-Hebert et al. 2012) have been recently reported as gamma MN markers. For alpha MNs the molecular markers are even fewer i.e. NeuN and Osteopontin (OPN) (Misawa, Hara et al. 2012). The discovery of concrete molecular markers is of utmost importance for elucidating the critical steps during locomotion and verifying the importance of different subtypes of MNs at each of those critical steps. The latest advancement in this direction was made in 2014 after the discovery of a transmembrane protein, delta homolog1 (Dlk1) as a marker for fast alpha MN and the first determinant of MN functional diversification identified so far. (Muller, Cherukuri et al. 2014).

Properties	α FF	α FR	α S	β	γ
Target Muscle fibre	Type IIB	Type IIA	Type I	Extrafusal And Intrafusal	Only Intrafusal Fibres
Membrane Input Resistance	High	Intermediate	Low	Intermediate	Low
Order of Recruitment	Late	Intermediate	Early	Unknown	Unknown
Molecular Markers	Dlk1, MMP9, Calca, Chodl	Unknown	Sv2a, PKC δ	Unknown	Err3, Gfra α , 5HT1D, Wnt7a
	High NeuN, OPN				Low NeuN

Table 2.3 Properties and Molecular Markers of MNs Subtypes

2.4 Dlk1 as a Determinant of Motor Neuron Functional Diversification

Delta-like 1 homolog (Dlk1) is a type 1 transmembrane protein constituted with a signal peptide for the secretory pathway, six epidermal growth factor (EGF) like repeats, a transmembrane region and a short cytoplasmic C-terminus. Its juxta-membrane region has a TACE (ADAM17)-mediated cleavage site which in some contexts seems to create a secretory soluble form of Dlk1 (Wang and Sul 2006). This protein was discovered independently several times and given different names and was reported as inhibitor of adipogenesis (Smas and Sul 1993), promoter of muscle development (Charlier, Segers et al. 2001), regulator of B cell maturation (Raghunandan, Ruiz-Hidalgo et al. 2008), tumour-suppressor (Li, Forman et al. 2005, Kawakami, Chano et al. 2006) and regulator of neurogenesis (Ferron, Charalambous et al. 2011).

Although expression of Dlk1 in central nervous system and its putative roles in differentiation of neurons was known for more than a decade (Jensen, Meyer et al. 2001), nothing was known or discussed about its role in neuronal development until recently. In 2014, it was shown that Dlk1 is expressed in one third population of spinal motor neurons and that its expression is important to promote fast MN properties. The population of MNs which express Dlk1 turn out to be both Hb9 and NeuN positive, with larger soma sizes indicating that Dlk1 expressing MNs are alpha MNs. Furthermore, in chicken spinal cord, overexpression of Dlk1 shifts the population of MNs towards 'fast' biophysical signature. Conversely, in Dlk1 knock-out mice, MNs fail to acquire the electrophysiological properties that normally characterize fast alpha MNs. Consequently, Dlk1 knock out mice which show reduced peak force generation during running tasks (Muller, Cherukuri et al. 2014).

The exact mechanisms through which Dlk1 promotes fast MN signature remains unknown. However, Dlk1 is necessary to promote fast MN specific gene expression including the neural activity modulator *KCNG4*, while there is evidence that Dlk1 acts through inhibition of Notch (Muller, Cherukuri et al. 2014). Also, it has been clearly shown that only MNs over-expressing Dlk1, but not the adjacent ones, exhibit fMN properties suggesting that Dlk1 acts cell-autonomously to promote fast MN properties (Muller, Cherukuri et al. 2014). Dlk1 in principle could act through multiple pathways, involving interactions of different proteins with its extracellular segment and intracellular segment and initiating different signalling pathways which influence various properties of the cell. A secondary structure of Dlk1 and probable signalling interactions is shown in Figure 2.4.

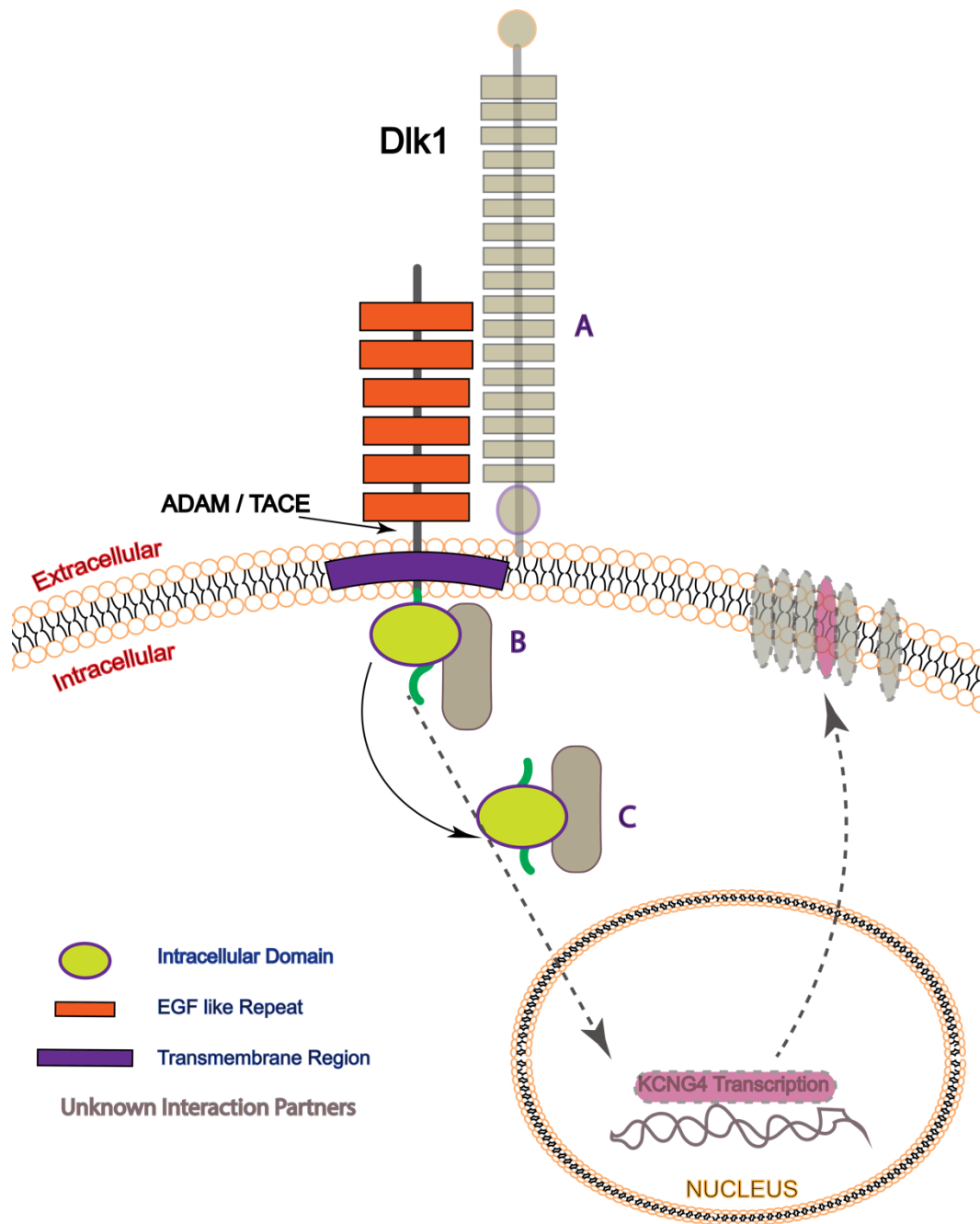


Fig.2.4 Dlk1 Transmembrane Protein Alters Motor Neuron Properties

Dlk1 is a transmembrane protein with 6 EGF-like repeats and can exhibit cis-interactions via EGF domain. Dlk1 is cleaved by metalloproteases (ADAM/TACE) and extracellular segment is secreted. Although exact signalling mechanism is unknown but Dlk1 alters gene transcription and changes the ion channel levels at membrane which ultimately changes motor neuron properties towards fast MNs. (A) shows the possible cis-interaction with Notch as speculated in literature. (B) and (C) depicts possible intracellular interactions which can ultimately alter gene transcription.

2.5 Notch Signalling and Dlk1 as a Ligand of Notch

Notch is a single pass type I transmembrane receptor protein which mostly exists as a heterodimer after maturation (Blaumueller, Qi et al. 1997) (Fig 2.5a). For three decades after cloning of Notch, a lot have been studied, discovered and outlined about the Notch signalling pathway and its functions which relates to almost every field of biological science. Notch signalling is an interface for short range cell-to-cell communication. Interestingly, Notch signalling is irreversible and each Notch molecule signals only once without amplification by secondary messenger cascades (Kopan and Ilagan 2009). Notch signalling can promote or suppress proliferation, acquisition of specific cell fates, cell death and activation of differentiation programs throughout development of an organism and after maturation during self-renewal.

During canonical Notch signalling, a canonical Notch ligand activates the mature receptor by trans- (cell-to-cell) interaction which leads to cleavage of Notch and generation of a Notch intracellular domain (NICD). NICD then translocates to the nucleus via unknown mechanism where it binds to a partner, the CSL protein, to affect transcription of genes (Fig. 2.5a). The canonical Notch ligand comprise several paralogues of the Jagged and Delta type I transmembrane protein that acts through EGF repeat 11-12 of Notch and differ in their structural domains and interaction with Notch (Fig. 2.5b). The jagged ligands interact via both DSL (Delta, Serrate and Lag2) and DOS (Delta and OSM-11-like) domain while delta ligands (except DLL1) interact only via DSL domain.

Apart from these canonical Notch ligands, non-canonical Notch ligands interact via different regions of Notch thus creating a non-canonical Notch signalling pathway. Most of the non-canonical Notch ligands exhibit cis (cell autonomous) interaction with Notch and are mostly inhibitory. Inhibitory ligands bind to EGF repeats 24-29 of Notch (de Celis and Bray 2000). However, there are also recent studies which claim that inhibitory and activating ligand binding regions overlap at EGF repeats 11-12 suggesting competition of canonical and non-canonical ligands for the same binding interfaces (Cordle, Johnson et al. 2008, Becam, Fiuza et al. 2010). Altogether, Notch ligands are mostly inhibitory, when they bind Notch in cis-configuration through EGF repeats 24-29 of the Notch receptor. Such cis-inhibitory ligands are thought to be important to maintain the unidirectional Notch signalling during cell differentiation and proliferation (Miller, Lyons et al. 2009, D'Souza, Meloty-Kapella et al. 2010).

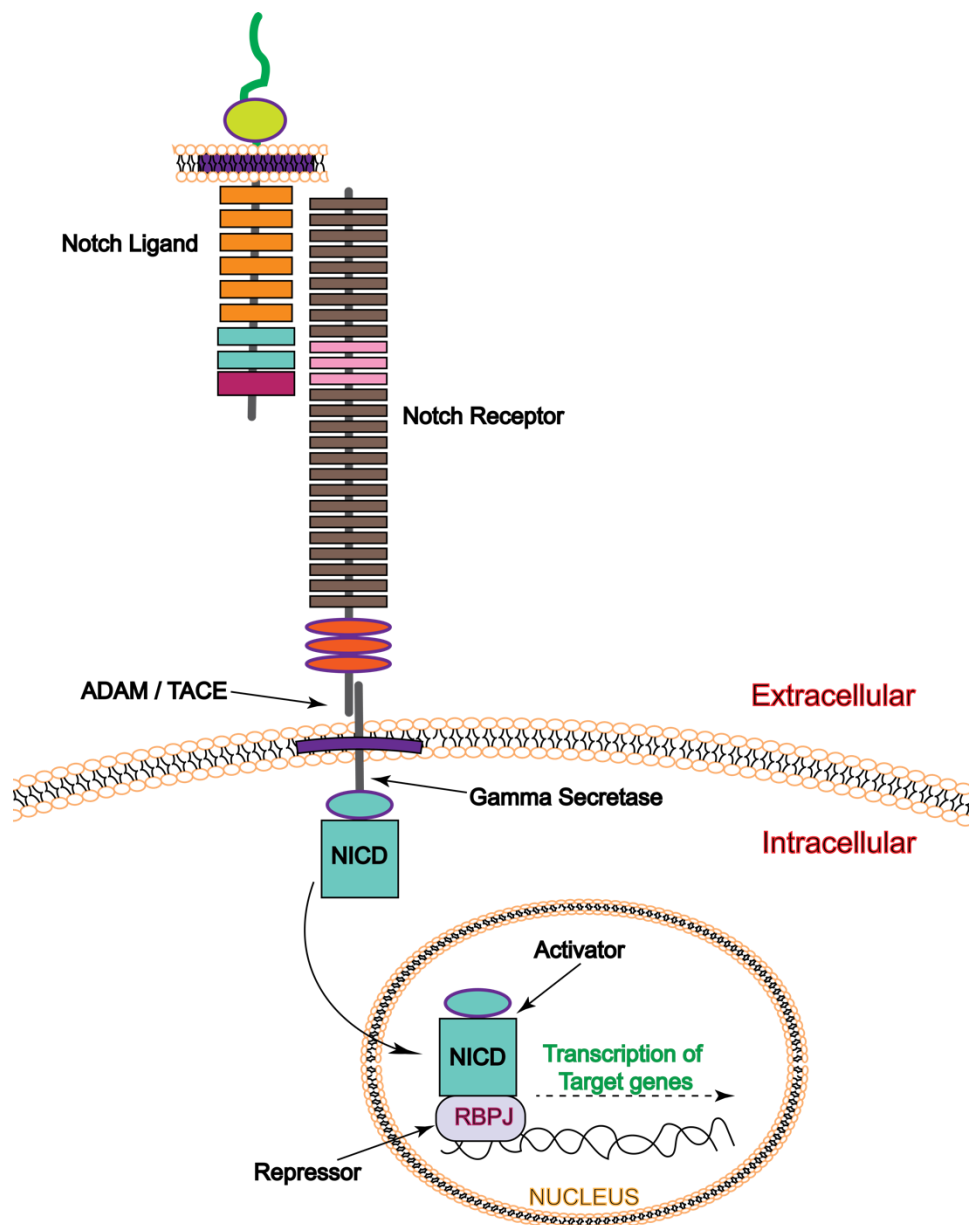


Fig.2.5a Canonical Notch Signalling

Schematic illustration of canonical Notch signalling. A trans-interaction, at EGF repeats 10-12 of heterodimeric Notch protein, with a canonical Notch ligand takes place. This interaction leads to cleavage of Notch protein near heterodimerization (HD) domain by ADAM and intracellular juxta-membrane region by gamma secretase. The cleavage creates a free cytoplasmic Notch intracellular domain (NICD) which translocates into the nucleus and where it suppresses the activity of repressors thus activating the transcription of target genes.

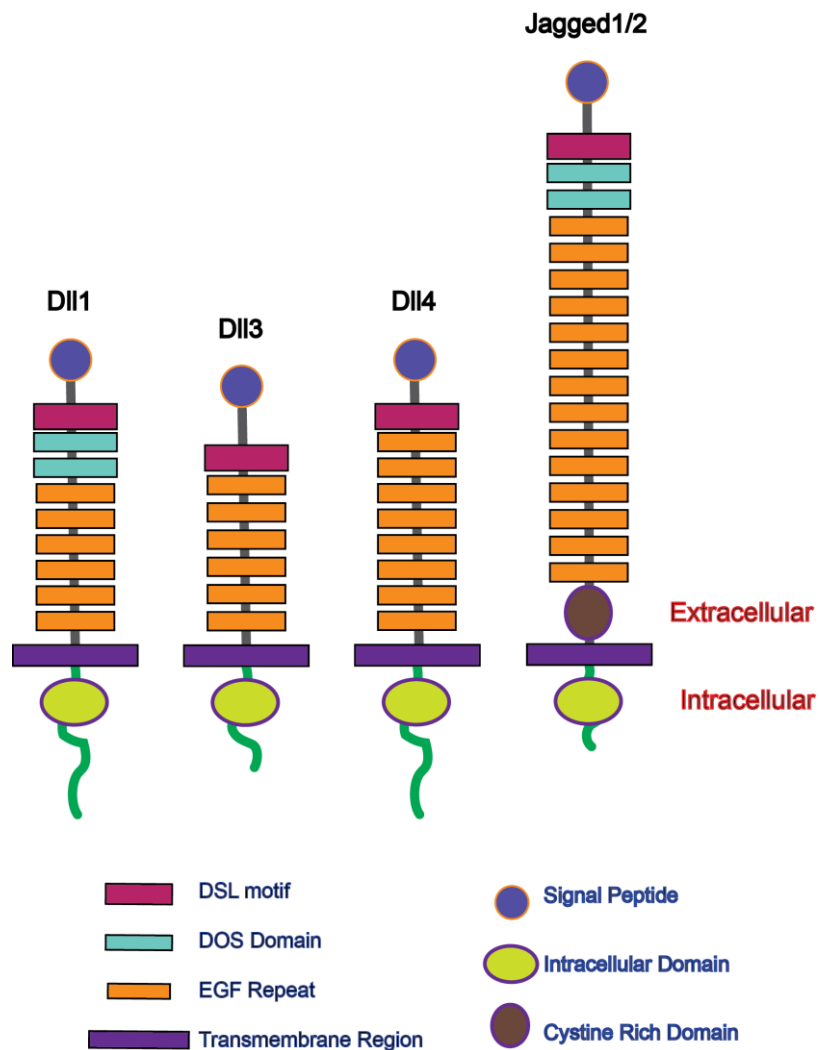


Fig.2.5b Canonical Notch Ligands

Representation of the secondary structures of canonical Notch ligands. Classical Notch ligands contain the DSL (Delta-Serrate-Lag-2), DOS (Delta and OSM-11-like proteins) and EGF (Epidermal growth factor) motifs. DLL3 and DLL4 are considered DSL-only ligands since they lack DOS domain. All of them are known to interact at EGF 10-12 of Notch protein.

Dlk1, the recently reported fMN marker, is structurally similar to canonical Notch ligand Dll1 (Fig.2.5c). There are several reports of Dlk1 interacting with Notch and that Dlk1 inhibits Notch (Baladron, Ruiz-Hidalgo et al. 2005) as a cis-ligand (Bray, Takada et al. 2008). Yeast two hybrid technique shows region of interactions as EGF repeats 10-15 of Notch and EGF domains 5-6 of Dlk1 (Sanchez-Solana, Nueda et al. 2011, Traustadottir, Jensen et al. 2016). Even so, the in-vivo interaction in mammals still remain unconfirmed since most of the

studies are done in-vitro. Also, if the non-canonical ligand Dlk1 also binds to the canonical interacting regions (11-12) then how it inhibits Notch in this configuration is still unclear. Moreover, the idea that Dlk1 signalling operates through Notch remains contested with evidences suggesting failure of Dlk1 to bind to Notch and Notch-independent roles of Dlk1 in adult neurogenesis (Ferron, Charalambous et al. 2011). Also, most of the evidences showing an inhibitory role of Dlk1 for Notch are indirect asserting inhibition of Notch target genes (Nueda, Baladron et al. 2007, Falix, Aronson et al. 2012) or failure of ligand function due to overexpression of Notch (Muller, Cherukuri et al. 2014).

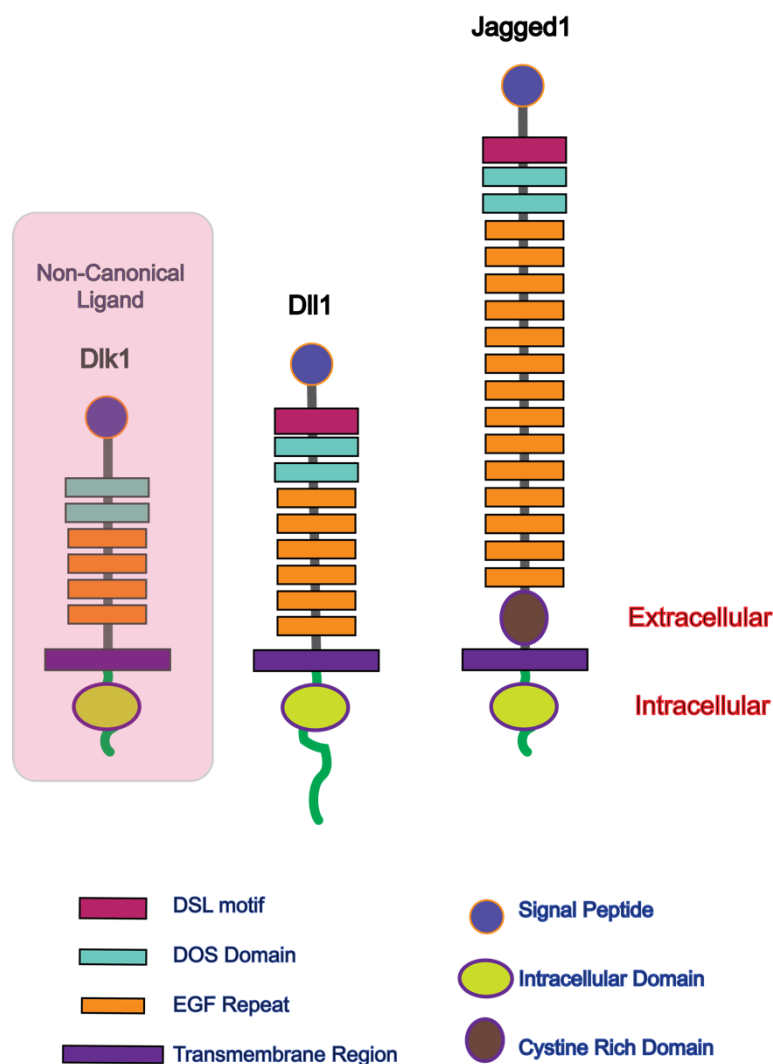


Fig.2:5c Dlk1 as a Non-Canonical Notch Ligands Compared with Canonical Ligands

Representation of the secondary structures of canonical Notch ligands compared with the non-canonical Notch ligand Dlk1. Dlk1 is similar to DII1 and lacks only the DSL motif. Hence Dlk1 is a DOS-ligand.

2.6 Notch Signalling During Spinal Neuron Diversification

Notch signalling is conducive for cell fate diversification during both vertebrate and invertebrate development. Notch is repetitively recruited whenever a binary fate decision is required throughout nervous system development. Establishment of neuronal diversity in central nervous system (CNS) depends on two main processes: patterning of neuroepithelium into discrete progenitor domains and intradomain diversification into neuronal and glial subtypes. During epidermal versus neural fate decisions, an inhibitory effect of Notch on neural fate is involved (lateral inhibition), whereas during making choice between different subtypes of neural cells, Notch permits one fate and prohibits the other (binary switch activity). For instance, it was shown that inhibition of Notch signalling induces premature neurogenesis (Nelson, Hartman et al. 2007) while in developing ventral spinal cord, Notch promotes V2b over V2a interneuron identity (Peng, Yajima et al. 2007).

Enhancer of split (Esp1), a bHLH transcription factor, is a primary downstream effector of Notch signalling. Esp1 suppresses neuronal differentiation by inhibiting other proneural bHLH transcription factors (Achaete-scute and Atonal). Inhibition of Notch thus upregulates the transcription proneural genes leading to neuronal differentiation (Yoon and Gaiano 2005). In addition to controlling neuron versus progenitor cell fate, Notch controls cell identity by temporal modulation of progenitor differentiation. For example, inhibition of Notch during early stages of chick retinal development (E3) results in increased population of ganglion cells while doing the same at later stages (E14.5) produces more amacrine cells (Nelson, Hartman et al. 2007). A similar temporal modulation by Notch signalling is observed during neuronal versus glial cell fate switch in zebrafish where a mutation in delta gene at early stages results in excess and early specified neurons (Appel, Givan et al. 2001) while conditional overexpression of Notch promoted excess of oligodendrocyte precursor cells (Park and Appel 2003). Studies using neurospheres clonally derived from neural stem cells of Dll mutant mice embryos, also revealed that Notch signalling controls the generation of neurons/glia from neural stem cells in a stepwise process based on temporal modulation (Grandbarbe, Bouissac et al. 2003).

Recent studies in the p2 domain of the ventral spinal cord suggest that Notch selects alternative cell fates by an evolutionarily conserved mechanism of Notch dependant asymmetric division observed during division of ganglion mother cells (GMCs) in drosophila. During GMC asymmetric division, only one of the daughter cell receives ability to respond to Notch signalling which is generated due to asymmetrical distribution of Numb (Notch

inhibitor) during GMC inhibition (Frise, Knoblich et al. 1996, Spana and Doe 1996, Buescher, Yeo et al. 1998). Similarly, the p2 daughter cell fate is regulated by Delta4 activation of Notch receptors and the daughter cell responsive to Notch signals activate a transcription factor code that specifies the v2bIN fate, whereas the daughter cell deprived of Notch signalling express another code for v2aIN formation (Peng, Yajima et al. 2007).

Within the motor neuron progenitor domain, it has been proposed that Notch controls motor neuron subtype identity primarily indirectly by controlling the timing of neurogenesis and gliogenesis (Crawford and Roelink 2007). Another study using Gde2-null mice, suggests that inhibition of Notch signalling regulates subtype-specific MN generation (Sabharwal, Lee et al. 2011) and that loss of Notch inhibitor GDE2 led to selective loss of hypaxial (HMC) or lateral motor columns (LMC). This study also implied that motor neuron subtype-specification initiates already at progenitor level when Notch is inhibited to generate post-mitotic neurons. Consistent with this observation is another study where reduction in Notch signalling promoted phrenic neuron identity which is a subpopulation of HMCs (Machado, Kanning et al. 2014). Even more recent study utilizing embryonic stem cell (ESC) differentiation model (Tan, Mazzoni et al. 2016) suggests that Notch directly controls motor neuron subtype identity. The study demonstrates that HMC generation peaks prior to MMC production in the ESC-to-motor neuron differentiation system and that inhibition of Notch signalling leads to accelerated neurogenic differentiation of pMNs due to repression of Ngn2 (Neurogenin2). The study also claims that MN subtype is controlled by an Ngn2-independent mechanism and that timing of neurogenesis and control of motor neuron subtype identity are functionally independent processes regulated by molecularly distinct Notch targets.

Altogether, various studies indicate Notch as a mediator of motor neuron versus glial differentiation and as interneuron fate selector in the ventral spinal cord. In vitro studies demonstrating Notch regulation of motor column identity suggests that Notch signalling may also regulate motor neuron functional diversity. A role for Notch in controlling functional diversification of motor neurons would fill a gap in our current knowledge of how motor neuron subtype identity is established.

2.7 NFATs as Interesting Signal Carriers from Cytosol to Nucleus

Regulated influx of Ca^{2+} and its release from internal reserves is critical a wide range of biological phenomena right from beginning of life during fertilization up to muscle contraction during movements made by living beings and even during death. Neurons exhibit Ca^{2+} -dependent gene transcription patterns which is very important aspect of nervous system development as it makes use of a broad signalling molecule for precise functions. For neurons, it is important for cell-to-cell communication, synaptic activity and also long-term survival (Marambaud, Dreses-Werringloer et al. 2009). A key mediator of Ca^{2+} -dependent gene expression is the Ca^{2+} /calcineurin dependent transcription factor NFAT (Nuclear Factor of Activated T-cell).

NFATs are family of transcription factors with five members: NFATc1, NFATc2, NFATc3, NFATc4 (Hugo Nomenclature) and NFAT5. NFATc transcription factors exist in two forms: a phosphorylated form which resides in the cytoplasm and a dephosphorylated form which is localised in the nucleus. The two forms shuttle between the nucleus and cytoplasm thus connecting the two compartments in response to cellular signals. These cellular signals can be versatile but the best-known pathway is outlined in Fig. 2.7. When intracellular calcium level increases to 400 nM it activates the serine/threonine phosphatase: Calcineurin via a calcium-binding messenger protein: Calmodulin. Calcineurin then dephosphorylates the cytoplasmic NFAT thus exposing its nuclear localisation signal (NLS). The dephosphorylated NFAT translocates to the nucleus within 5-30 minutes. In nucleus, NFATs form a transcription complex with other proteins or cofactors and alters gene transcription. Important to mention here is that NFATc transcription factors cannot directly bind to DNA, instead they always need another factor to bind to DNA. Hence, NFATc proteins integrate a calcium signal and other signal to reach a final outcome of gene transcription. For example, cardiac hypertrophy is caused when calcium signal triggers NFATc4 nuclear translocation and GATA4 binds to NFATc4 thus integrating two independent signals/information (calcium influx and GATA4) in the cardiac muscles (Molkentin, Lu et al. 1998). NFAT proteins have several interaction partners and the interaction can lead to either synergistic activation or repression of NFAT mediated transcription (Mognol, Carneiro et al. 2016). Also, different members of NFAT family have different specific roles which indicates that the amount of NFAT proteins activated and the cell-type dependant environment of the protein will decide the targets of NFAT mediated transcription.

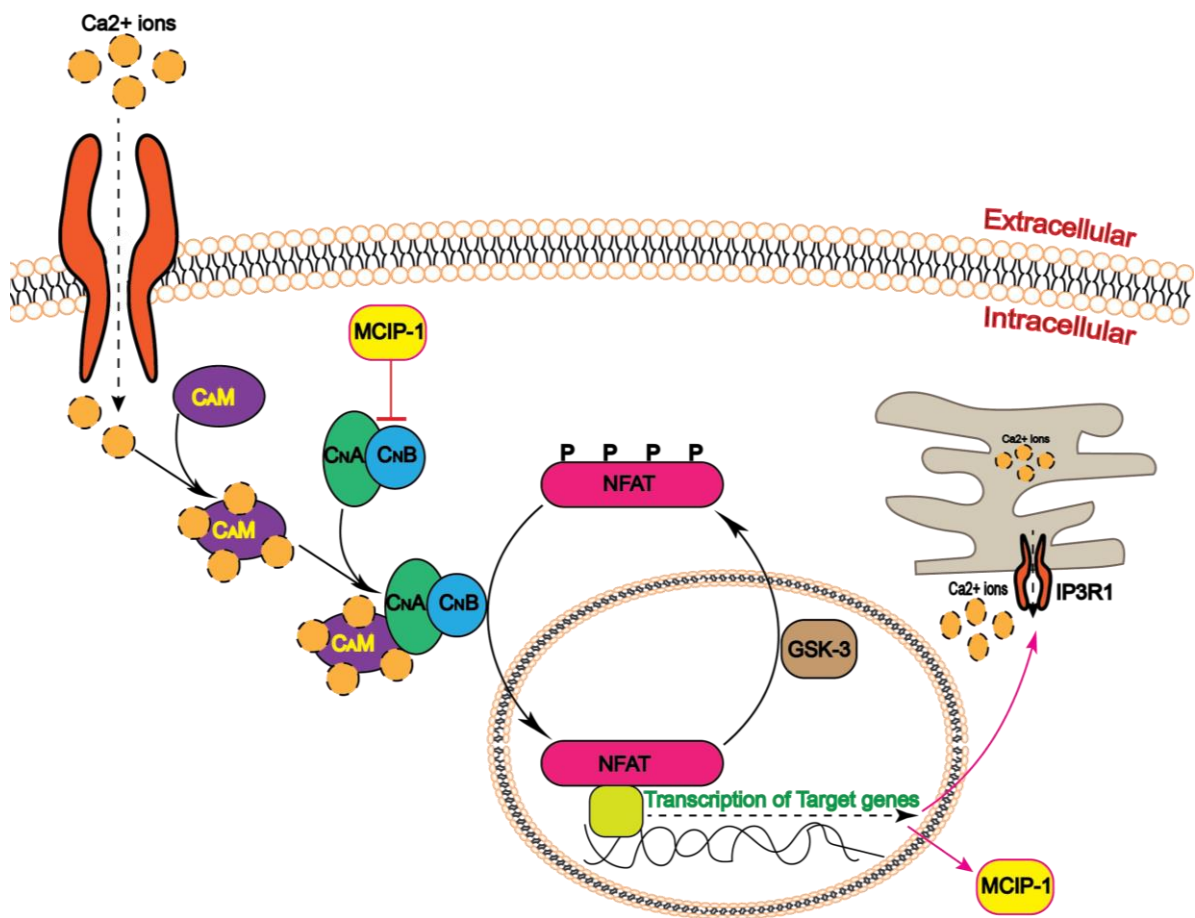


Fig.2.7 Illustration of NFAT Signalling Pathway

Calcium ion influx during developmental processes or cellular activities, leads to activation of calmodulin (CaM) which then binds and activates Calcineurin (CaN-CnB). Calcineurin being a phosphatase, dephosphorylates cytoplasmic NFAT and exposes its nuclear localisation signal hence leading to nuclear import of NFAT. In nucleus, NFAT dimerizes with other transcription factors and alters gene transcription. Regulation of NFAT mediated gene transcription occurs by regulation of Ca^{2+} levels; nuclear export of NFAT by a kinase GSK-3 which phosphorylates NFAT and by feedback control mediated by MCIP-1 (myocyte-enriched calcineurin interacting protein) which inhibits calcineurin. A positive feedback regulation also exists by transcription of intracellular receptor inositol triphosphate which release the intracellular reserves of calcium thus increasing intracellular calcium levels.

Like most other signalling pathways, NFAT signalling pathway is also regulated at multiple levels and several modulators take part in it. First regulation occurs during nuclear import by calcium levels, calcineurin levels and calcineurin activators/inhibitors. Secondly, once

NFATc is in the nucleus the nuclear export becomes regulatory because more it will stay in nucleus more/longer will be the transcriptional alterations. In nucleus GSK-3 (glycogen synthase kinase-3) is the main kinase taking part in exit of NFAT by rephosphorylating the protein while other kinases like p38, MAP-kinase, casein kinase and MEKK-1 are also known to rephosphorylate NFATc1 and NFATc3 proteins at least in vitro. The third level of regulation is via feedback control. For instance, NFATc2 is known to induce NFATc1 in T-lymphocytes (Zhou, Cron et al. 2002) while in hippocampal and cortical neurons, IP3R1 gene is induced by NFATc4 signalling (Genazzani, Carafoli et al. 1999, Graef, Mermelstein et al. 1999), which in turn will activate NFAT signalling by increasing intracellular calcium levels. Similarly, a feedback inhibition is observed in muscle cells where expression of MCIP-1 (a calcineurin inhibitor) transcription is activated by NFAT signalling (Yang, Rothermel et al. 2000).

2.8 NFAT Signalling During Development of Central Nervous System

NFAT signalling has been first implicated in lymphoid development (Shaw, Utz et al. 1988, Riegel, Richie et al. 1990) and was initially mostly studied in immune cells (Boom, Sol et al. 1990). Advancements in past three decades have shown presence of different NFAT paralogues in different tissues during vertebrate development because NFATc proteins have vertebrate specific functions (Graef, Chen et al. 2001). NFAT signalling is one of those signalling pathways which integrates and transmits signals from cytosol to nucleus only in vertebrates because calcium sensitive NFAT homologs are not found in invertebrates (Graef, Gastier et al. 2001). Also, NFAT signalling appears to be involved in those developmental processes which are advanced in vertebrates e.g. lymphoid development (Rao and Avni 2000, Macian 2005), organisation of vascular system (Graef, Chen et al. 2001, Nilsson, Nilsson-Ohman et al. 2008), nervous system development (Graef, Wang et al. 2003, Benedito, Lehtinen et al. 2005) and skeletal development (Hill-Eubanks, Gomez et al. 2003, Schulz and Yutzey 2004, Zhao, Irie et al. 2006, Cheng, Zhao et al. 2012).

The presence of NFAT proteins in neurons was first detected in the murine nervous system and it indicated role of NFATs in transcription of specific neuronal genes in response to increases in cytosolic calcium (Ho, Jain et al. 1994). The activity of NFAT proteins in nervous system was first observed in hippocampal neurons (Graef, Mermelstein et al. 1999) where it was shown that calcium ion influx (via L-type voltage gate calcium channels and NMDA receptors) activates NFAT-dependent transcription. At the same time activity of NFATs in microglia was also reported where extracellular ATP was shown to modulate early gene expression within nervous system via P2Z purinoreceptor mediated activation of NFATs (Ferrari, Stroh et al. 1999). Soon enough, several roles of NFATs in nervous system development began to unravel. It was discovered that, NFATc is required for Neurotrophin dependent axon outgrowth in mouse embryos (Graef, Wang et al. 2003); NFATc4 mediates and supports survival of granule neurons of the developing cerebellum (Benedito, Lehtinen et al. 2005); the morphological and electrophysiological properties of neurons depend on transcriptions mediated by distinct NFAT interactions (Schwartz, Schohl et al. 2009); NFAT signalling is important for diversification of neural crest cells and differentiation of Schwann cells (Kao, Wu et al. 2009). Altogether, NFATs emerged as key regulators of development and plasticity in nervous system but its precise role at cellular level in terms of interaction partners and direct influence on cellular properties remained vague due to complexity of vertebrate nervous systems and cellular diversity.

Later, after discovery of the single *Drosophila* homolog of NFATs (dNFAT), which is 53% similar to NFATc2 and 64% similar NFAT5 (Keyser, Borge-Renberg et al. 2007, Franciscovich, Mortimer et al. 2008), NFAT was studied in simpler nervous system of *drosophila* and it was shown that dNFAT homolog is expressed widely in the nervous system including motor neurons; Neuronal dNFAT negatively regulated pre-synaptic bouton number; reduced pre-synaptic transmitter release at the neuromuscular junction; suppressed excitability of motor neurons and abolished synaptic plasticity (Freeman, Franciscovich et al. 2011).

Due to established functions of NFAT signalling during development of nervous system, NFAT proteins were also studied in relation to nervous system disorders like Alzheimer disease (Abdul, Sama et al. 2009, Abdul, Furman et al. 2010), Parkinson's disease (Luo, Sun et al. 2014) and Timothy Syndrome (Tian, Voineagu et al. 2014). It was shown that constitutively active NFAT expression in mouse model of Alzheimer's disease recapitulates the phenotypes of amyloid beta ($A\beta$) neurotoxicity (Hudry, Wu et al. 2012) and that overexpression of NFAT3 (NFATc4) significantly increased $A\beta$ 42 protein in SAS1 cells (Mei, Yan et al. 2015). On the other hand, NFAT inhibition leads to cure of Lithium-induced apoptosis and motor deficits observed in mouse models undergoing lithium therapy (Gomez-Sintes and Lucas 2010) and suppression of $A\beta$ induced microgliosis in Alzheimer's mouse model (Rojanathammanee, Floden et al. 2015).

2.9 NFAT Regulates Transcription of K⁺ Channels

NFAT-signalling has been reported as transcriptional regulator of several ion channels in neurons and in muscles. A study in cardiomyocyte reported transcriptional upregulation of Kv4.2 channel subunits by NFAT activation (Gong, Bodi et al. 2006). Another study revealed that transcription of M-type K⁺ channels, encoded by KCNQ2-5, is regulated by NFAT transcription-factors organized together with A-kinase anchoring proteins (AKAPs) in sympathetic neurons (Zhang and Shapiro 2012). Even recent study using in-vitro models has provided direct evidence that NFATc4 is recruited to Kv4.2 gene promoter loci and in NFATc4(-/-) mice Kv4.2 transcriptional upregulation is abolished. In all these studies the membrane excitability of the cell was shown to be reduced due to increased K⁺ channel expression and vice-versa.

Also, hyperexcitability is a norm in many Motor Neurone Diseases (MNDs). In case of Spinal Muscular Atrophy (SMA) for example, it has been shown that MNs derived from SMA patients show hyper-excitable electrophysiology (Liu, Lu et al. 2015) while similar hyperexcitability exists in hippocampal cortical neurons together with spinal MNs in (Amyotrophic Lateral Sclerosis) ALS patients (Benedetti, Ghilardi et al. 2016, Geevasinga, Menon et al. 2016). In all of such cases of hyperexcitability voltage gated calcium, sodium and potassium were held responsible and NFATs have been shown as transcriptional regulators of many of those channels (Chang and Martin 2016, Noto, Shibuya et al. 2016). Also, a role of NFAT in supporting neuronal survival is already known (Benedito, Lehtinen et al. 2005, Vashishta, Habas et al. 2009, Mojsa, Mora et al. 2015) which further strengthens the idea that lack of NFAT signalling might cause neurodegenerative disease.

Altogether, inhibition of NFAT which causes hyperexcitability also resembles an unhealthy state of MNs and signifies the importance of NFAT in MNs where NFATc4 is significantly expressed as seen by *in-situ* hybridization (Website: © 2015 Allen Institute for Brain Science. Allen Spinal Cord Atlas).

In case of MNs, the fast MNs differ from the gamma MNs or the slow alpha MNs primarily in the property of excitability. While fast MNs promoted by Dlk1 show highly reduced excitability, the slow MNs and the gamma MNs are easily excitable. Kcng4 transcriptional upregulation was shown to be responsible for the decreased excitability and increased firing frequency observed in Dlk1 over-expressing MNs (Muller, Cherukuri et al. 2014). Since *KCNQ4* expresses potassium channel subunit that forms functional heteromeric channels

with other potassium channel (Kv2.1) and also alters excitability of MNs, I hypothesized that induction of Kcng4 expression and reduction of excitability observed in fast MNs should also be possible through NFATc4 signalling pathway. Hence, a link between Dlk1 and NFAT or NFAT and Kcng4 will strengthen the idea of a role of NFAT in MN functional diversification.

2.10 Dlk1 and NFAT Linked Together in Several Different Cellular Systems

Both Dlk1 and NFAT transcription factors are implicated in a number of related biological processes, although a direct link between Dlk1 and NFAT signalling pathway has never been discussed. Interestingly, a comparison of Dlk1 and NFAT functions reveals that they co-relate both antagonistically and synergistically depending on the tissue of reference.

1. Adipogenesis: Dlk1 is known as an inhibitor of adipogenesis, since it inhibits the differentiation of preadipocytes to mature adipocytes (Smas and Sul 1993, Smas, Chen et al. 1997). In contrast to this, inhibition of NFAT transcription factors in preadipocytes inhibits their differentiation (Ho, Kim et al. 1998).
2. Muscle Development: Dlk1 positively regulates muscle fibre growth during development and loss of Dlk1 in muscles decreases the number of muscle fibres (Charlier, Segers et al. 2001, Waddell, Zhang et al. 2010). NFATs also play important role in muscle fibre type specification and acts as nerve activity sensor leading to expression of relevant myosin heavy chains (McCullagh, Calabria et al. 2004, Calabria, Ciciliot et al. 2009).
3. Lymphocyte Development: Both Dlk1 and NFATs are important players of lymphoid development. On one hand expression of Dlk1 is essential for differentiation and function of B-lymphocytes (Raghunandan, Ruiz-Hidalgo et al. 2008) while on the other T-cell differentiation and function requires NFAT signalling (Macian 2005).
4. Angiogenesis: Inhibition of NFAT signalling inhibited VEGF-mediated angiogenesis (Hernandez, Volpert et al. 2001). Recently, Dlk1 has been reported as inhibitor of VEGF-mediated angiogenesis (Rodriguez, Higuera et al. 2012).

2.11 Goals of the Present Study

Our group has established Dlk1 as a determinant of MN functional diversification by promoting fast MN biophysical properties (Muller, Cherukuri et al. 2014). Previous electrophysiological studies in chick indicated that inhibition of Notch was a prerequisite for Dlk1 actions on MN properties (Muller, Cherukuri et al. 2014). Although inhibition of Notch is important, it is most likely 'not sufficient' to promote fast neuron properties, suggesting the involvement of additional factors or pathways through which Dlk1 promotes fast MN properties. *KCNG4*, a gene encoding a β -subunit of a potassium channel, was identified as a Dlk1 dependent fast MN specific gene which contributes to the implementation of fast MN biophysical signature by increasing both the rheobase and firing frequency of MNs. However, the pathway through which expression of genes like *KCNG4* are altered by the type I transmembrane protein Dlk1 remained unresolved.

Based on a Split-Ubiquitin two-hybrid screen for Dlk1 interaction partners, several potential Dlk1 interaction partners were identified including Notch1 and NFATc4. As already described, NFATc4 is Ca^{2+} dependent carrier of signals cytosol to nucleus where they directly regulate gene expression. Since Dlk1 and NFATs were implicated in similar developmental pathways, my thesis is based on the working hypothesis that NFAT would be an essential intermediate factor of Dlk1-mediated gene expression.

Because whether Dlk1 directly interacts with Notch, and whether Dlk1 would inhibit or activate Notch remained controversial, my thesis starts with the investigation of Dlk1-Notch interaction and its effects. The second goal of my thesis was to study Dlk1 and NFAT interaction and its contribution to Dlk1-dependent control of gene expression.

III Materials

3.1 Laboratory consumables and plastic wares

Consumables were purchased from Starlab GmbH (Ahrensburg), Eppendorf (Hamburg), and Sarstedt AG (Nürnberg). Dissection instruments were bought from Fine Science Tools GmbH.

3.2 Antibodies:

- **Primary antibodies**

Antibody Against	Host Species	Working Dilution	Company
ChAT	Goat	1:200	Merck-Millipore
Dlk1	Rabbit	1:500	Santa Cruz
DsRed	Rabbit	1:1000	Clontech
Err3	Mouse	1:1000	Perseus Proteomics
FLAG Tag	Mouse	1:1000	Sigma
FLAG Tag	Rabbit	1:1000	Sigma
GFP	Rabbit	1:1000	Life Technologies
GFP	Chicken	1:2000	Abcam
HA Tag	Mouse	1:1000	Abcam and Sigma
Islet1/2	Mouse	1:200	DHSB
MMP9	Goat	1:1000	Merck-Millipore
MNR1/2	Mouse	1:100	DHSB
NeuN	Mouse	1:1000	Merck-Millipore
PKCdelta	Mouse	1:1500	Abcam
Tuj1	Mouse	1:1000	DHSB

vAChT	Rabbit	1:1000	Synaptic Systems
-------	--------	--------	------------------

- **Secondary antibodies**

Target Species	Host Species	Conjugate (Alexa)	Working Dilution	Company
Mouse	Donkey	488, 555, 647	1:1000	Life Technologies
Rabbit	Donkey	488, 555, 647	1:1000	Life Technologies
Chicken	Donkey	488, 555, 647	1:1000	Life Technologies
Goat	Donkey	488, 555, 647	1:1000	Life Technologies
Mouse IgG2a	Donkey	488, 555, 647	1:1000	Life Technologies
Mouse IgG2b	Donkey	488, 555, 647	1:1000	Life Technologies
Mouse IgG1	Donkey	405	1:500	Life Technologies
Rabbit	Donkey	405	1:500	Life Technologies
Rabbit	Donkey	700	1:15000	Licor
Mouse	Donkey	800	1:15000	Licor

3.3 Enzymes

Enzyme	Supplier
Phusion (thermostable polymerase)	Thermo Scientific
Restriction enzymes	Thermo Scientific
T4 DNA ligase	Thermo Scientific
Dream Taq Polymerase	Thermo Scientific

Shrimp alkaline phosphatase	Thermo Scientific
Protein Nucleotide Kinase	Thermo Scientific

3.4 Chemicals and reagents

Name	Supplier	Catalogue Number
Acetic Acid	Roth	6755.1
Agar-Agar	Roth	5210.4
Agarose	Roth	3810.4
Ampicillin Natriumsalt	Applichem	A0839.0010
Anode Buffer	Roth	L510.1
Blocking reagent Roti-Block	Roth	A151.2
Bovine serum albumin (BSA)	Roth	0163.4
Calcium Chloride x 2H ₂ O	Roth	5239.1
Calcium Chlorid-Dihydrate	Roth	T885
Cathode Buffer	Roth	L511.1
Chloroform	Roth	3313.1
D+ Glucose Anhydrous	Roth	X997
D (+) Sucrose	Roth	4621.2
DABCO(1,4-diazabicyclo-[2,2,2]-octane)	Roth	718.1
Diethylpyrocarbonate (DEPC)	Roth	K028.2
DMEM	Merck	FG0445
DMEM	Gibco	10566-032
Dimethylsulfoxide (DMSO)	Roth	A994.2

Dodecylsulfate Na-salt (SDS)	Serva	20765
DNA Ladder 100bp plus	Thermo Scientific	SM0321
DNA Ladder 1kb plus	Thermo Scientific	SM1333
DTT	Sigma	10197777001
dNTP Mix	Thermo Scientific	18427013
Ethanol 100%	Applichem	A4230.2500
Ethanol 99%	Chemie Vertrieb Hannover	603/002-00-5
Ethylenediaminetetraacetate (EDTA)	Applichem	A1103.1000
EGTA	Sigma	E3889-10G
Foetal Bovine Serum	GIBCO	10270
Glutamine	Sigma	G8540-100G
Glycerol	Roth	3783.2
Glycine	Roth	3908.1
HEPES	Roth	HN77.5
Isopropanol	Roth	CP41.4
Kallium Chloride	Roth	6781
L-15 medium	SAFC Biosciences	SLBC6273
Lysogeny Broth (LB) Agar	Roth	X965.3
Lysogeny Broth (LB) Medium	Roth	X964.3
Magnesium Acetate	Sigma	M5661-250G
Magnesium Chloride- Hexahydrate	Roth	2189.1
Magnesium Chloride-Solution	Sigma	M1028-100ML
MES Running Buffer	Novex	NP0002

Methanol	Roth	4627
Methyl Sulphonate	Sigma	471356
Mg-ATP	Sigma	A9187-1G
MOPS Running Buffer	Novex	NP0001
Mowiol 4-88	Roth	0713.1
Na3-GTP	Sigma	G8877-1MG
Nu-PAGE Bis-Tris Gel 4-12 %	Thermo Scientific	NW04122BOX
Nonident NP40 substitute	Sigma	74385
OCT embedding medium	Tissue-Tek	25608-930
PAGE Ruler	Thermo Scientific	26616
PAGE Ruler INR	Thermo Scientific	26635
Paraformaldehyde	Roth	0335.3
PBS pH 7.2 10X	Gibco	70013-065
PBS pH 7.2	Gibco	20012-019
Penicillin-Streptomycin	Gibco	15070063
Phosphatase Inhibitor Cocktail	Sigma	P5726
Picric Acid	Sigma	P6744-1GA
Potassium Hydroxide	Roth	6751.1
Protease Inhibitor Cocktail	Sigma	P1860
Proteinase K	Applichem	A7932.0100
RNAse Away	MBP	7005-11
Roti-Block	Roth	A151.2
Roti-Load	Roth	K929
Sodium Chloride	Roth	9265.2

Sodium dodecyl sulphate	Roth	0183.3
Sodium Hydrogen Carbonate	Roth	8551
Sodium Hydroxide	Roth	T135.1
Sucrose	Roth	4621.3
Tris-HCl	Roth	9090.3
Tris Ultra	Roth	5429.3
Triton X-100	Roth	3051.2
Trypsin 0.05%	Gibco	15400054
Tween 20	Sigma	P1379
Venno FF super	Menno	5019-ghs
Qiazol	Qiagen	79306
β -Mercaptoethanol	Roth	4227.1

3.5 Plasmids

Vector	Supplier
Hb9-Cre	(Lee, Jurata et al. 2004)
pCAGEN	Addgene Inc.
pCAGGS::T2TP	(Sato, Kasai et al. 2007)
pCRII-TOPO	Invitrogen GmbH
pGK-Cre	Addgene Inc.
pMES	Dr. Till Marquardt

3.6 Kits

Kit	Supplier
PrimeScript 1st strand cDNA synthesis Kit	Takara Bio Inc.
GeneJET Gel Extraction Kit	Thermo Scientific
pCR-IITOPPO TA Cloning Kit	Invitrogen GmbH
GeneJET Plasmid Miniprep Kit	Thermo Scientific
Qiagen Maxiprep Kit	Qiagen GmbH

3.7 Primers

Construct (Mus)	Primers (5'-3'); Forward (F); Reverse (R)
HA-NFATc4 full length	F: CTCTAGACATGTACCCATACGATGTTCCAGA TTACGCTGGGGCCGCAAGCTGCGAGGATGA R: GCGCGGATATCGCGCGTCAGGCAGGAGGCTCTTCT
HA-NFATc4 dominant negative (DN)	F: GCTCTAGACCATGTATCCATATGATGTTCCAG ATTATGCTGGGGCCGCAAGCTGCGAGGATG R: GGCTCACGAGGTCTGGCGGGTCAGGCGTGGGAGAGATG
HA-NFATc4 constitutively active (CA)	F: GCTCTAGACCATGTATCCATATGATGTTC CAGATTATGCTGTGGGTGCTCCACCAAC R: GGGCGATATCGCGCTCAGGCAGGAGGCTCTTCTCCAGGAC

3.8 Software

Name	Application	Developer
Adobe Illustrator	Vector Construction	Adobe Inc.
Adobe Photoshop	Image Processing	Adobe Inc.
ApE	Molecular cloning tools	M. Wayne Davis
Axograph	Electrophysiological Recording Analysis	Dr. John Clements
GraphPad Prism	Data Analysis and Representation	GraphPad
Image J	Image Processing	National Institutes of Health
Microsoft Office	Documentation and Presentation	Microsoft
pCLAMP	Patch Clamp Recording Acquisition	Molecular Devices
ZEN2012	Confocal Image Acquisition	Zeiss

3.9 Animal Models for experiments

- ✓ Chick: Fertilized chick eggs (*Lohmann LSL* strain) were purchased from Geflügelzucht-Horstmann GmbH. According to the German “Tierschutzgesetz” (BGBl. I S. 1206, 1313), *in-ovo* chick experiments do not require animal protocol permission.

- ✓ Mouse: The experiments were performed on mice using procedures approved by the animal care committee of the Bezirksregierung Braunschweig (permit no. G42/08 and no. T9.07), Germany. Animals were fed *ad libitum* and were maintained on a 12-hour light-dark cycle by the animal facility of the ENI-Göttingen under the control of a veterinarian.

3.10 Equipment

1. Axon Instruments Digidata 1322A digitizer
2. Axon Instruments MultiClamp 700B Amplifier
3. Bio-Rad Sub-Cell GT Electrophoresis Chamber
4. BTX-Harvard Apparatus ECM 830 Square Wave Electroporation System
5. Consort EV 231 Power Supply
6. Custom built Faraday Cage
7. Custom built Micromanipulators
8. Eppendorf Centrifuge 5417R
9. Eppendorf Centrifuge 5424
10. Eppendorf Centrifuge 5810 R
11. Eppendorf Mastercycler epgradient S
12. Eppendorf Research Plus pipettes
13. Eppendorf Thermostat Plus
14. Harvard Apparatus Genetrode Kit Gold Plate Model 512
15. Intas Gel Imager
16. Leica CM1850 UV Cryostat
17. Leica S6 E Greenough stereomicroscope
18. Leica VT1200 S vibratome
19. Licor Odyssey Clx Imaging System
20. NanoDrop 2000
21. Narishige Japan PN-30 Magnetic Glass Microelectrode Horizontal Puller
22. New Brunswick Galaxy 170 R CO₂ Incubator
23. Olympus SZX16 Wide Zoom Versatile Stereo Microscope
24. Schott KL 1500 LCD halogen light source
25. Stuart End-to-End Rotator SB3 1.5 ml and 50 ml
26. Sutter Instruments P-97 Micropipette Puller
27. Thermo Scientific Heracell CO₂ Incubator 240
28. Thermo Scientific Herasafe Microbiological Safety Cabinet
29. Thermo Scientific XCell SureLock™ Mini-Cell Electrophoresis System
30. X-Cite 120 LED Fluorescence Microscope Light Source
31. Zeiss LSM 710

IV Methods

4.1 Molecular Cloning

4.1.1 RNA Extraction and Synthesis of cDNA library

Necessary reagents and solutions:

1. Tissue
2. QIAzol lysis reagent
3. Chloroform
4. Isopropanol
5. 75% ethanol
6. DEPC-water (0.1% DEPC in ddH₂O, mix and let it sit at room temperature overnight. Then autoclave)

Total RNA was isolated from embryonic and adult mouse brain by single-step method of RNA isolation by acid guanidinium thiocyanate-phenol-chloroform extraction (Chomczynski and Sacchi 1987). Tissue was homogenized in 1 ml of QIAzol lysis reagent per 50 mg of tissue in a 1.5 ml tube. Homogenized sample was then incubated for 5 minutes at 30°C. For 1 ml of QIAzol 0.2 ml of Chloroform was then added to the sample. Tubes were shaken vigorously for 15 seconds and incubated again for 3 minutes at 30°C. Sample was then centrifuged at 12000 x g for 15 minutes at 4°C. Due to centrifugation, phase separation takes place (Fig. 4.1.1). The aqueous phase was transferred to a fresh 1.5 ml tube. 0.5 ml of isopropyl alcohol per 1 ml of QIAzol was added to the aqueous phase and incubated at 30°C for 10 minutes. After incubation, it was again centrifuged at 12,000 x g for 10 minutes at 4°C. After centrifugation, RNA is concentrated as pellet, so supernatant was removed and pellet was washed with 75% ethanol (1 ml for 1ml of QIAzol). After washing and removal of alcohol by centrifugation, pellet was allowed to dry for 5-10 minutes. The pellet was then dissolved in 100 µl of DEPC-water (RNAase free sterile water) to get a stock of total RNA which could be stored at -80°C for further usage.

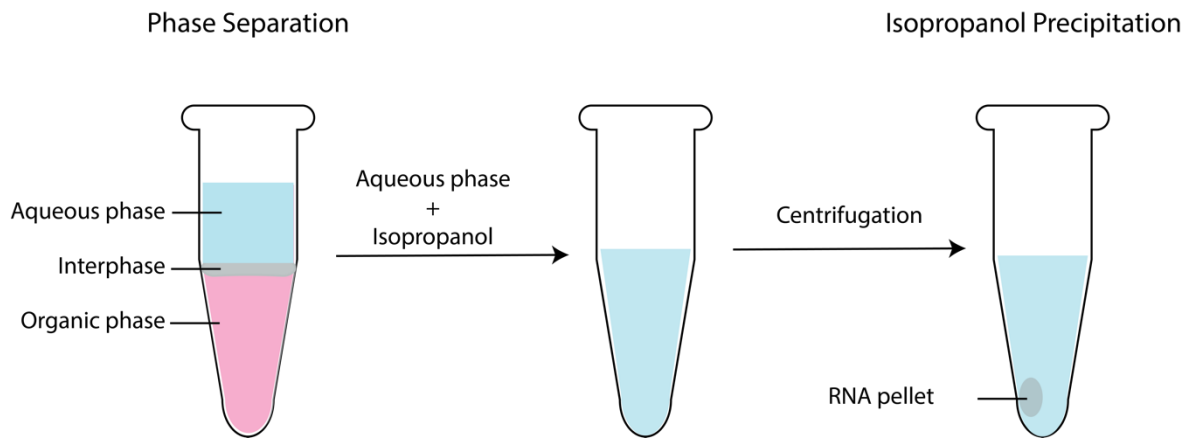


Fig.4.1.1: Phase separation and RNA isolation

The homogenate is separated into 3 phases: an aqueous phase, an organic phase and an intermediate phase. In the aqueous phase, only RNA is present, and DNA and protein are present in the intermediate phase and the lower phase. The aqueous phase is collected, and RNA is precipitated by adding isopropanol followed by centrifugation.

cDNA library was created by PrimeScript 1st-strand cDNA Synthesis Kit from TaKaRa as per manufacturer's protocol using Oligo dT primers and 2 µl of total RNA. The end product, cDNA, was further diluted 5 times and stored at -80° for further usage.

4.1.2 Polymerase Chain Reaction (PCR)

Necessary reagents and solutions:

1. Sterile water
2. 100 mM stock of forward and reverse primers
3. Phusion enzyme and its buffer
4. DMSO
5. dNTPs
6. cDNA or template DNA

PCRs were performed as per instructions from the Thermo-Scientific user guide for the Phusion DNA polymerase enzyme. The pipetting and cycling protocol is tabulated below:

<u>Component</u>	<u>3 X 20 µl Reaction</u>	<u>Final Concentration</u>
Sterile Water	35.4 µl	
5X Phusion HF Buffer	12 µl	1X
10 mM dNTPs	1.2 µl	200 µM
DMSO	1.8 µl	3 %
10 µM Forward Primer	3 µl	0.5 µM
10 µM Reverse Primer	3 µl	0.5 µM
Template DNA / cDNA (0.5 µg/µl)	3 µl	0.025 µg/µl
Phusion DNA polymerase	0.6 µl	0.02 U/µl

Table 4.1.2.a: Pipetting Protocol

<u>Cycle Step</u>	<u>Temperature</u>	<u>Time</u>	<u>Number of Cycles</u>
Initial Denaturation	94°C	3 min.	1
Denaturation	94°C	1 min.	35
Annealing	67°C	1 min.	35
Extension	68°C	50 seconds/Kb	35
Final Extension	68°C	5 min.	1

Table 4.1.2.b: Cycling Protocol

The PCR was carried out in a Mastercycler eppgradient (Eppendorf AG)

4.1.3 Agarose Gel Electrophoresis

Necessary reagents and solutions:

1. TAE buffer: 40 mM Tris; 1mM EDTA adjust pH 7.5 with glacial acetic acid
2. EtBr
3. DNA molecular weight marker

PCR products or mixed populations of DNA were always separated in agarose gels by isoelectric focussing (Takahashi, Ogino et al. 1969). 1 % (w/v) of agarose, dissolved in 1 X TAE buffer with 3% (v/V) EtBr (1% w/V stock) was used to cast agarose gels. DNA samples were mixed with loading dye before loading onto the gel-wells. The molecular weight reference markers were used to determine the size of DNA bands, hence at least one well of the gel is occupied by the DNA ladder (1 Kb plus or 100 bp plus, Thermo-Scientific). 1 X TAE buffer was also used as running buffer. The voltage used for electrophoresis was 5-7 V/cm. The DNA bands were observed and photographed using Gel Jet Imager (Intas GmbH).

4.1.4 PCR Product / DNA purification after Electrophoresis

Necessary reagents and solutions:

1. Thermo Scientific Gel Extraction Kit / PCR purification Kit

After sufficient segregation, the DNA bands were precisely cut out from the gel with the help of clean & sharp blade and collected in 1.5 ml tubes. The weight of each gel sample was determined and the DNA was purified using Thermo-Scientific Gel Extraction Kit as per manufacturer's protocol which is based on scientific discoveries (Vogelstein and Gillespie 1979, Vogelstein 1987, Boom, Sol et al. 1990).

4.1.5 TOPO Cloning of PCR Products

Necessary reagents and solutions:

1. pCRII-TOPO TA-cloning kit

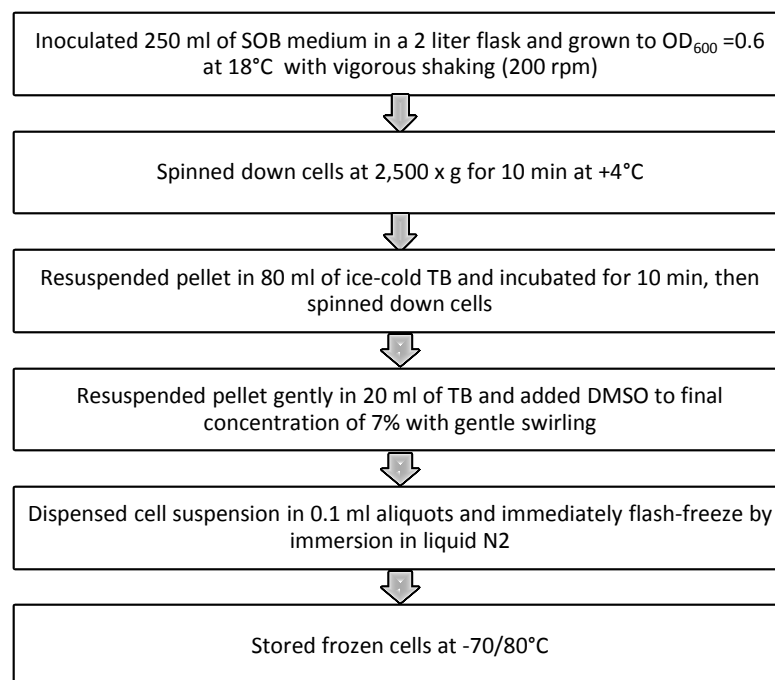
Purified PCR products were sub-cloned into pCRII-TOPO vector using the TA-Cloning Kit according to the manufacturer's protocol (Thermo-Scientific). TA-Cloning in pCRII-TOPO vector requires A-overhang. Hence the blunt PCR products created using Phusion (proofreading polymerase) were incubated with Taq polymerase to add 3' A-overhangs and re-purified before setting up a TOPO-cloning reaction.

4.1.6 Preparation of chemically competent *E. coli* cells

Necessary reagents and solutions:

1. SOB media: 0.5% (w/v) yeast extract; 2%(w/v) tryptone; 10 mM NaCl; 2.5 Mm KCl; 20 mM MgSO₄
2. Terrific Broth (TB)
3. DMSO

Competent *E. coli* cells of the Top10 strain (Invitrogen GmbH) were prepared according to the protocol demonstrated as flowchart below (Inoue, Nojima et al. 1990) and checked for competence by a test transformation with the pBluescript KS (-) plasmid. The cells were stored at -80°C until use.



4.1.7 Transformation of chemically competent *E. coli* cells

Necessary reagents and solutions:

1. Aliquot of competent cells
2. SOB media
3. Antibiotic containing agar plates

Transformation of *E. coli* was performed by simple and efficient method (SEM) (Inoue, Nojima et al. 1990) by adding 50 µl of competent cells (thawed on ice) to a maximum amount of 10 µl (50 ng) of DNA solution (after TOPO cloning or Ligation). The cells were incubated on ice for 30 min and heat shocked at 42°C for 1 min. Afterwards they were chilled on ice for 2 min and 0.5 ml SOC medium was added. Subsequently they were incubated for 1 h on a 37°C shaker and plated on an agar plate containing the appropriate selection antibiotic. *E. coli* cells were grown over night at 37°C in an incubator.

4.1.8 Plasmid isolation

Necessary reagents and solutions:

1. Thermo-Scientific Miniprep Kit / Qiagen Maxi-prep Kit
2. Isopropanol

A rapid alkaline extraction procedure was used for plasmid isolation (Birnboim and Doly 1979). Bacterial cells were grown from single colonies. Small-scale plasmid isolation was performed using 5 ml of an *E. coli* overnight culture using the Thermo-Scientific Miniprep kit according to the manufacturer's instructions. Finally, the DNA was eluted in 40 µl of elution buffer.

For higher amount and purer plasmid preparations, 150 ml of *E. coli* liquid culture was grown over night. Plasmid DNA was extracted with the Qiagen Plasmid Maxi kit according to the manufacturer's protocol. Concentration of nucleic acids was determined based on UV absorption using a Nanodrop ND-1000 UV-Vis spectrophotometer (Peglab Biotechnologie GmbH).

After successful plasmid isolation, the prescribed amount of plasmid with appropriate primers were sent for sequencing to Seqlab.

4.1.9 Restriction Digestions and Ligation

Necessary reagents and solutions:

1. Restriction enzymes and relevant buffers
2. T4 Ligase and T4 Buffer
3. Sterile water

For analytical DNA digestions 2 µl (app. 500 ng) of DNA were incubated with 2 units (one unit cleaves 1 µg of DNA per hour) of the appropriate restriction enzyme. The incubation was carried out in the reaction buffer and at the temperature recommended by the manufacturer for 1 h.

For preparative digestions 10 µg of DNA were incubated with 10 units of the restriction enzyme for at least three hours at the appropriate reaction temperature. If a double digestion was not possible according to the manufacturer's recommendations, the DNA was ethanol precipitated and suspended in nuclease free water prior to the second restriction digest.

To prevent religation of vector DNA leading to false positive colonies, it was treated with shrimp alkaline phosphatase after restriction digestion. For this, 0.5 units of the phosphatase enzyme were added to the restriction digest per 10 µg of DNA. Then the reaction mixture was incubated for 15 min at 37°C.

Vector and insert DNA concentration were determined and ligation reaction was prepared with molar vector to insert concentrations of 1:3 to a total volume of 8 µl. Subsequently 1 µl each of T4 DNA ligase and T4 10X buffer were added. The reaction was incubated at 22°C for sticky end ligations or at 16°C for blunt end ligations for 2 h. After 2 hours the ligation mixture was transformed as described before.

4.1.10 Cryopreservation and recovery of *E. coli* clones

Necessary reagents and solutions:

1. 100% Glycerol
2. Overnight plasmid containing *E. coli* culture

1 ml of an *E. coli* overnight culture was mixed with 0.25 ml of 100% glycerol in 1.5 ml Eppendorf tube to create a 20% glycerol stock of the bacterial clone generated. Subsequently the sample was stored at -80°C until reuse. In order to regrow the culture approximately 20 µl of the frozen stock were grown for 12 h in 5 ml LB medium for mini-prep DNA purification or for 16 h in 200 ml LB medium for maxi-prep purification.

4.1.11 Ethanol Precipitation of DNA

Necessary reagents and solutions:

1. 3M sodium acetate (pH 5.2)
2. Cold 100% Ethanol
3. 70% Ethanol
4. Sterile water or Elution buffer

This is a simple and useful method to clean DNA from impure samples or to change to concentration of DNA from lower to higher. For this the total volume of DNA sample is measured and 1/10th volume of 3M sodium acetate (pH 5.2) is added so that final concentration of sodium acetate is 0.3M. After mixing it well, 2.5 volumes of chilled 100% ethanol is added and mixed well. The complete mixture is incubated at -20°C for more than 20 minutes and centrifuged at maximum speed for 15 minutes. The supernatant is decanted and pellet is washed with 70% ethanol. After air-drying the pellet for 10 minutes, pellet is suspended in desired volume of TE buffer or sterile water.

4.2 Cell Culture

Cell culture protocols were adapted from widely used protocols and necessary precautions were taken based on published literatures (Hayflick and Moorhead 1961)

Sources:

1. Freshney, R. Ian. (1994) Culture of Animal Cells, Third Edition. Wiley Publishing, New York.
2. Gey, G.O., Coffman, W.D., Kubicek, M.T. (1952) Tissue culture studies of the proliferative capacity of cervical carcinoma and normal epithelium. Cancer Research, 12:364-365.
3. Hayflick, L., Moorhead, P.S. (1961) The serial cultivation of human diploid cell strains. Exp. Cell Res. 25:585-621.
4. Sweeney, Catherine. BS Biology, SLCC-CS Biotechnology
5. Warmke, Timothy. SLCC-AAS Biotechnology

4.2.1 Thawing the cells

Necessary reagents and solutions:

1. Hela Culture Media: 10% FBS; 1% Pen-Strep; in DMEM-High Glucose
2. PBS

When vial containing cells are removed from either the liquid Nitrogen freezer, it should be thawed quickly. In order to prevent damage to the cells, the Hela culture media was warmed to 37°C in a 15 mL falcon tube. The cells were thawed at 37°C in the water bath until about ½ of the sample has melted. The vial with ethanol and the warm media was added dropwise to the thawed cells. The diluted cells in fresh media were then centrifuged at 200 rpm for 10 minutes. The supernatant after centrifugation was carefully decanted and the cell pellet was re-suspended in fresh Hela media. This suspension of cells was then used seeding new flasks (labelled with passage number and date) for Hela cell culture.

4.2.2 Passaging and Maintaining a Culture

Necessary reagents and solutions:

1. Hela Culture Media: 10% FBS; 1% Pen-Strep; in DMEM-High Glucose
2. PBS

Cells were passaged when they reach 70 – 90% confluency. In order to passage these cells, old media was removed and flask was rinsed with 5 ml PBS (0.1M) two times using vacuum filtration. For T-75 flask I added 2 ml of 0.05% trypsin solution and incubate 3 minutes at 37°C to detach the adherent cells. The trypsin reaction was then quenched by adding 8 ml of warm media. This media was then sucked up and dispensed a few times to detach and collect all the cells from flask. The whole cell suspension was then transferred in a 15 ml falcon tube and centrifuged at 200 rpm for 5 minutes. After centrifugation, supernatant was decanted and the cell pellet was suspended in 0.9 ml of media. 100 µl of this suspension was then added to 10 ml of fresh media in a new T-75 flask as seed. For accurate seeding, cells were first counted and then seeded according to the required cell density (Table 4.2.3). The new passage number and date was noted. The new flask was swirled horizontally to evenly distribute the cells and incubated in the incubator.

	Surface Area (cm ²)	Seeding Density	Cells at Confluency ¹	Versene (ml of 0.05% EDTA)	Trypsin (ml of 0.05% trypsin, 0.53 mM EDTA)	Growth Medium (ml)
Dishes						
35mm	9	0.3 x 10 ⁶	1.2 x 10 ⁶	1	1	2
60mm	21	0.8 x 10 ⁶	3.2 x 10 ⁶	3	2	3
100mm	55	2.2 x 10 ⁶	8.8 x 10 ⁶	5	3	10
150mm	152	5.0 x 10 ⁶	20.0 x 10 ⁶	10	8	20
Culture Plates						
6-well	9	0.3 x 10 ⁶	1.2 x 10 ⁶	2	2	3 - 5
12-well	4	0.1 x 10 ⁶	0.4 x 10 ⁶	1	1	1 - 2
24-well	2	0.05 x 10 ⁶	0.2 x 10 ⁶	0.5	0.5	0.5 - 1.0
Flasks						
T-25	25	0.7 x 10 ⁶	2.8 x 10 ⁶	3	3	3 - 5
T-75	75	2.1 x 10 ⁶	8.4 x 10 ⁶	5	5	8 - 15
T-160	162	4.6 x 10 ⁶	18.4 x 10 ⁶	10	10	15 - 30

Table 4.2.3 Seeding Densities for Hela Cells (adapted from cell culture protocols Gibco)

4.2.3 Freezing Cells

Necessary reagents and solutions:

1. Freezing Media: 20% FBS; 10% DMSO; in DMEM-High Glucose
2. PBS

Cells were frozen when at low passage number (P3 and P4), healthy and confluent. To freeze the cells were grown in the large 75 cm² culture flasks. When the cells were ~80 – 90% confluent, freezing protocol was followed as follows:

- Warmed PBS (-), appropriate media and freezing media in water bath.
- Pre-labelled 18X 2 ml cryovials with the following information:
 - Cell line
 - Passage number
 - Date
- Prepared a styrofoam-holder (cooling box with tube holders) filled with isopropanol to store at -80°C.
- Removed the media from the flask using suction.
- Rinsed with ~ 8 mL of PBS twice.
- Added about 1.5 mL of trypsin (0.05%) and placed the flask in the incubator for 3 minutes until they detach.
- The trypsin reaction was quenched by adding 8 ml of warm media and collected all the cells from flask into a 15 ml falcon tube.
- Centrifuged at 200 rpm for 5 minutes, then supernatant was discarded completely leaving the large pellet of cells behind.
- 19 ml of freezing media was then added to the pellet and cells were dispensed several times to create a homogenous suspension of cells.
- Added 1mL of the suspended cells in freezing media to each of the labelled cryovials. Placed the cap on tightly.
- Placed each tube in the styrofoam holder and closed the lid tightly.
- The complete styrofoam holder with 18 tubes was placed in -80°C refrigerator for 24 hours.
- After 24 hours, the frozen cryovials were removed from styrofoam holder and placed in boxes in liquid nitrogen tank.

4.2.4 Transfection

Necessary reagents and solutions:

1. Lipofectamine 2000
2. DMEM serum free media
3. Optimem
4. Plasmids

Lipofectamine 2000 was used as per manufacturer's protocol to transfect cells in 6 well plates. Cells were grown to 80% confluency in a 6 well plate. Transfections were done in the laminar flow. 2 hours prior to transfection the growth media from each of the wells was removed and replaced with serum free DMEM media. For each well 1 tube with 100 μ l of Optimem was aliquoted in 1.5 ml tubes. 2 μ g of desired plasmid for each well was added in respectively labelled tube with Optimem. In a separate tube 100 x 6 (no. of wells) Optimem was taken to dilute 6 μ l/well of Lipofectamine i.e. 24 μ l Lipofectamine in 600 μ l of Optimem media. Diluted plasmid and diluted Lipofectamine were incubated at room temperature for 5 minutes and then 106 μ l of diluted Lipofectamine was added into each tube containing plasmid. The Lipofectamine-DNA mixture was further incubated for minimum of 25 minutes before finally adding into each well dropwise. The 6 well plate was then placed in incubator. After 6-8 hours the serum free media was replaced with complete Hela media and cells were allowed to grow and express protein for another 2 days.

4.2.5 Cell lysis for protein extraction

Necessary reagents and solutions:

1. Ice cold PBS
2. Lysis Buffer: 0.32M Sucrose, 3mM CaCl₂, 2mM MgOAc, 0.1 mM EDTA, 10 mM DTT, 0.5% NP-40 Substitute
3. Protease Inhibitor Cocktail
4. Phosphatase Inhibitor Cocktail

The transfected 6-well plates lysed for protein extraction after 60 hours of transfection. The 6-well plate was kept on cooling gel pack. Media was sucked out with the help of vacuum filtration and 1 ml of ice-cold PBS was added in each well for washing of the cells. PBS was also removed with vacuum-filtration. After 2 more such washings, 60-70 µl of lysis buffer (freshly supplemented with protease inhibitors) was added into each well. Cells from each well scraped and collected in separate 1.5 ml labelled tubes and kept immediately in tube mini-coolers. After careful collection, all tubes containing cell lysates were then kept on ice for 20 minutes for complete lysis of cells. After 20 minutes, all samples were centrifuged at 12000 rpm for 10 minutes at 4°C. After centrifugation, cell debris is seen as white pellet in the bottom while the whole cell protein lysate is present in clear supernatant. The supernatant is then carefully transferred to new tubes for further analysis or experiment. A small aliquot of this lysate is saved and boiled for analysis.

4.3 Co-immunoprecipitation

Necessary reagents and solutions:

1. Tris Buffer Saline (TBS): 50 mM Tris, 150 mM NaCl, pH 7.5
2. TBS-T: TBS with 0.05% Tween-20
3. Lysis buffer
4. Anti-HA magnetic beads
5. Elution Buffer (Thermo Scientific) pH 2.3 or 0.1M Glycine pH 2.0

The Co-IP experiments were carried out using commercially available Pierce anti-HA magnetic beads from Thermo-Scientific, since HA-tagged proteins were used as a bait for pull down. Manufacturer's protocol was carefully followed with slight modifications. The beads were mixed well before use.

15 µl of anti HA beads were placed in a low protein bind 1.5 ml tube for each sample of cell lysate (protein). To the beads 85 µl of 0.05% TBS-T was added and mixed. Tubes were placed in magnetic stand for 30 minutes and the supernatant was removed. Then tubes were removed from magnetic stand and 100 µl of lysis buffer used for lysis of cells was added to the beads. After mixing, again the buffer was magnetically separated from beads and supernatant was discarded. After one more such washing, 70-90 µl of cell lysate containing HA tagged protein was added to the beads and incubated on end-over-end rotator for 3 hours at 4°C. After 3 hours, beads were separated magnetically and unbound sample lysate was collected in separate tube for analysis. To the beads, 200 µl of TBS-T was added for washing. Washing step was repeated and TBS-T was discarded completely with the help of pipette.

For elution of proteins bound to the beads, acidic elution protocol from the manufacturer was used. 15 µl of elution buffer (pH 2.3), was added to the beads and after mixing it was incubated at 37°C for 10 minutes. The supernatant was collected in fresh tubes after magnetic separation and another round of elution with additional 15 µl of buffer was carried out. Final volume of 30 µl of eluted protein was collected and to this 10 µl of 4X Roti-Load buffer from Roth was added and mixed. This final mixture was boiled at 95°C for 5-6 minutes.

After boiling the protein was ready for SDS-PAGE or for short term storage at -20°C.

Alternate elution of protein was done by direct boiling of beads in 40 μ l of 1.5X Roti-Load buffer. However, this protocol was used only when the antibody bands did not interfere with the eluted protein bands.

4.4 SDS-PAGE

Necessary reagents and solutions:

1. NuPAGE 4-12% Bis-Tris Gradient Gels OR self-casted gels
2. MES or MOPS Running Buffer
3. PAGE Ruler

Equal amounts of protein were loaded in each well. For Co-IP experiments, eluted sample were always loaded together with the whole cell lysate aliquots for protein expression reference. The running buffer was supplied with NuPage anti-oxidant in the inner tank. After loading the samples and the PAGE ruler in the gel wells, a constant voltage of 120 V was applied for 2 hours to the SDS-PAGE apparatus (Figure 4.4).



Fig.4.4: Apparatus used for SDS-PAGE

The apparatus for SDS-PAGE shows the tank in which a precast gel is placed vertically and after loading the protein sample, they are size-resolved with help of constant voltage using electrophoresis power supply

4.5 Western Blot

4.5.1 Wet Transfer

Necessary reagents and solutions:

1. Transfer Buffer: 25mM Tris; 190mM Glycine; 20% Methanol

The gel after PAGE was carefully cut-out and placed in transfer buffer for 10 minutes. A nitrocellulose membrane was cut out with same dimensions as the gel and also incubated in transfer buffer for 10 minutes. After incubation, a sandwich with gel and membrane was prepared as shown in figure 4.5.1. This sandwich was then kept in wet transfer tank filled with transfer buffer and the protein was transferred on to the membrane by electrical force overnight at 15 mA current.

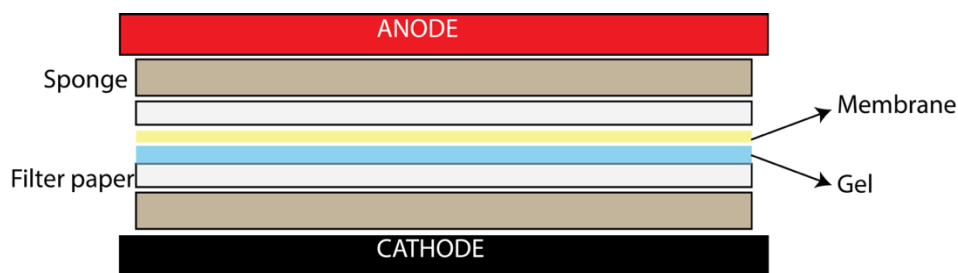


Fig.4.5.1: Sandwich for Western Blot

4.5.2 Semi-dry Transfer

Necessary reagents and solutions:

1. Anode Buffer
2. Cathode Buffer

The gel after PAGE was carefully cut-out and placed in anode buffer for 10 minutes. A nitrocellulose membrane was cut out with same dimensions as the gel and also incubated in anode buffer for 10 minutes. Two thick filter papers (0.5 cm) were also incubated in anode and cathode buffers to support the membrane and gel respectively. Finally, a sandwich was prepared as shown in figure 4.5.1 and placed in semi-dry transfer chamber. Proteins were transferred to membrane by applying constant current of 120 mA for 2 hours.

4.5.3 Protein Detection by Antibody Staining

Necessary reagents and solutions:

1. Blocking Buffer in TBS
2. Primary Antibodies
3. Secondary Antibodies from Licor
4. TBS-T

The blotted membrane after transfer was rinsed with TBS and blocked in blocking buffer for 1 hour. Post blocking, primary antibodies were added in blocking buffer and membrane was incubated in antibodies at 4°C overnight. Following day, the membrane was washed with TBS-T for 10 minutes three times. Membrane was then incubated in secondary antibodies for 1 hour and again washed 3 times. The membrane was then imaged under Licor imaging system to detect the protein bands.

4.6 Chick Experiments

In the field of developmental biology, chick embryos (*Gallus gallus domesticus*) are a classical model for studying embryogenesis and neurogenesis, because they are easy to access and manipulate. Moreover, the chick is a precocial species which show early neuromuscular maturity and mobility from the time of hatching. Due to lower generation time of chick and easy visualization of chick embryos. It was chosen as model system.

4.6.1 The long-term expression vector utilizing *Tol2* system

In order to ensure high-level transgene expression within embryonic chick spinal cord postembryonic day 9 a novel vector system was created in our lab. This system was based on the *tol2* transposase, which stably integrates DNA fragments into the chicken genome (Kawakami and Shima 1999). The *tol2* transposase system requires specific recognition sites flanking the DNA fragment to be integrated into the genome, therefore in our vector system the *tol2* sites are flanking the entire expression cassette. The expression cassette consists of pCAGGS followed by lox-stop-loxP site, multiple cloning site(MCS), and IRES-eGFP (Fig.4.6.1), and is referred as *tol2*-pCAGEN from here on. The transposase is introduced into the cells by co-electroporation of the transposase gene bearing plasmid (pCAGGS-T2TP) driving transposase expression in all cell types. To maintain expression specificity within motor neurons together with a high expression level the strong unspecific CAGGS promoter derived from the pCAGEN vector has been combined with a lox-STOP-lox cassette consisting of two loxP recognition sites for the CRE recombinase flanking three beta-globin polyadenylation signals (Hoess, Ziese et al. 1982). Hb9:Cre (gift from Samuel Pfaff) was used in combination with the *tol2*-pCAGEN to express the desired gene specifically in MNs.

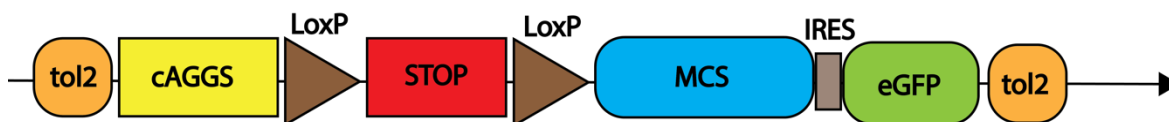
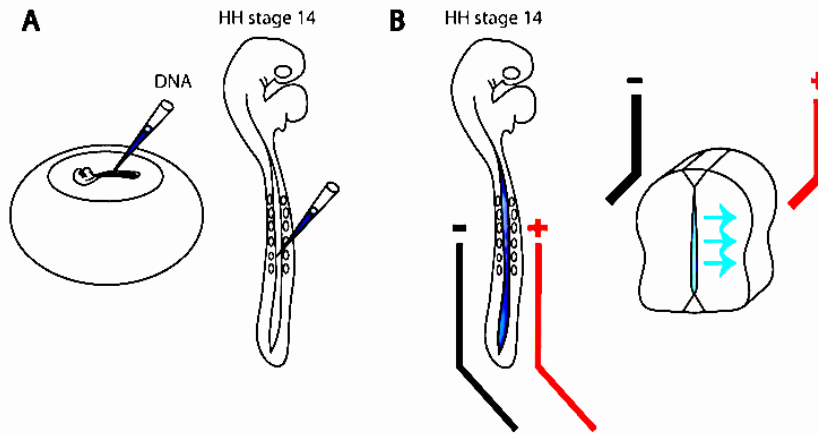


Figure 4.6.1: Stable Expression Vector Outline (*tol2*-pCAGEN)

4.6.2 *In-ovo* Injection and Electroporation of Chick Neural Tube

Fertilized eggs of the Lohmann LSL strain were incubated for 65 h at 37.0°C in the humidity chamber (Hemel-Brutgeräte GmbH) until embryos reached Hamburger–Hamilton (HH) stage 18. A small hole was made in the shell on the side of the air chamber, and then 5 ml albumin was removed from the egg using a syringe. An oval window was made in the eggshell to visualize the embryo (Fig.4.6.2). A micropipette was filled with 0.2% fast green/DNA solutions. The DNA mixture was injected into the neural tube and the embryo was kept moist by adding L-15 medium on top of the vitelline membrane. Unipolar electroporation of the DNA solution was then carried out using ECM 830 electroporator (Harvard Apparatus) and L-Shaped Genetrodes (5 mm in length and 0.5 mm diameter) conducting 25 V pulses (50 ms duration and 200 ms interval). Subsequently, the eggs were sealed and put back to the incubator until desired stages of development were reached.



Adapted from Master Thesis: Özge Demet Özçete

Fig.4.6.2: In-ovo Electroporation of Chick Neural Tube

A: Injection of Chick neural tube with desired DNA solution after making a small window in egg shell.
B: Unipolar electroporation of the injected DNA solution.

4.6.3 Isolation of Chick embryonic spinal cord and sample preparation for IHC

Necessary reagents and solutions:

1. 1X PBS
2. 4% PFA in PB
3. 30% Sucrose in 0.1M PBS

After the embryo reached the desired stage, the neural tube/spinal cord of embryos were dissected and fixed in 20 ml of 4% PFA solution for 1.5-5 hours. The PFA was then replaced with PBS to wash the tissue overnight. After washing, fixed tissue was dehydrated using 30ml 30% sucrose solution until the tissue sinks to the bottom. The dehydrated tissue was then embedded in OCT and stored frozen for cryosectioning.

4.6.4 Electrophysiology

Patch-clamp recordings to evaluate the electrophysiological properties of chick MNs were performed in E12.5-E13.5 chick embryos. The embryos were electroporated on embryonic day 2.5 with the long-term expression vector tol2-pCAGEN in combination with the Hb9-Cre and the pCAGGS-T2TP vector.

Necessary reagents and solutions:

1. Artificial Cerebral Spinal Fluid (aCSF) for chick (2 L): Always freshly prepared

NaCl	16.24 g
KCl	0.446 g
NaHCO ₃	2.856 g
Glucose	4.38 g
CaCl ₂ ·2H ₂ O	1.19 g
MgCl ₂ ·6H ₂ O	0.40 g

Dissolved in water to final volume of 2 L and continuously bubbled with carbogen. Final osmolality should be around 320.

2. 2% Agarose in aCSF moulded in tubes: Prepared in advance; stored at 4°C
3. 20% Gelatine in aCSF stored in syringes: Prepared in advance; stored at 4°C
4. Patch Clamp Internal Solution (100 ml) pH 7.3:

This solution should be prepared completely on ice since it contains ATP and GTP. After making small aliquots in 1.5 ml tubes on ice, it should be immediately stored at -80°C. A tabulated composition of internal solution for chick spinal motor neuron patch clamp is mentioned here:

Stock Solution	Mol. Wt.	Per 100 ml	Final Conc.
KOH 8N	56.11	1.5 ml	For adjusting pH to 7.3
MeSO ₃ H	96.11	840 µl	130 mM
KCl	74.55	75 mg	10 mM
MgCl ₂	95.2	19 mg	2 mM
EGTA	380.4	15.2 mg	0.4 mM
CaCl ₂	147	1.47 mg	0.1 mM
HEPES	238.4	238.4 mg	10 mM
Mg-ATP	551.14	137.8 mg	2.5 mM
Na ₃ -GTP	523.2	13.1 mg	0.25 mM

After the solutions were ready, 200 ml of aCSF was cooled to 4-6°C on ice and vibratome was set up for sectioning. The chick eggs were anaesthetized on ice and dissected to isolate lumbar region of spinal cord. This lumbar region of spinal cord was inserted in agarose molds and filled with gelatine to minimize the movement of spinal cord. The mould was quickly moved in cold aCSF in vibratome and 300 µm thick acute slices of lumbar spinal cord were sectioned. The slices were then moved in aCSF at room temperature with continuous carbogen aeration. Acute slices were incubated in aCSF for 30 minutes before patch clamp recordings.

Current clamp recordings were done to record electrophysiological properties of chick Motor-Neurons. Electroporated chick embryos expressed GFP in motor neurons along with desired gene expression, so GFP positive cells were patched under fluorescence microscope.

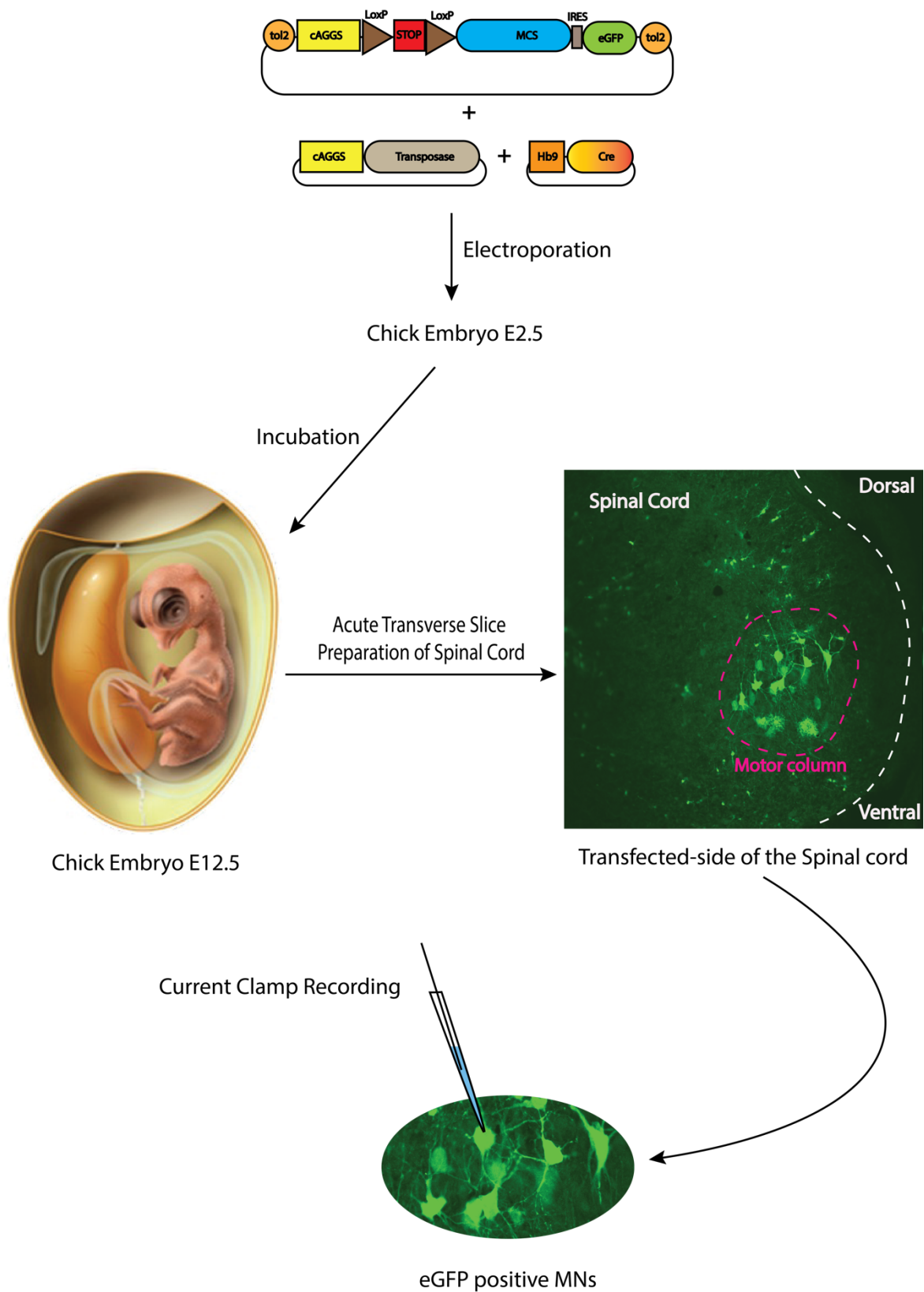


Fig.4.6.4: A Chronological Outline of Patch-Clamp Recordings from Chick Spinal Cord

4.7 Mouse animal experiments

All animal experiments have been carried out in accordance with the animal protection law of Germany and were approved by the district government.

The experimental animals were housed under standard conditions with access to food and water ad libitum.

4.7.1 Pronuclear Injection and Mouse Line Generation

Necessary reagents and solutions:

1. Sterile, Purified DNA (30 µg/ml) in TE Buffer
2. TE Buffer: 5mM Tris (pH 7.5); 0.1 mM EDTA
3. Qiagen Maxi-prep Kit

tol2-pCAGEN- NFAT-dominant negative (NFAT-dn) plasmid was isolated from 200 ml of bacterial culture using Qiagen Maxi-prep Kit. The plasmid was then digested using PshAI and Swal restriction enzymes to remove all the bacterial promoters and resistance genes. The digested plasmid was then isolated via agarose gel electrophoresis followed by gel extraction. For elution of DNA after gel extraction only filter sterile TE buffer was used. The concentration of DNA was then measured with Nanodrop and final concentration of DNA was adjusted to 30ng/µl. 200 µl of this sterile and pure DNA was sent to animal facility of MPI-BPC Göttingen for pronuclear injection and mouse line generation.

After the pups were born, they were tested for presence of desired gene by genotyping. The positive pups, after reaching adult stage, were mated with a desired Cre line of mouse to direct desired gene expression in desired type of cells or tissue. For present study, NFAT-DN positive mouse were bred with Olig-Cre mice and ChAT-Cre carrying transgenic mouse line to express NFAT dominant negative in Olig2 positive or ChAT positive cells in nervous system hence making a Motor-Neuron specific expression of NFAT-dominant negative.

4.7.2 Mouse genotyping

Necessary reagents and solutions:

1. 1M Tris (pH 8)
2. 5M NaCl
3. 0.1M EDTA
4. 10% SDS
5. Proteinase K
6. Lysis Buffer(10ml): 1ml Tris; 60µl NaCl; 20µl EDTA; 50µl SDS; 250µl Prot.K; in water
7. Dream Taq Polymerase
8. Primers

DNA was extracted from tail biopsies by incubation of tail tips in 500 µl lysis buffer overnight at 56°C. The lysate was cleared by centrifugation for 10 min at 14000 rpm and the supernatant was mixed with 500 µl isopropanol. Mixture was then centrifuged for 10 min at 14000 rpm. Subsequently, supernatant was discarded and the DNA pellet was washed with 500 µl 70 % Ethanol. Afterwards the DNA was dried at 37°C and 50 µl of water was added to dissolve the DNA pellet.

The extracted DNA was then used as a template for genotyping. The genotyping was performed via PCR with the reaction components tabulated below:

	1X (µl)	4X (µl)	6X (µl)	7X (µl)	9X (µl)	11X (µl)	13X (µl)
10X Dream Taq Buffer	2.5	10	15	17.5	22.5	27.5	32.5
dNTPs	0.5	2	3	3.5	4.5	5.5	6.5
100 µM Forward Primer	0.5	2	3	3.5	4.5	5.5	6.5
100 µM Reverse Primer	0.5	2	3	3.5	4.5	5.5	6.5
Dream Taq Pol.	0.125	0.5	0.75	0.875	1.125	1.375	1.625
Sterile Water	19.875	79.5	119.25	139.13	178.87	218.62	258.37

For genotyping of Mouse NFAT-DN-Olig-Cre and NFAT-DN ChAT-Cre mice, PCR reactions were set up for:

1. NFAT dominant negative AND
2. Olig-Cre OR ChAT-Cre

4.7.3 Isolation of Mouse embryonic tissue and sample preparation for IHC

Necessary reagents and solutions:

4. 1X PBS
5. 4% PFA in PB
6. 30% Sucrose in 0.1 M PBS

The pregnant mother mouse was sacrificed by spinal dislocation and its belly was cut open. The uterus was then incised carefully at one end and scissors were then inserted to widely open the uterus lengthwise. All embryos were then collected carefully in cold PBS. The embryos were washed in PBS and their heads were removed. The trunks of the embryos were then fixed in 30 ml of 4 % PFA for 2 hours. After 2 hours, PFA was replaced with PBS for overnight washing. The following day, PBS was replaced with 30% sucrose and incubated until the trunks sank to the bottom. After sinking, the tissue was ready for embedding and storage for further processing.

4.7.4 Isolation of Mouse postnatal tissue and sample preparation for IHC

Necessary reagents and solutions:

1. 0.2M Phosphate Buffer (PB): 27.4g $\text{Na}_2\text{HPO}_4 \cdot 2\text{H}_2\text{O}$; 8.32g $\text{NaH}_2\text{PO}_4 \cdot 2\text{H}_2\text{O}$ in 1L water
2. Freshly prepared and chilled 4% PFA in PB (pH 7.3)
For 1000 ml of 4% PFA: Take 350 ml of water, add 25 drops of 10 N NaOH and heat water to 60°C. Add 40 g of solid paraformaldehyde and dissolve on hot water bath. Cool and make the volume to 500 ml with water. Mix this solution with equal amount of 0.2M PB to get 4% PFA.
3. Ketamine-Xylazine as anaesthesia
4. PBS
5. 30% Sucrose in 0.1M PBS

PFA and PBS were chilled to 4°C and kept on ice. P10 or P21 mice were sacrificed by transcardial perfusion with 4 % PFA under deep ketamine (100mg/kg) -xylazine (10mg/kg) anaesthesia. The mice were anesthetized with ketamine-xylazine anaesthesia and after few minutes, they were checked for the presence of reflexes. When the reflexes

were totally absent, the heart was exposed and a needle connected to the tubing from a perfusion pump with circulating ice-cold PBS, was inserted into the left ventricle. The atrium was then cut with a sharp pair of scissors. This allowed for the flushing of the blood from the system. After three minutes of perfusion with ice-cold PBS, the tubing was moved to ice-cold 4 % PFA. The pump was stopped while the tubing was shifted to limit the inclusion of air bubbles. The animal was then perfused with PFA for 7 min (P10 mice) or 10 min. (P21) mice. Flow rate during the whole experiment was kept at 8.5ml/min. After the completion of 10 minutes, the animal was eviscerated and a ventral laminectomy was performed to remove the whole spinal cord (all levels) and muscles. The spinal cord was post fixed for an additional three hours in 4 % PFA at 4°C. Then it was washed with PBS for 15 hours on a shaker. After washing, the spinal cord was transferred to 30 % sucrose solution and was incubated at 4°C until the floating tissue sank to the bottom. Tissue was then removed from sucrose and embedded in OCT compound to form a cryo-block. The blocks were then stored at either -20 or -80°C until cryo-sectioning was performed.

4.8 Embedding tissue in Cryo-molds and Cryo-sectioning

Necessary reagents and solutions:

1. O.C.T. Compound

The fixed and dehydrated tissue was immersed in OCT compound for 1 minute to equilibrate. Meanwhile, cryomolds were labelled with description of tissue, age of tissue and date. Cryomolds were then filled with OCT and tissue was placed in the mold with desired arrangements and orientation. The cryo-mold containing OCT and tissues was then rapidly frozen at -80°C and stored at -20°C until use.

For cutting, the solidified OCT blocks were removed from the molds and mounted in a CM 1510 S cryostat (Leica Microsystem GmbH). 10-60 µm thick sections were sectioned and collected on glass slides (SuperFrost Plus). The slides were labelled with mold description, thickness of section and date. Then they were air dried for 30 minutes at room temperature and stored in slide holder boxes. Subsequently they were stored at -20°C until use.

4.9 Immunohistochemistry (IHC)

Necessary reagents and solutions:

1. PBS 1X
2. PBS-T (1XPBS with 0.01 % TritonX100)
3. Protein Block: 1% BSA; 0.5% TritonX100 in PBS
4. Antibodies
5. Mowiol 4-88 mounting medium*

Cryo-sections on slides were rinsed thrice for 10 min with PBS at room temperature. 500 µl of protein block was applied to each slide at room temperature for 30 minutes. Appropriate amounts of primary antibodies were diluted in 500 µl of protein block. Protein block was then drained from the slides and 500 µl of diluted primary antibodies were added. The slides with primary antibodies were incubated overnight in cold room. The following day, slides were rinsed with PBS-T three times for 10 minutes. Appropriate amount of target species specific secondary antibodies was diluted in 500 µl of protein block. Diluted secondary antibodies (500 µl) were then added to the slides for 1 hour at room temperature. After one hour, slides were washed two times with PBS-T and once with PBS for 10 minutes. PBS was completely drained out and 50 µl of Mowiol mounting medium was added. Slides were carefully covered with cover slip, preventing any bubble and incubated at 37°C for 30 minutes for Mowiol to solidify. After solidification of Mowiol, slides were ready for image acquisition or short term storage.

* Add 2.4 g of Mowiol 4-88 to 6 g of glycerol. Stir to mix. Add 6 mL of H₂O and leave for several hours at room temperature. Add 12 mL of 0.2 M Tris-Cl (pH 8.5) and heat to 50°C for 10 min with occasional mixing. After the Mowiol dissolves, clarify by centrifugation at 5000g for 15 min. For fluorescence detection, add DABCO (1,4-diazabicyclo-[2,2,2]-octane) to 2.5% to reduce fading. Aliquot in airtight containers and store at -20°C. Stock is stable at room temperature for several weeks after thawing. Cold Spring Harbor Protocols (2006)

4.10 Image Acquisition

Confocal fluorescence images were taken on a Zeiss LSM 710 confocal laser scanning upright microscope Using a 20x / 0.8 Plan-Apochromatic air objective for overviews and a 40x /1.3 and a 63x / 1.4 plan-apochromatic oil objectives for high resolution images. Fluorescent dye excitation at 488 nm, 561 nm, and 633 nm was provided by Ar/Kr, DPSS (Diode-pumped Solid-State), and He-Ne lasers, respectively. The fluorescent dye detection channel (PMT, photomultiplier tube) bandwidth was adjusted to 505-550 nm, 572-640 nm, and 655-720 nm for Alexa Fluor 488, Alexa Fluor 555, and Alexa Fluor 647, respectively. Images were acquired after the acquisition settings (laser power, PMT voltage and offset) were optimized while preventing pixel clipping. Once the acquisition parameters were established, they remained unchanged during the course of an experiment. The saved images were imported to Fiji software and were processed for adjustment of brightness/contrast. All the effects mentioned were applied uniformly across the whole images.

4.11 Luciferase Reporter Assay

This assay was performed in collaboration with group of Dr. Kristine Henningfeld. In brief, at 4-celled stage of Xenopus laevis embryo (blastomeres), 250pg of Gal4-fused Notch1 mRNA was injected with 10 pg. of UAS-firefly-luciferase (positive control) and 10 pg. of CMV-renilla-luciferase DNA into 2 of the 4 cells. The embryos were then cultured until onset of gastrulation (E10.5), after which they were collected in tubes. The luciferase assay was then performed using Dual Luciferase Reporter Kit (Promega) according the manufacturer's protocol. Embryos were homogenized in 10 µl/embryo passive lysis buffer (Promega) followed by 15 minutes' incubation at room temperature. After incubation, the homogenate was centrifuged for 10 min. at 13000 rpm. Supernatant was collected in fresh tubes and centrifuged again at 10000 rpm for 10 min. to remove any residual debris. 10 µl of final lysate supernatant was then loaded on luciferase assay well plate and measured via Centro LB960 luminometer (Berthold Technologies) using firefly and renilla luciferase substrates from the Promega Kit as per manufacturer's protocol. Notch activation was then calculated by normalization with UAS-Firefly luciferase (positive control). Similarly, the activation of different Notch variants was calculated and for each Notch variant, its activation after co-injection of Dll1, Dlk1 and GFP mRNA was also experimented and calculated.

4.12 Statistical analysis

Statistical analysis and graphs were made using GraphPad Prism software. Error bars indicate the standard error of mean (SEM) unless otherwise stated. Significance was calculated using non-parametric Students t-test with two samples and unequal variance.

V Results

To dissect the Dlk1 signalling pathway, I have divided my study into two parts: Dlk1 extracellular signalling and Dlk1 intracellular signalling. In sections 5.1 to 5.5 experimental evidences for Dlk1 extracellular interaction with Notch receptor and its influence on Notch activity is shown. In sections 5.6 to 5.13, the newly identified interaction of Dlk1 via its intracellular segment with another interaction partner, NFAT, is shown and its effects are documented. Before describing each experiment, I have detailed the generation of different protein variants in separate sections.

PART-1: Dlk1 extracellular interaction

5.1 Generation of Dlk1 Variants with Specific Deletions to Track the Extra and Intracellular signalling

The longest isoform of native Dlk1, referred to here as Dlk1-WT with 385 amino acids was tagged with FLAG epitope at its N-terminal end to detect the expression and localisation of the protein by immunodetection in western blot (Fig.5.1). To study the requirement of the extracellular segment of Dlk1, a truncated version of Dlk1, Dlk1 Δ ICD, was created in which the intracellular segment was replaced with 6XHistidine residues. The 6XHis tag was added to ensure that the protein product remains anchored in the membrane. A construct expressing Dlk1 intracellular segment was also cloned separately to study its interactions with other intracellular proteins. Since the intracellular segment had only 65 amino acid residues and was difficult to detect after Co-IP experiments, GFP (green fluorescent protein) was fused N-terminal to Dlk1 along with a FLAG tag at C-terminal, to enable detection in western blots (Fig.5.1).

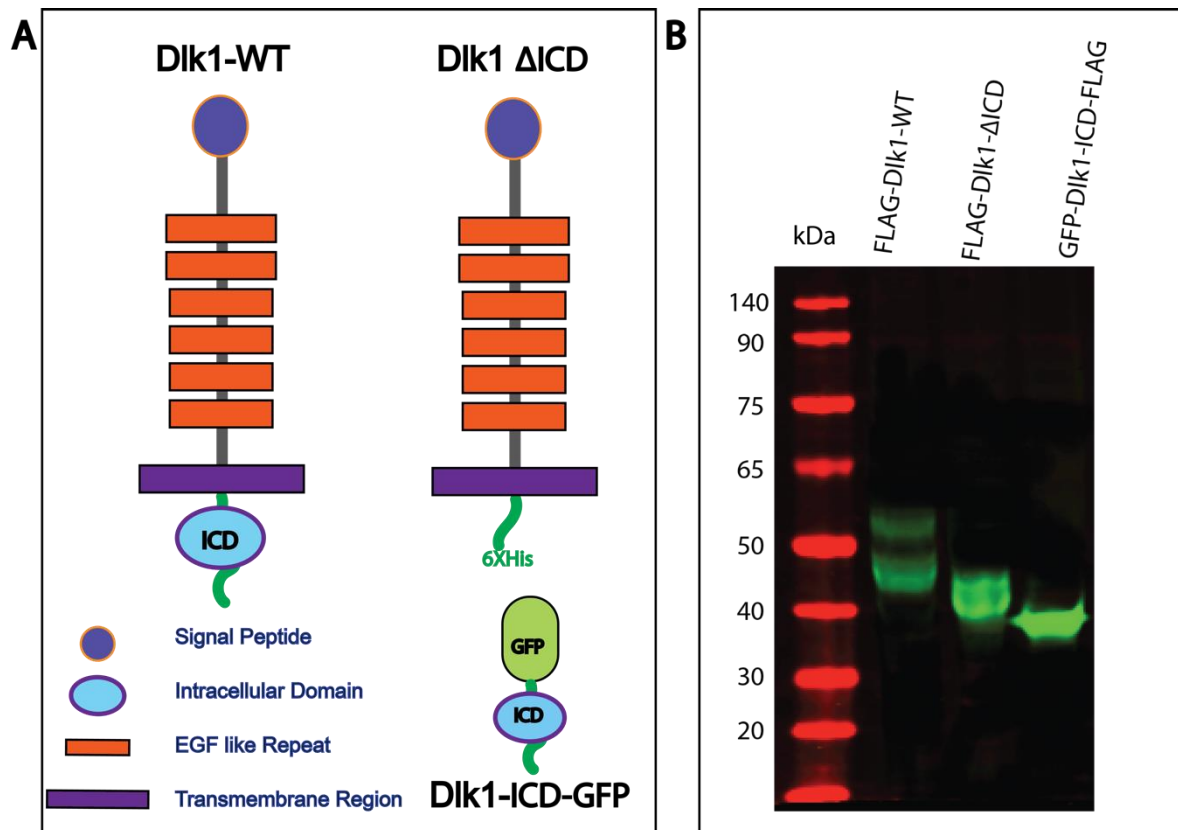


Fig.5.1 Mouse Dlk1 wild type and truncated versions cloned with FLAG tag.

A: To study the signalling mechanism of Dlk1, the Dlk1 protein was divided into two. An extracellular only version, Dlk1 Δ ICD and an intracellular only version Dlk1-ICD were cloned with N-terminal FLAG tag. B: A western blot picture of the protein products of each Dlk1 version is also shown with FLAG staining. While the Dlk1 full length shows two bands around 50kDa, the Dlk1 Δ ICD band is closer to 40kDa and even shorter is Dlk1ICD-GFP (35 kDa) band as expected.

5.2 Generation of Notch Variants with Specific deletions to find out interacting regions with Dlk1

While canonical Notch ligands activate Notch signalling (de Celis and Bray 1997), non-canonical ligands tend to inhibit Notch signalling (Micchelli, Rulifson et al. 1997). The Abruptex region of Notch (EGF 24-29) was proposed to be required for cis-inhibitory interactions (de Celis and Bray 2000, Pei and Baker 2008), while another study suggested that EGF repeats 10-12 of Notch are responsible for cis-inhibition (Becam, Fiuza et al. 2010). Moreover, depending on the study or system used, the non-canonical Notch ligand has been concluded to activate and suppress Notch signalling, while yet other studies have failed to detect physical interaction between Notch and Dlk1 at all (Wang, Zhao et al. 2010). Part of the ambiguity in these findings could be due to the use of relatively small fragments, rather than the entire extracellular segment of Notch, to study its interactions with putative ligands.

Therefore, I addressed this ambiguity of Notch-Ligand interaction by testing the interaction of the entire Notch extracellular segment (ECD), referred to here as Notch1-WT for simplicity with Dlk1 using biochemical assay as well as luciferase assay. I generated variants of Notch1-WT from mouse by introducing different deletions (Fig. 5.2a). I considered dividing the Notch-ECD into two parts: the proposed Notch activating region (EGF 3-19) and the proposed Notch inhibitory region (LNR1-3). Hence, I generated truncated version of Notch1-WT with deleted LNR1-3 called as Notch Δ LNR (Fig. 5.2a). Another truncated version lacked the activating regions EGF3-19 and was called Notch Δ EGF (Fig. 5.2a) while a third deletion construct of Notch lacked both the activating regions and inhibitory regions called as Notch Δ EGF Δ LNR (Fig. 5.2a). Notch Δ EGF Δ LNR was left with only few EGF repeats and dimerization domains (Fig. 5.2a). The expression of all native and truncated versions of Notch1 was verified by western blotting (Fig. 5.2b).

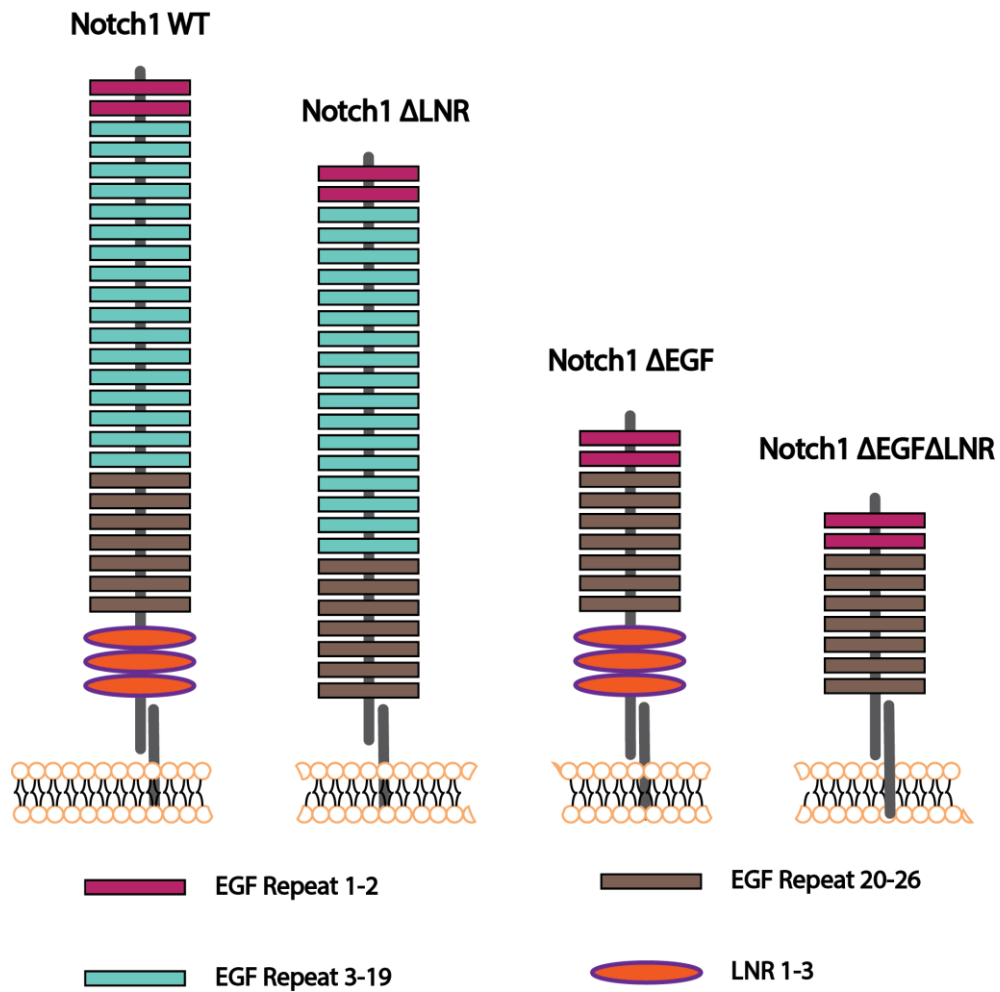


Fig.5.2a Generation of Notch1 Truncations Lacking Putative Activating or Inhibitory Regions or Both.

To study the interaction of Dlk1 with Notch, several deletion constructs of native Notch1-ECD were generated. Notch1WT contained entire ECD of Notch including transmembrane region. In Notch1 Δ LNR the three Lin-12 repeats were deleted. EGF repeats 3-19 were deleted in Notch1 Δ EGF and another version of Notch1, called as Notch1 Δ EGF Δ LNR, with both these deletions was also created.

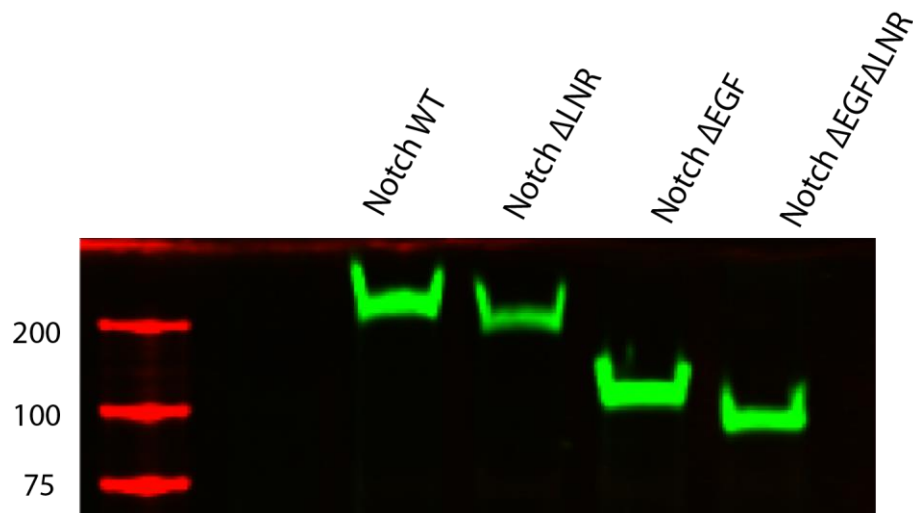


Fig.5.2b Western blot analysis of Notch1WT and truncated versions.

Western blot analysis upon transfection into Hela cells showed stable expression and the expected sizes for Notch1-WT ($\cong 215$ kDa). Notch Δ LNR ($\cong 200$ kDa) was expected to be 13 kDa smaller, while Notch Δ EGF ($\cong 100$ kDa) expected to be 100 kDa smaller than Notch1-WT. Notch Δ EGF Δ LNR was expected to be 13 kDa smaller than Notch Δ EGF.

5.3 Dlk1 Extracellular Segment Interacts with Notch Like a Canonical Notch Ligand

Different HA-tagged Notch constructs were co-expressed with FLAG-tagged canonical Notch ligand Delta1 (Dll1) or FLAG-tagged non-canonical Notch ligand Delta like homolog1 (Dlk1) in HeLa cells and a pull-down assay using anti HA magnetic beads was performed to test for interaction. After pull down, SDS-PAGE and western blot was performed to visualize the protein bands. The results of the experiment are shown in Figure 5.3a. and 5.3b. for Notch-Dll1 interaction and Notch Dlk1 interaction respectively.

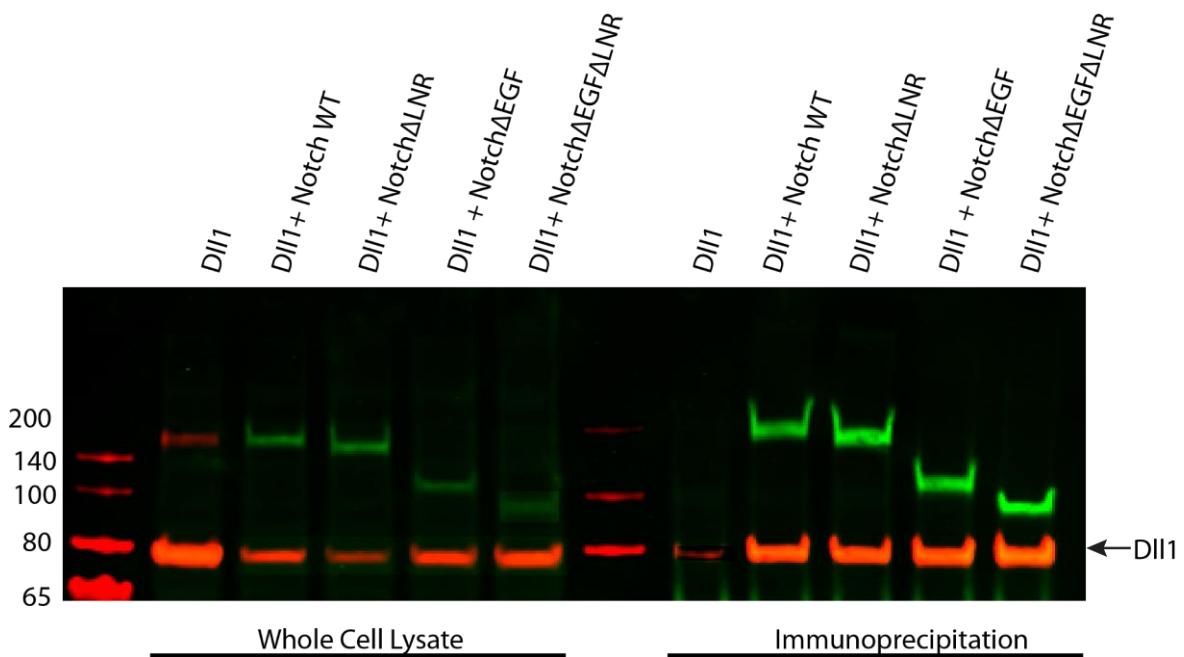


Fig.5.3a Interaction of Canonical Notch Ligand Dll1 with Native and Truncated Versions of Notch1

Co-immunoprecipitation of co-expressed Dll1 with Notch1. Overexpressed FLAG-tagged Dll1 was immunoprecipitated from HeLa cell lysates with anti HA magnetic beads when HA-tagged Notch1 constructs were co-expressed. Immunoprecipitation with anti-HA magnetic beads in absence of Notch co-expression was done as control. Co-immunoprecipitation of Dll1(red bands) with Notch1(green bands) was detected by western blotting using anti-FLAG antibody and anti-HA antibody in different channels scanned by Licor imaging system.

Dll1 is a canonical Notch ligand which induces Notch signalling by trans-activation. Dll1 appears to bind between EGF repeats 11-12 of Notch1 (Rebay, Fleming et al. 1991, Rebay, Fehon et al. 1993). Since then EGF 11-12 was univocally established as the Notch-Delta interacting region. Few other reports suggested that Notch EGF 11-12 also binds at its own Abruptex region (EGF 24-29 in human Notch) to maintain inactive state (Pei and Baker 2008). However, my results from co-immunoprecipitation experiments suggest that Dll1 additionally interacts with other regions of Notch1. Fig. 5.3a tells that Dll1 has the capacity to bind Notch at both activating and inhibitory regions (Notch Δ LNR and Notch Δ EGF respectively). Not only this, Dll1 can still bind to Notch Δ EGF Δ LNR i.e. the EGF 20-26 of Notch. If we compare this to the literature, the EGF 20-26 of mouse Notch is similar to Abruptex region of human or *Drosophila* Notch. Hence, it can be concluded from figure 5.3a that the canonical Notch-ligand Dll1 can interact with Notch at multiple regions at EGF repeats region or LNR region. Therefore, I further hypothesized that activation or inhibition of Notch signalling after Notch-Dll1 interaction will depend on where exactly Dll1 binds. Experimental evidence to prove this hypothesis is provided in section 5.4.

I next tested with which region of Notch1 the non-canonical ligand Dlk1 would binds to. Unlike what was recently reported that Dlk1 interacts at EGF 10-15 of Notch (Traustadottir, Jensen et al. 2016), in my experiment I confirmed that Dlk1 also binds at multiple regions of Notch ECD (shown in Figure 5.3b) just like its canonical ligand Dll1. It again raises the question whether Dlk1, which is known as Notch inhibitor, will activate Notch when bound at activating region of Notch or not. This question is addressed later in section 5.4 and 5.5

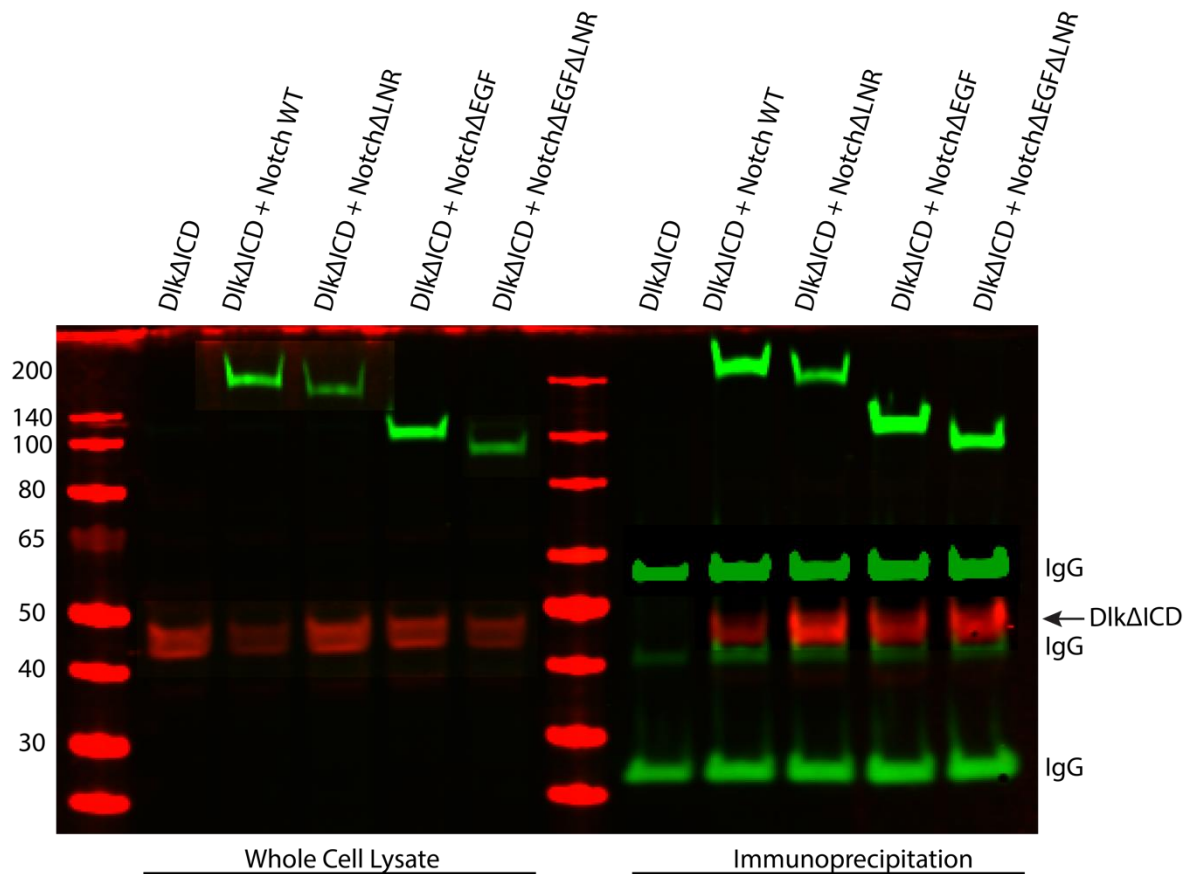


Fig.5.3b Interaction of the Non-Canonical Notch Ligand Dlk1 extracellular segment with Native and Truncated Versions of Notch1

Co-immunoprecipitation of co-expressed Dlk1ΔICD with Notch1. Overexpressed FLAG-tagged Dlk1ΔICD was immunoprecipitated from HeLa cell lysates with anti HA magnetic beads when HA-tagged Notch1 constructs were co-expressed. Immunoprecipitation with anti-HA magnetic beads in absence of Notch co-expression was done as control. Co-immunoprecipitation of Dlk1ΔICD (red bands) with Notch1 (green bands) was detected by western blotting using anti-FLAG antibody scanned by Licor imaging system.

5.4 What Luciferase Assay Reveals About Notch-Dll1 and Notch-Dlk1 Interaction, Activation and Inhibition

While some studies provided evidence that Dlk1 is an inhibitor (Baladron, Ruiz-Hidalgo et al. 2005) of Notch signalling, others suggested that Dlk1 activates Notch (Li, Tan et al. 2014) while yet other studies seem to deny an involvement of Dlk1 in Notch signalling at all (Wang, Zhao et al. 2010). To address these issues, I collaborated with Dr. Kristine Henningfeld's laboratory (UMG Göttingen) to perform Notch activity assays in *Xenopus laevis* embryos. The Notch1-WT and its deletion constructs (Fig.5.2a) were fused to Gal4 and Notch activation was tested using a Gal4-UAS-Luciferase assay in presence and absence of Dll1 and Dlk1. Luciferase assay is used to study gene expression and events involved in regulation of genes due to its extreme sensitivity which allows quantification of small changes in transcription (section 4.11). The result of this experiment is reported as relative activation of Notch with respect to its basal activation by endogenous Notch ligands (Fig. 5.4).

In these experiments, co-expression of canonical ligand Dll1 led to a very strong increase in Notch activity (Fig.5.4). Since Notch1 and Dll1 are forcedly co-expressed *in vivo* and are thus equally likely to interact in trans- as well as cis-configuration, transactivation of Notch by Dll1 appears to largely overrule cis-inhibition when both occur at the same time. In contrast to Dll1, Dlk1 completely suppressed both Notch1 basal activity and Notch1 activation by Dll1 (Figure 5.4). Consistent with previous studies, both basal as well as Dll1-mediated activation of Notch1 were abolished upon deleting a region of Notch1 containing EGF repeats 3-19 implicated in trans-activation (Figure 5.4). In contrast to deleting the trans-activation region, deleting the LNR region implicated in inhibiting Notch1 auto-activation led to very strongly elevated basal Notch1 activity that was even higher compared to that resulting from Dll1 co-expression. Co-expression of Dll1 was not able to further elevate Notch Δ LNR activity (Figure 5.4). Notably, co-expression of Dlk1 completely suppressed the Notch Δ LNR activity, strongly suggesting that it operates as a bona fide suppressor of Notch activation rather than by competing with canonical ligands for binding the EGF10-13 trans-activation region. Indeed, Dlk1 still completely suppressed auto-activation of Notch lacking both the LNR and EGF10 repeats, Notch Δ EGF Δ LNR (Figure 5.4). Interestingly co-expression of Dll1 either with Notch Δ EGF Δ LNR or Notch Δ LNR slightly yet significantly decreased Notch auto-activation, which is likely explained by the retained ability of Dll1 to interact with the EGF20-26 cis-inhibitory region in these constructs, consistent with the results I obtained through the co-IPs (see Figure 5.3a). These results

are further consistent with the binding of Dlk1 to both constructs detected by co-IP (see Figure 5.3b). Together these data seem to confirm Notch EGF3-19 and EGF20-26 as the respective trans-activating and inhibitory binding interfaces of Dll1, while Dlk1 suppresses Notch by both direct inhibitions at inhibitory regions of Notch and by competitive inhibition at activating regions of Notch.

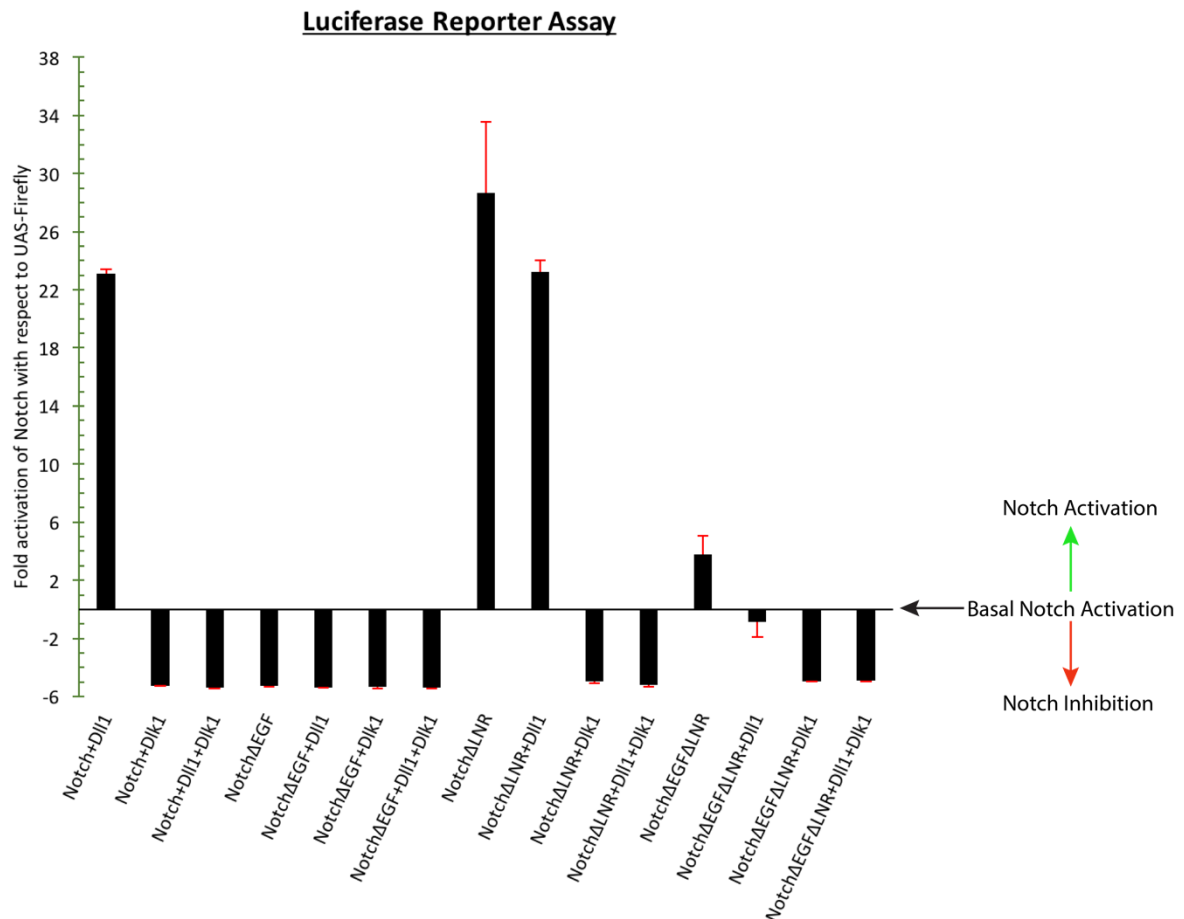


Fig.5.4 Dlk1 is a Potent Suppressor of Notch Signalling

Vertical bars represent the activation of Notch1-Wt and its variants in presence or absence of Dll1 and Dlk1 plotted with reference to basal Notch Activation. Dlk1 completely suppresses Notch-WT basal activity as well as Dll mediated Notch1-WT activation. In the absence of Dlk1, Dll1 strongly activates Notch and this activation is lost in case of NotchΔEGF. High level of Notch auto-activation is observed for NotchΔLNR. Additionally, removing EGF3-19 in NotchΔEGFΔLNR still leads to auto-activation, although to a lesser degree. Despite deletion of EGF and LNR repeats, Dlk1 nevertheless completely blocks NotchΔEGFΔLNR activation.

5.5 Ectopic expression of Dlk1 Inhibits Notch Protein and Promotes Early Cell Cycle Exit *in vivo* in Chick Neural Tube

I next decided to test whether Dlk1 would promote biological actions linked to Notch signalling or the inhibition of Notch signalling *in vivo*. I hypothesized that if Dlk1 were to suppress Notch signalling in neural progenitors, then it would promote cell cycle exit and Neuronal differentiation. Therefore, I forcedly expressed Dlk1 in the neural tube of chick embryos, by *in ovo* electroporation of E2.5 chick embryos and determined the number of differentiated MNs in transverse sections of chick neural tube by immunostaining.

The transverse sections of chick neural tube have a GFP positive transfected side while a GFP negative untransfected side (Fig. 5.5 A). MNR1/2 (blue) staining determines the total number of motor progenitor cells including the ones which have undergone differentiation. Islet1/2 staining indicates only those motor neurons which have exited cell cycle. The quantification of MNR1/2 and Islet1/2 positive cells revealed that while the total number of MN progenitors remained unchanged, the Islet positive cell count was higher in transfected side indicating early cell cycle exit of MN progenitors (Fig. 5.5 B and C).

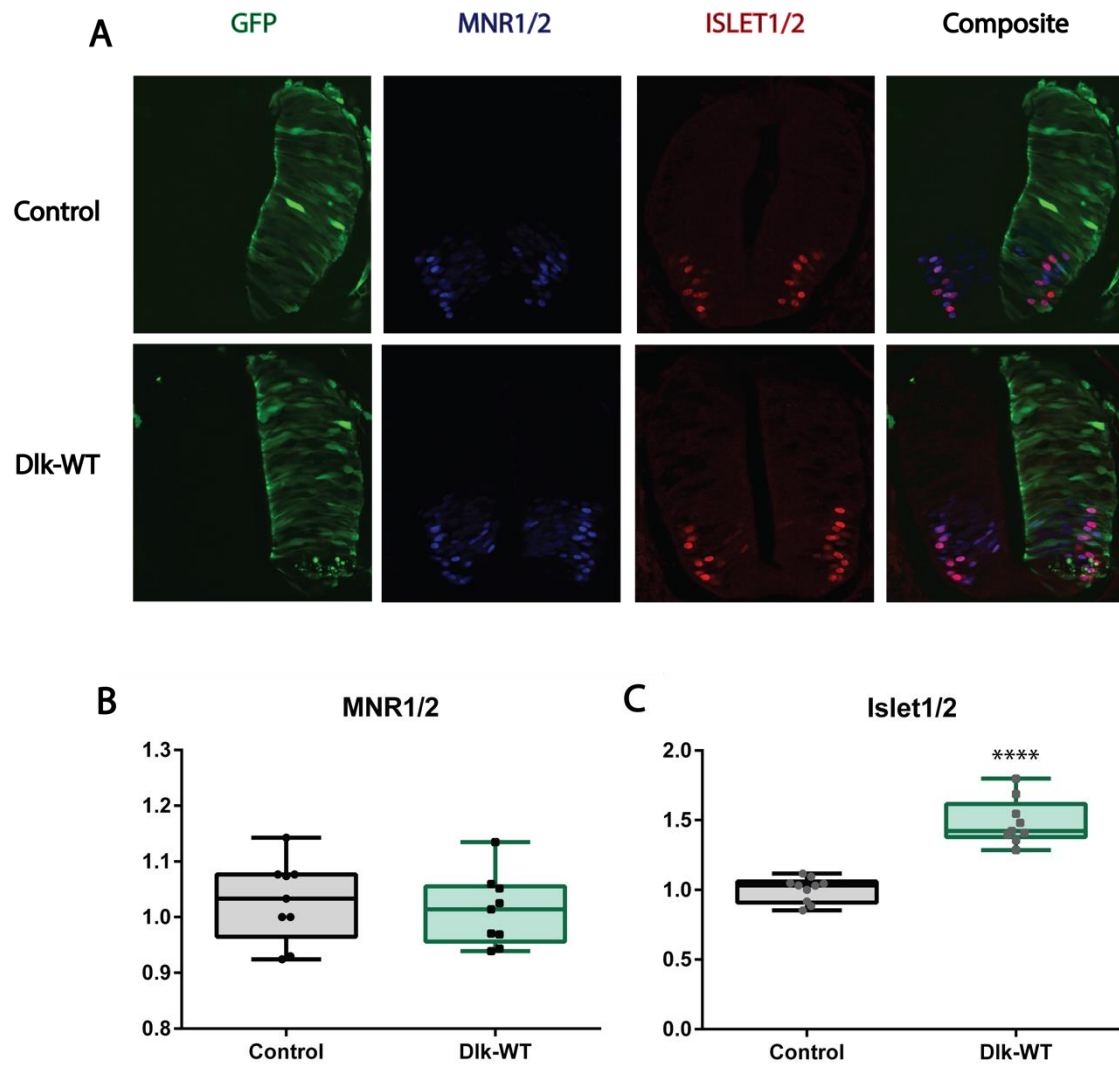


Fig.5.5 Dlk1 Induces Early Cell Cycle Exit in Chick Neural Tube

A: Transverse section of chick neural tube at E3.5, 24 hours after electroporation of control GFP (n=7) and Dlk1-WT (n=9) expressing vector. B: Ratio of MNR1/2 positive cells in transfected side of neural tube over the untransfected side of neural tube. C: Ratio of Islet1/2 positive cells in transfected side of neural tube over the untransfected side of neural tube. ****: $p < 0.0001$ as per non-parametric t-test.

PART-2: Dlk1 Intracellular Signalling

Because a screen by the laboratory for Dlk1 interaction partners using the yeast split-ubiquitin two-hybrid system (DualSystems) detected interaction of the intracellular segment of Dlk1 with the nucleo-cytosolic NFATc transcription factors I focus in the second part of my thesis on the interaction between Dlk1 with NFAT and its contribution to Dlk1 intracellular signalling.

5.6 Dlk1 Processing and Release of its Intracellular Segment (DLK1-ICD)

When expressing Dlk1 with a C-terminal epitope tag in *HeLa* cells and analysing the resulting protein product by western blotting I noticed the presence of a short Dlk1 fragment of 10 kDa together with the two larger bands around 50 kDa (due to its post-translational modifications like glycosylation or ubiquitination) corresponding to the non-cleaved Dlk1 holoprotein (Figure 5.6), indicating that the Dlk1 intracellular segment (Dlk1-ICD) predicted to be around 10 kDa in size, is post-translationally cleaved from the holoprotein. Moreover, since Dlk1-ICD was present in similar abundance compared to the larger Dlk1 forms these observations suggest it is remarkably stable considering its small size. Because an artificial epitope-tagged construct containing the entire intracellular portion of Dlk1 was slightly larger than 10 kDa, Dlk1 appears to be cleaved a few residues C-terminal to the transmembrane segment to generate Dlk1-ICD (Figure 5.6). To exactly pinpoint the site of Dlk1 processing and the generation Dlk1-ICD I am in the process of collaborating with Dr. Oliver Valerius to perform mass spectrometry of the Dlk1 cleavage products.

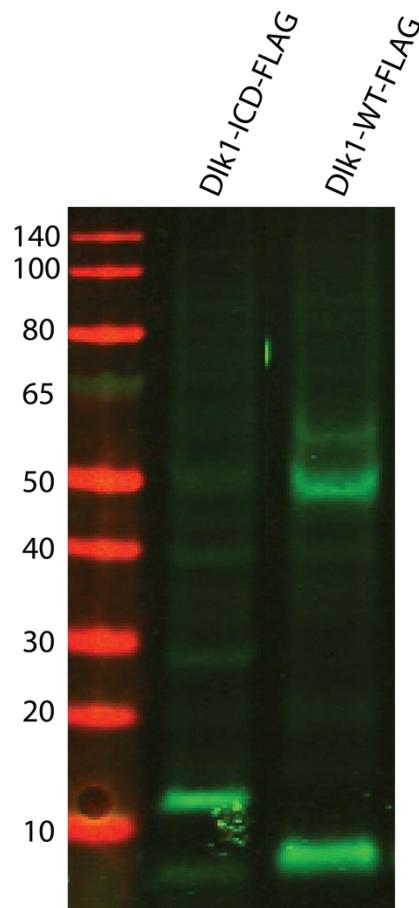


Fig.5.6 Cleavage and Release of Dlk1 Intracellular Segment in HeLa cells

Mouse Dlk1-WT expression with C-terminal FLAG tag together with FLAG-tagged Dlk1-ICD expression in HeLa cells: The Dlk1-ICD-FLAG has size of 11 kD. A cleaved C-terminal fragment of Dlk1-WT shows a band near 10 kD, indicating Dlk1-ICD might be cleaved further C-terminally in its cytoplasmic portion.

5.7 Generation of NFAT Constitutively Nuclear and NFAT Dominant Negative Versions of NFAT

NFATc proteins consist two domains: An N-terminal regulatory domain called as NFAT-homology region (NHR) and the C-terminal Rel-Homology Domain (RHD) which binds the DNA. NHR contains docking site for calcineurin and kinases while rest of the protein is having phosphorylation site, nuclear localisation sequence (NLS) and DNA binding RHD which are responsible for NFAT localisation and activity. By competing for and sequestering Ca^{2+} /Calcineurin from endogenous NFAT proteins, the N-terminal portion of NFATc4 can act as a dominant negative inhibitor of the transcriptional activity of all proteins of the NFAT family (Chow, Rincon et al. 1999) Similarly, the C-terminal DNA without the transactivation domains contained in the N-terminal portion of NFATc4 yield a constitutively nuclear and perpetually active transcription factor (Chin, Olson et al. 1998, Bai and Kerppola 2011). To study NFAT interaction with Dlk1 and its role in motor neuron functional diversification I therefore generated C-terminally and N-terminally truncated versions of native NFATc4 (called NFAT-wt): NFAT-dn and NFAT-cn, (Figure 5.7).

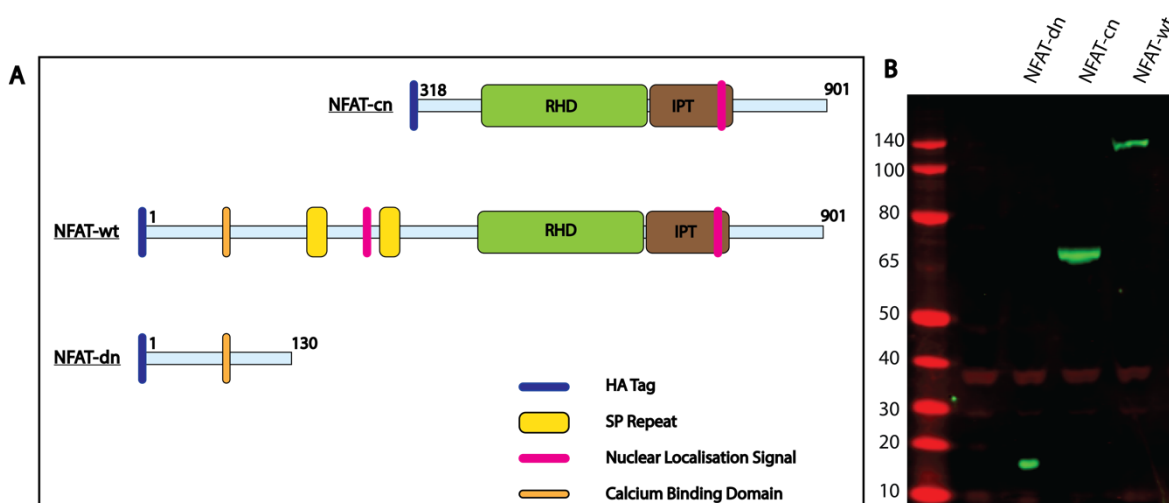


Fig.5.7 Construction and expression of native, constitutively-active and dominant-negative NFATc4

A: Based on literature, NFAT constitutively nuclear (NFAT-cn) and NFAT dominant negative (NFAT-dn) were cloned with the outline of amino-acid residues as shown. B: A western blot picture of the protein products of each NFAT construct is also shown with anti-HA staining along with the protein ladder which shows NFAT-dn at 15 kDa, NFAT-cn at 65 kDa and NFAT-wt at 140 kDa.

5.8 Localisation of NFAT Variants in Cell culture and in Chick Embryos

I confirmed the localisation of all NFAT variants both in cell culture and in the neural tube of chick embryos. As expected (Chin, Olson et al. 1998, Chow, Rincon et al. 1999), NFAT-dn expression was cytosolic as well as nuclear due to its small size, NFAT-cn was constitutively nuclear (Chin, Olson et al. 1998) while NFAT-wt was predominantly cytosolic in both cell culture (Figure 5.8a) and chick neural tube progenitor cells (Figure 5.8b). Also the distribution of NFAT-cn in the nucleus was not uniform, instead a punctate pattern was observed which is also consistent with observation from previous studies.

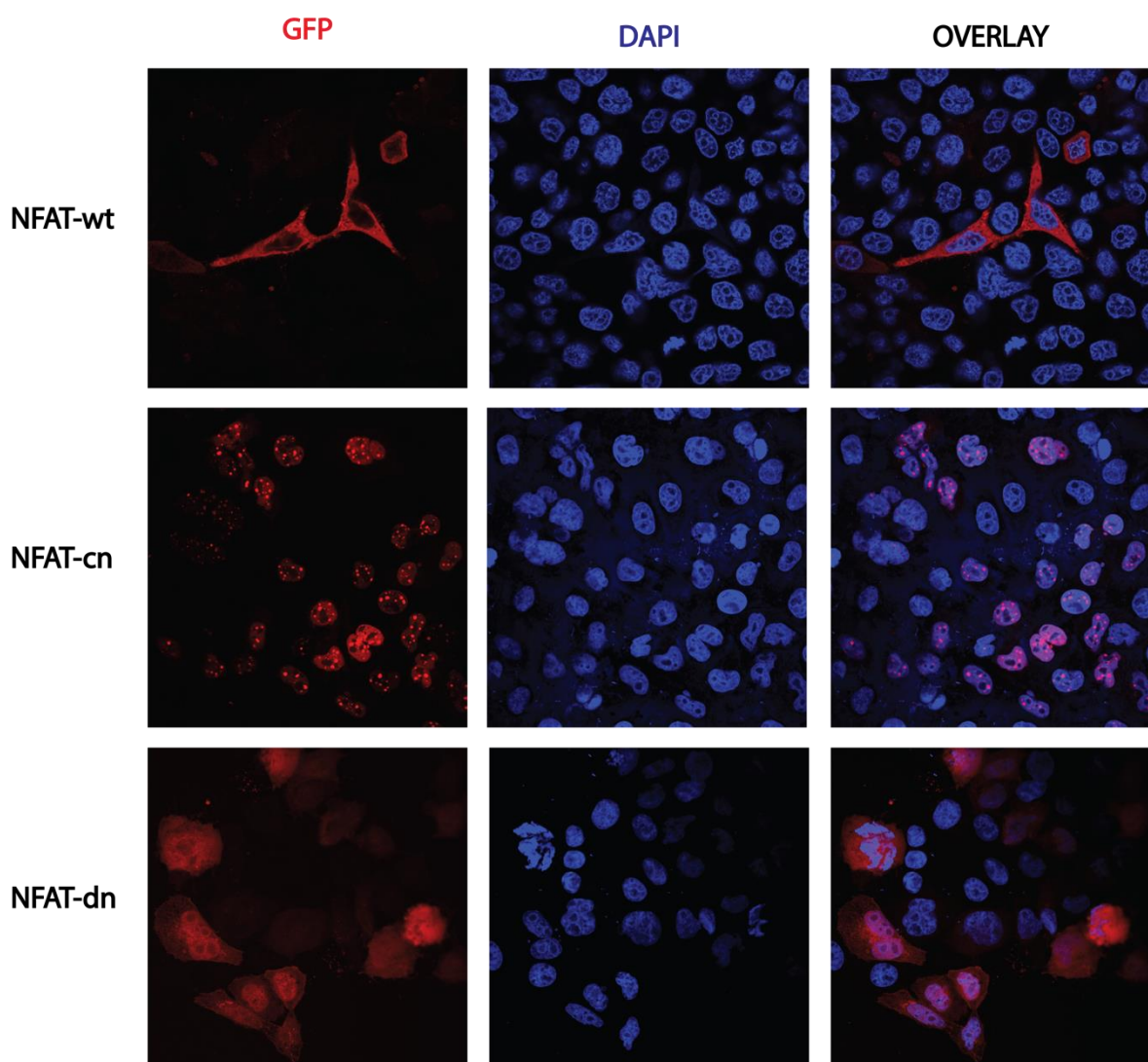


Fig.5.8a Localisation of native, dominant negative and constitutively nuclear NFATc4 in HeLa cells

NFAT-wt is localised in cytosol while NFAT-cn has nuclear localization. NFAT-dn has both cytosolic and nuclear localisation.

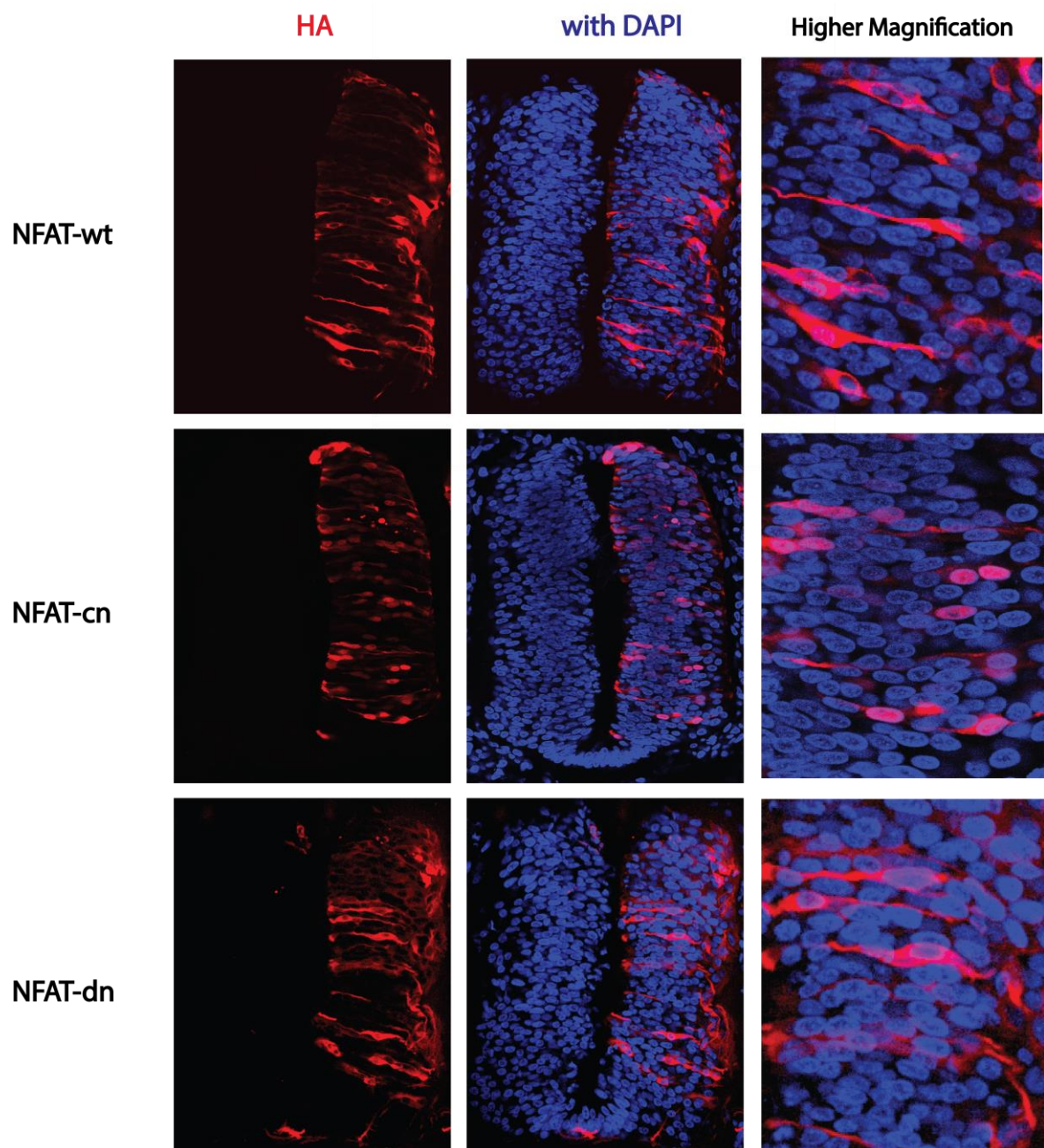


Fig.5.8b Localisation of native, dominant negative and constitutively nuclear NFATc4 in the chick neural tube.

NFAT-dn is localised in cytosol while NFAT-cn has nuclear localization. NFAT-wt has both cytosolic and nuclear localisation.

5.9 Direct Physical Interaction of the Dlk1-ICD with the C-terminal portion of NFATc4

Upon co-expression in HeLa cells with HA-tagged NFATc4-wt or NFAT4-cn, but not when expressed alone, Flag-tagged Dlk1-ICD was co-immunoprecipitated by anti-HA antibody along with HA-NFAT4, thus confirming that Dlk1-ICD physically interacts with the C-terminal portion of NFATc4 (Figure 5.9). At the same time Dlk1 did not interact with the NFAT-dn protein (Figure 5.9), consistent with the Two-Hybrid-based screen in which Dlk1 was found to interact with the C-terminal portion of NFATc4. Thus, Dlk1 interacts only with that part of NFATc protein required for DNA binding and transactivation and thus being responsible for implementing NFAT-mediated signalling, together suggesting that the binding of Dlk1 would directly influence NFAT-signalling: either by activating or suppressing NFAT-signalling, which still needs to be addressed (see section 5.11).

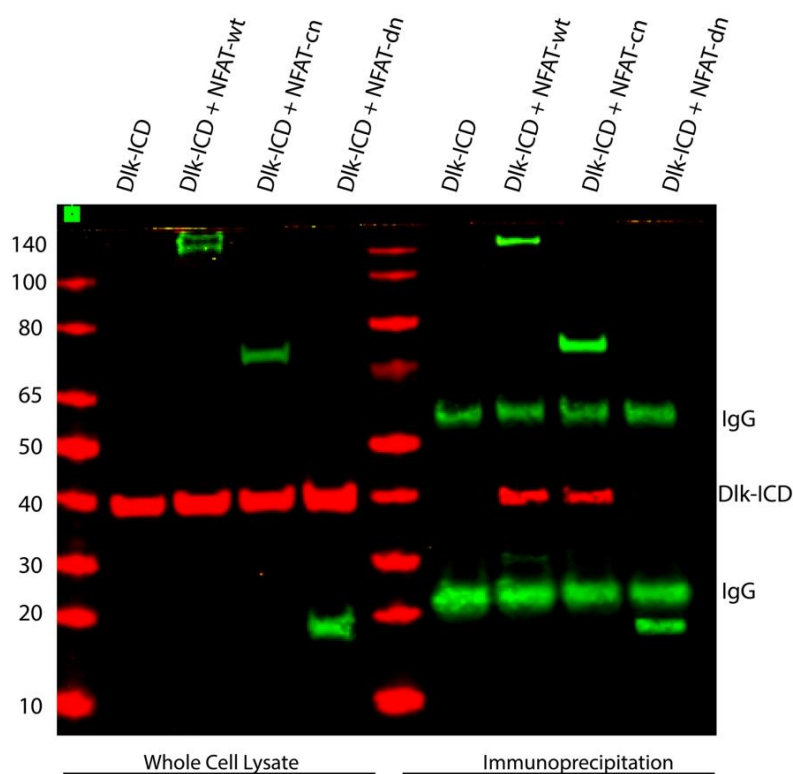


Fig.5.9 Dlk1-ICD Physically Interacts with the C-terminal Portion of NFATc4

Overexpressed FLAG-tagged Dlk1-ICD was Co-immunoprecipitated from HeLa cell lysates with anti HA magnetic beads only when HA-tagged NFAT-wt and NFAT-cn constructs were co-expressed. Immunoprecipitation with anti-HA magnetic beads in absence of NFAT co-expression was done as control. Co-immunoprecipitation of DIK1-ICD with NFAT was detected by western blotting using anti-FLAG antibody (red bands) in and anti-HA antibody (green bands) scanned by Licor imaging system.

5.10 NFAT-cn Interacts with *KCNG4* Cis-Regulatory Module

A preliminary protein-DNA interaction test using a Reporter assay indicates that the constitutively nuclear NFAT (NFAT-cn) interacts with the cis-regulatory module (CRM) of *KCNG4* (Fig. 5.10). When different NFAT versions were co-transfected with the *KCNG4* enhancer element fused with a reporter DNA (tomato) with minimal promoter (TATA), the expression of tomato was increased only with NFAT-cn and not with NFAT-dn (Fig.5.10).

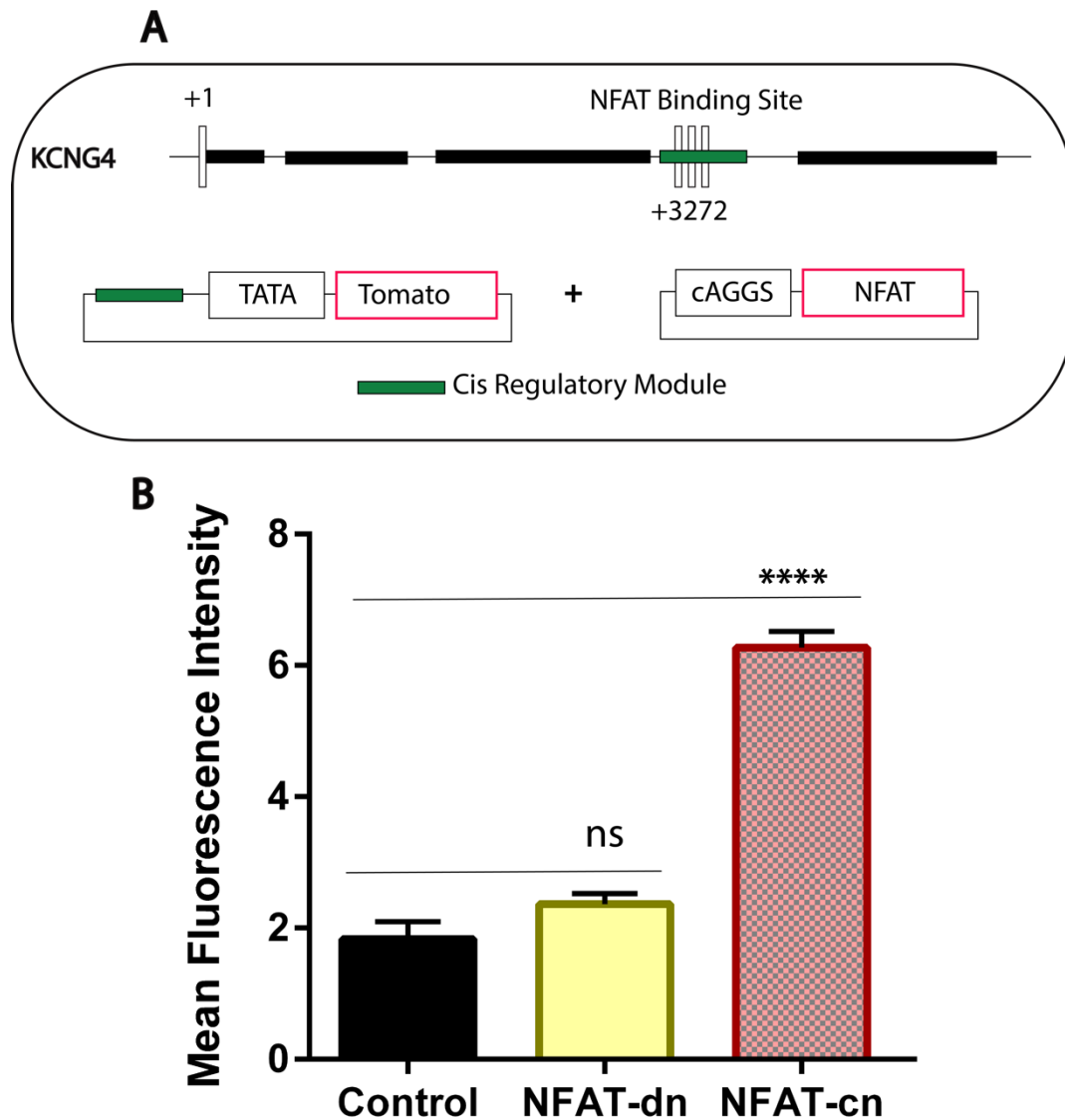


Fig.5.10 Effect of NFAT-cn on the *KCNG4* Cis-Regulatory Module

A: NFAT binding to *KCNG4*-CRM (+3272 to +3483 bp) was determined by reporter assay. B: While the constitutively active NFAT-cn increased the expression of reporter gene, the inhibitory NFAT-dn did not alter the reporter expression. Fluorescence intensity measured in arbitrary units; ****: $p < 0.0001$ as per non-parametric t-test. Number of cells counted for each group was 50.

5.11 NFAT-cn Overexpressing Cells Exit from Chick Motor Column

Although, NFAT had been reported to support neuronal survival and had been shown to express in MNs using in-situ hybridization (Website: © 2015 Allen Institute for Brain Science. Allen Spinal Cord Atlas), I discovered that NFAT-cn overexpressing cells exit the motor column. Already at E7 of chick embryonic stage, none of the NFAT-cn expressing cells were seen in the motor column. An example of chick neural tube section demonstrating the exit of GFP positive, HA-tagged NFAT-cn expressing cells is shown in Figure 5.11.

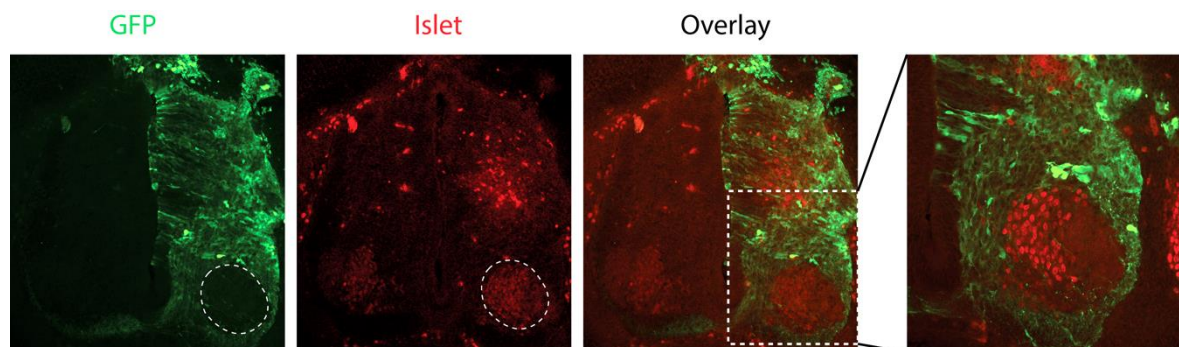


Fig.5.11 Mouse NFAT-cn Overexpression is Incompatible with Motor Columnar Cell Localization

Transverse section of Chick neural tube after 7 days of embryonic development when electroporated with tol2-lox-stop-loxp-NFAT-cn-IRES-GFP under P_{gk}-cre. No cells with reporter GFP or with anti-HA staining were found in motor column. Motor column outline is shown is white dashed line in the overlay image.

Due to the above reason, a current clamp recording of NFAT-cn overexpressing MNs was not possible.

5.12 Overexpressing NFAT-dn in MNs Induces Hyperexcitability

I studied the loss of function effect of NFATs by overexpressing NFAT-dn in chick spinal cord. It was already shown previously by our group that when Dlk1 is overexpressed in chicken spinal cord, it changes the electrophysiological properties of motoneurons towards fast signature. Fast alpha motoneurons (α fMNs) are larger in size and have higher activation thresholds with higher firing frequencies. These intrinsic properties are reflected in current clamp recordings in terms of Rheobase, Input Resistance, After-hyperpolarization spike width (AHP1/2width), After-hyperpolarization decay time (AHP1/2dT) and firing frequency. Essentially, higher rheobase means higher threshold for firing, lower AHP1/2width and AHP1/2dT reflects ability to fire faster while input resistance represents the soma size of neurons i.e. larger the cell, lower will be the input resistance and vice-versa. Also, the ability to fire faster (determined by AHP1/2width and AHP1/2dT) does not conclude a cell to be a faster firing MN. Firing frequency ultimately depends on several other factors, most essential of which is stimulus; larger the stimulus, higher will be the firing frequency. For example, the same cell can have two different AHP1/2width and AHP1/2dT values at different stimulus. Hence, AHP parameters should always be compared with a reference of 'Rheobase' i.e. if two cells with same rheobase, have different AHP1/2width then it can be concluded that the cell with lower AHP1/2width is a faster firing neuron. Also, the firing frequency should be compared always with reference to the rheobase to claim if an MN is a slow MN or a fast MN. Therefore, in my study I have included two sets of data for firing frequency: one, firing frequency at twice the threshold (i.e. Rheobase) to conclude a relatively slower or a faster MN and the peak firing frequency of the cell to determine the firing abilities of the cell at stimulus of 1000 pA.

Both the rheobase and firing frequency at twice rheobase of NFAT-dn overexpressing MNs significantly reduce (Fig.5.12) while they retain their cell size (input resistance). Despite having lower rheobase, the cells have the ability to fire at higher frequency with lower AHP1/2width, AHP1/2dT and higher Peak firing frequency (Fig.5.12). This observation concluded that MNs due to overexpression of NFAT-dn become hyper-excitable and gain ability to fire even with very low stimulus. This observation negatively correlated to what we observe when Dlk1 is overexpressed i.e. Rheobase and Firing frequency at twice Rheobase increased. Fast MNs in general are large in size, and are recruited very late during muscle contraction due to their low excitability and once excited they fire with higher rates as compared to early recruited MNs. Overexpression of NFAT-dn pushes the MNs away from the properties of a fast MN by increasing its excitability and reducing its firing rate.

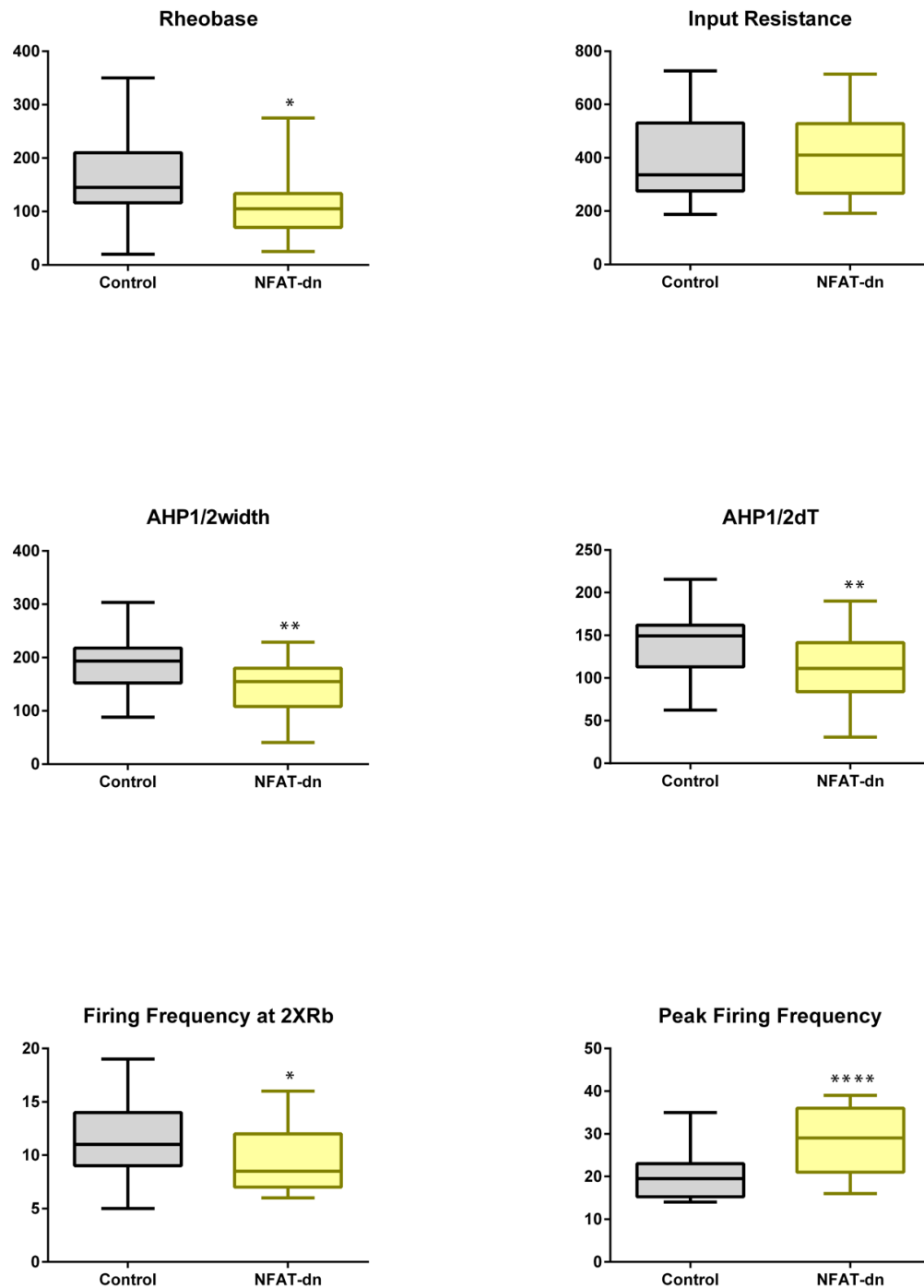


Fig.5.12 NFAT-dn Overexpression Induces Hyperexcitability in MNs

A minimum to maximum box-plot with midline representing mean for all electrophysiological parameters. NFAT-dn (n=24) significantly reduces the Rheobase, Firing Frequency at twice Rheobase, AHP1/2width and AHP1/2dT as compared to control group (n=32). Peak firing frequency on the contrary is increased in the NFAT-dn overexpressing cells as compared to the control group.

*: $p < 0.05$; **: $p < 0.01$; ****: $p < 0.0001$ as per non-parametric t-test.

5.13 NFAT-dn overexpressing MNs fail to acquire Fast MN properties

A combination of input resistance vs rheobase of the motor neurons can correctly identify 95% of the Motor unit types. For instance, fMNs have high Rheobase (Rb) and low Input Resistance (IR), the slow MNs have low Rb and high IR while the intermediate neurons have intermediate membrane properties (Zengel, Reid et al. 1985). I used to same combination of membrane properties of NFAT-dn overexpressing MNs to determine the motor unit type of these neurons. When compared with the control, I observed a reduction in population of neurons with high rheobase and low input resistance which correspond to the neurons of fast motor units. Hence, the electrophysiological study of NFAT-dn overexpressing MNs indicates a loss of fMN population when NFAT is inhibited in the developing motor neurons.

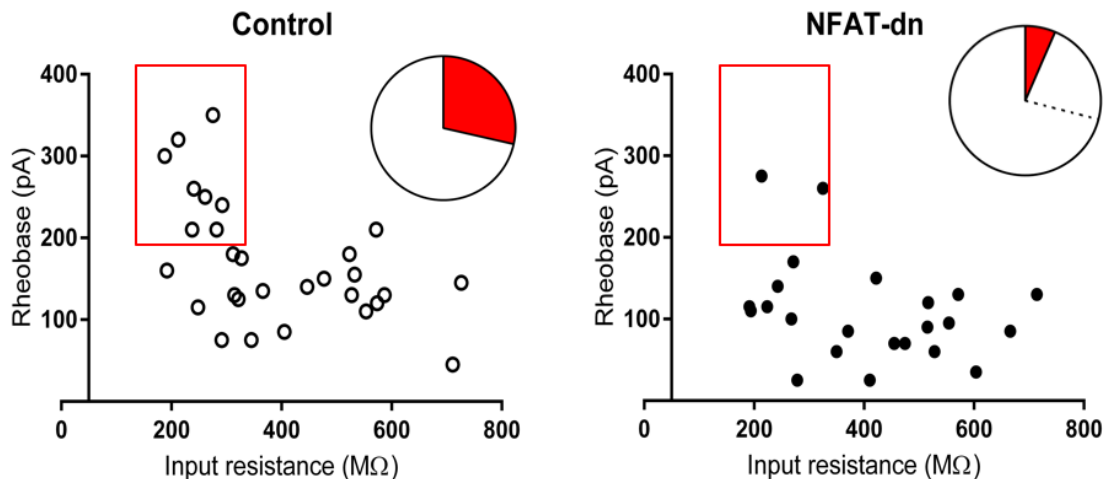


Fig.5.13 NFAT-dn overexpression leads to reduction of fast MN population

A significant reduction of fast Motor Neuron population was observed as compared to control when NFAT-dn was overexpressed in motor neurons. The population of neurons under the red box exhibit the properties of a fast MN and is approximately 28% in case of control. In case of NFAT-dn over-expression, number of neurons in red box is reduced to almost 9%.

5.14 Generation of Conditional NFAT-dominant Negative Mouse Line

While biological effects caused by overexpression of a protein can be informative as to its endogenous function, it can also cause misleading artefacts. I therefore decided to study the requirements of NFAT in MNs by loss-of-function through stable genetic manipulation in mice. Several functionally redundant NFAT paralogues are expressed in MNs in mouse (Website: © 2015 Allen Institute for Brain Science. Allen Spinal Cord Atlas). Moreover, mice homozygous for NFATc3/c4 or NFATc2/c3/c4 compound null mutations were previously found to die around embryonic day 11 (Graef, Chen et al. 2001, Graef, Wang et al. 2003). To selectively study NFAT requirements in MNs, I therefore decided to use a strategy allowing conditional suppression of NFAT activity in MNs. To achieve this, I generated a transgene (Fig. 5.14a) facilitating selective expression of dominant negative NFAT (NFAT-dn) upon co-expression with Cre-recombinase. Mice carrying the Caggs::loxP-stop-loxP-NFAT-dn-IRES-GFP transgene were generated by random insertion transgenesis following male pronuclear injection.

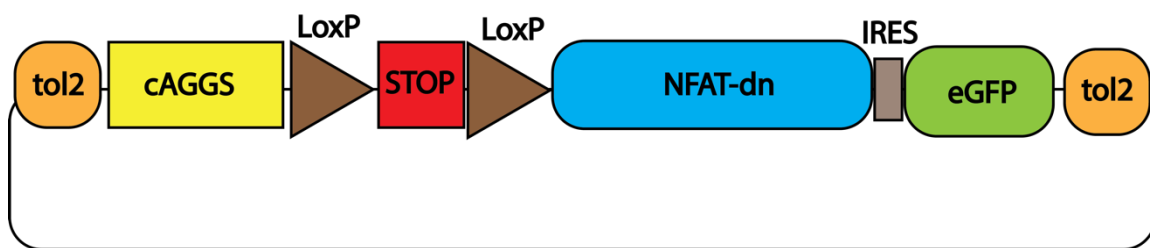


Fig.5.14a The Transgene Introduced in Mice by Random Insertion

Illustration of the transgene used to create a conditional NFAT-dn expressing mouse line. The entire expression cassette is flanked with tol2 sequences to facilitate random insertion of the transgene. The expression cassette contained lox-stop-lox sites to aid the selective Cre driven expression

To study the role of NFAT in spinal motor neuron development I chose two Cre-driver lines i.e. Oligo2-cre (Zhou and Anderson 2002, Zawadzka, Rivers et al. 2010) and ChAT-cre (Rossi, Balthasar et al. 2011). Oligo2-Cre mice express Cre recombinase under the direction of the Olig2 locus in pMN progenitor cells giving rise to MNs and oligodendrocytes (Zhou and Anderson 2002) and MNs. Upon interbreeding the founder mice (n=2) with Oligo-2Cre, I was able to identify a line showing stable expression of NFAT-dn in MN progenitors (Fig. 5.14b). Similarly combining the transgene with ChAT-Cre, expressing Cre recombinase in cholinergic neurons, allowed expression of NFAT-dn specifically in post mitotic MNs (Fig. 5.14c)

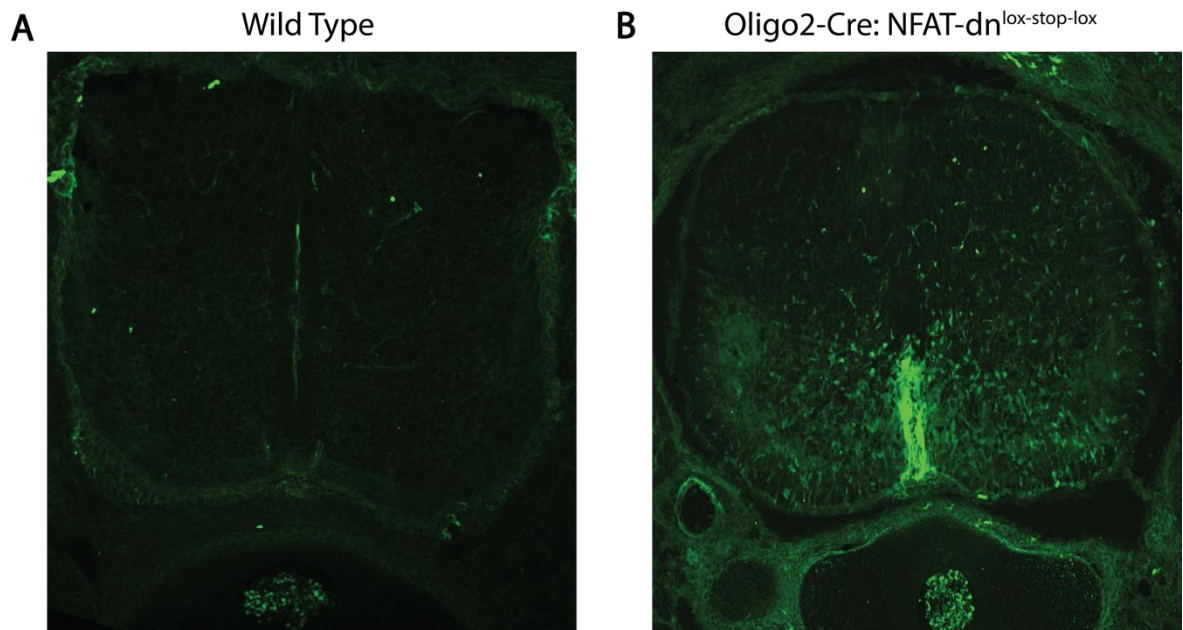


Fig.5.14b Selective Expression of NFAT-dn in mouse MN/oligodendrocyte lineage

Transverse sections of mouse embryos show absence or presence of GFP in spinal cord depending on the genotype as confirmed with PCR-genotyping. A: Wild type mice lack GFP positive cells in spinal cord. B: In the Oligo2-Cre: NFAT-dn^{lox-stop-lox} mice GFP was strongly expressed in a ventral domain of the spinal cord that corresponds to pMN.

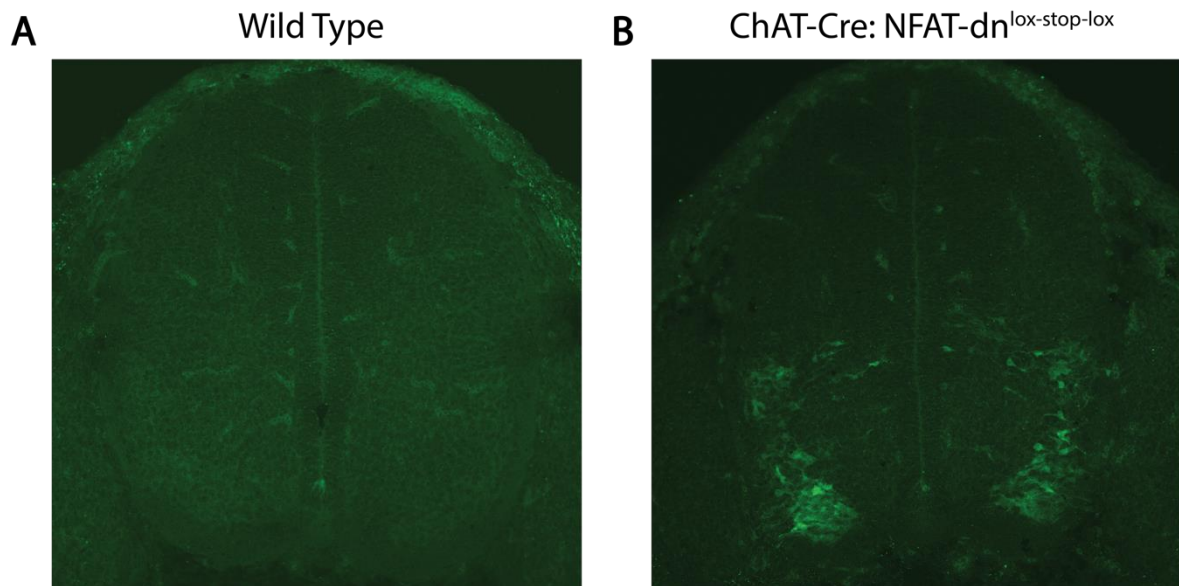


Fig.5.14c Targeted Expression of NFAT-dn-IRES-GFP Driven by ChAT-Cre in Post-mitotic MNs

Transverse sections of mouse embryos show absence or presence of GFP in spinal cord depending on the genotype as confirmed with PCR-genotyping. A: Wild type mice lack GFP positive cells in spinal cord. B: In the ChAT-Cre: NFAT-dn^{lox-stop-lox} mice GFP was strongly expressed in a ventral domain of the spinal cord that corresponds to MN.

VI Discussion

During development of central nervous system (CNS), hundreds of dissimilar neuron types are created. Establishment of this diverse population of neurons is essential since loss of particular classes of CNS neurons causes neurodegenerative disorders with improper formation of neuronal circuits. Spinal motor neurons (MNs) are one of those CNS neuronal subtypes for which an outline of transcriptional cascades, such as directed by Hox and Lim homeodomain proteins leading to formation of neuronal subclasses and types, is available. Spinal MNs further diversify into 'functional' subtypes: alpha (which in turn comprises of slow, fast and intermediate types), beta and gamma MNs. In recent years, several molecular markers have been found to identify particular subsets of MNs. For instance, NeuN and OPN seem to identify alpha MNs while Err3, Gfra, Wnt7a identify gamma MNs. Alpha MN subtypes may be further identified by presence of MMP9, Calca, Chodl as fast MNs or Sv2a, PRKCδ as slow MNs. However, in case of all these molecular markers, a clear understanding of the molecules and pathways involved in acquisition of alpha, beta or gamma MN identity and their respective properties is largely missing. Dlk1, a type I transmembrane protein, was recently reported to promote fast MN properties. Loss of Dlk1 in its knock-out mice also co-related with loss of fast MN properties while *KCNG4* was reported as a Dlk1 target gene and intermediate factor for promoting fast alpha MN specific properties. Yet, how Dlk1 promotes transcription of *KCNG4* remained elusive. The present study attempted a step-by-step dissection of Dlk1 signalling pathway for promoting fast MN properties.

6.1 Dlk1 Interacts with Notch and Inhibits Notch

The signalling pathways that synchronise gene expression during early metazoan development relies, among others, on five main pathways, namely Notch, Hedgehog, receptor tyrosine kinase (RTK) transforming Growth factor-beta (TGFbeta), and wingless/WNT (Gerhart 1999). Out of these five signalling pathways, Dlk1 appears to specifically affect the Notch signalling pathway. It is clear from the Co-IP experiments (Fig. 5.3a and Fig 5.3b) that Dlk1 interacts with Notch. This finding is against what was previously reported (Wang, Zhao et al. 2010) but a luciferase reporter assay for activation of Notch in presence or absence of Dlk1 (Fig. 5.4) further confirmed that Dlk1 not only interacts with Notch but completely abolishes any Notch activation. This observation was consistent with early cell cycle exit due to ectopic expression of Dlk1 observed *in-ovo* in chick E3.5 embryonic neural tube (Fig. 5.5). Inhibition of Notch by Dlk1 during early embryonic neural tube development in chick signifies that the role of Dlk1 in MN diversification starts right from the beginning of spinal neuron generation. Delta-Notch signalling is already known to control generation of neurons and glia in step wise process (Grandbarbe, Bouissac et al. 2003). Delta is a trans-activating Notch ligand and activation of Notch by juxtacrine Delta keeps the Notch expressing cell into cell-cycle. Delta expressing cells on other hand exit the cell cycle and differentiate into neurons. In this context, identification of Dlk1 as a cis-inhibitor (Muller, Cherukuri et al. 2014) is an additional pathway of cell-cycle exit and differentiation i.e. while Delta expressing cells become neurons by lateral inhibition, Dlk1 expressing cells become neurons by cis-inhibition thus already generating two pools of neurons (Delta expressing versus Dlk1 expressing) from the very beginning of neuronal emergence.

How Dlk1 acts as a potent inhibitor of Notch remains unresolved and was not the subject of present study. However, from the evidence that Dlk1 is able to bind at multiple regions of Notch (Fig. 5.3b) more likely explanation would be as follows. Dlk1 binds to inhibitory regions of Notch (LNR1-3) to directly inhibit Notch by blocking the cleavage of Notch and further activation. In addition, binding of Dlk1 to the activating regions of Notch (EGF 6-15) blocks activation of Notch by its canonical trans-activating ligands such as Delta and Jagged. Thus Dlk1 inhibits Notch both by direct inhibition and competitive inhibition which exaggerates the inhibitory capacity of Dlk1.

6.2 Is Inhibition of Notch Sufficient for fast MN properties?

Although inhibition of Notch is a prerequisite for Dlk1 activity to promote fast MN properties (Muller, Cherukuri et al. 2014), it remains unconfirmed whether inhibition of Notch is sufficient for fast MN properties. This aspect is difficult to study due to the 'unitary function' of Notch (a common, underlying molecular mechanism that is independent of developmental context), which makes it difficult to isolate the Dlk1-Notch inhibition for study of MN diversification. Additionally, a major hurdle to studying the role of Notch in the motor neuron progenitor domain is the lack of techniques to specifically manipulate Notch signalling in motor neuron progenitors. However, inhibition of Notch signalling at different time points of development is known to create different identities synchronizing with progenitor cell differentiation. During retinal development for example, early inactivation of Notch signalling (chick stage E3) promotes differentiation into ganglion cells while inhibition of Notch signalling at later stages (chick E 14.5) promotes amacrine cells (Nelson, Hartman et al. 2007). Similar stepwise activity of Notch is observed during neuron/glia differentiation where initially, Notch inhibits the neuronal fate while promoting the glial cell fate and in a second step, Notch promotes the differentiation of astrocytes, while inhibiting the differentiation of both neurons and oligodendrocytes (Grandbarbe, Bouissac et al. 2003). Despite of such existing examples, diversification of MNs merely due to inhibition of Notch seems unlikely due to the fact that MN diversification is very fine tuned and MN subtypes do not differ as broadly as a neuron and a glial cell or as seen between ganglion cells and amacrine cells. The MN subtypes actually differ at functional level but share a lot at molecular and anatomical level. For instance, all MNs express all the different ion channels and there is no sorting in positioning of alpha, beta or gamma MNs, they are mixed and can be found next to each other. The actual difference among the MN subtypes arises due to variation in composition of the different ion channels they express, the inputs they receive and the effectors they innervate. Moreover, differentiation and maturation of MN into functional subtypes occur much later than the time when progenitor cells exit cell cycle due to inhibition of Notch. Altogether, functional diversification of MNs entirely by time modulated Notch inhibition is not 'impossible' but knowing the complexity involved in MN diversification, a simpler module of Notch signalling inhibition appears to be the less likely pathway.

A detailed and stepwise experiment with transient and temporal inhibition of Notch during early development of a model organism or during differentiation of MN progenitor cells will give a concrete evidence about this possibility but is currently out of scope of this study.

6.3 Dlk1 is Cleaved Intracellularly and the Cleaved Intracellular Segment is Stable

In present study it is shown for the first time that Dlk1 is cleaved and the cleaved intracellular form is stable at least in Hela cells (Fig. 5.6). This observation is also partly consistent with the previous study that Dlk1 is cleaved, however the inconsistency is observed in the sizes of cleaved forms of Dlk1 (Smas, Chen et al. 1997). Although it was previously reported that Dlk1 is cleaved at an extracellular juxta-membrane site by TACE (Wang and Sul 2006), in my study it is observed that the size of stable cleaved form of Dlk1 ($\cong 9$ kDa) is even smaller than the size of Dlk1-ICD ($\cong 11$ kDa). This indicates that Dlk1 is also cleaved intracellularly. However, the enzyme responsible for the intracellular cleavage remains to be identified.

Irrespective of the enzyme responsible, the cleavage of Dlk1 and its stabilisation signifies a function of Dlk1 intracellular segment with several possibilities. Firstly, Dlk1 intracellular segment can interact with several cytoplasmic proteins and alter their functions by causing conformational changes and alter the signalling status of its binding partner or secondly, changing the localisation of itself or binding partner or both together from cytoplasm to nucleus. The wide range of possibilities in Dlk1 signalling due to cleavage of Dlk1 is further expanded by the sequence analysis of Dlk1 intracellular segment which shows a weak nuclear localisation signal (NLS). The presence of weak NLS in Dlk1-ICD but absence of any DNA binding site indicates that Dlk1 is capable of translocating into nucleus and altering the gene expression by acting as a cofactor to transcription factors.

6.4 Dlk1 Interacts with the Transcription Factor NFATc4

The biochemical assay of co-immunoprecipitation reveals a strong and stable interaction between Dlk1 intracellular segment and NFATc4 (Fig.5.9). Now this novel interaction revealed in this study can either demonstrate a new function that neither protein can exhibit by itself or Dlk1 can simply act as a modulator of NFAT transcriptional activity. In any case, Dlk1-NFAT interaction reveals a new signalling pathway which is significant not only in present context but in all those biological processes where Dlk1 and NFAT have been implicated together (section 2.8). In present study, interaction of Dlk1 with NFAT narrows the gap between a membrane protein Dlk1 and its target gene *KCNG4* indicating that a signal which starts from Dlk1, reaches to the nucleus via cleavage of Dlk1, interaction of Dlk1 intracellular domain with NFAT and NFAT translocating into the nucleus as an outcome of interaction. It is already known from previous studies that NFATc4 upregulates voltage gated potassium channels (Gong, Bodi et al. 2006, Zhang and Shapiro 2012) and same might be the case in fast MN pools where NFATc4 is highly expressed (Allen Brain Atlas) and *KCNG4* expression is upregulated. NFAT normally translocates into the nucleus due to exposure of its NLS after dephosphorylation by Calcineurin. How Dlk1 interaction alters the translocation of NFAT still needs to be confirmed.

6.5 NFATc4 Regulates Transcription of *KCNG4*

Using the tools of bioinformatics, we have found that NFATc4 can bind to non-coding regions of *KCNG4* and in our sequence analysis we found 4 such regions ranging from 200-400 base pairs (bp). A reporter assay has indicated binding of NFATc4 to 1 of the *KCNG4* non-coding region (cis-regulatory module) (Fig. 5.10). However, due to the known limitations of reporter assays a confirmatory Chromatin-immunoprecipitation (CHIP) assay still needs to be performed. Nevertheless, the indication that NFATc4 can regulate the Dlk1 target gene *KCNG4* contributes in completing the missing puzzle of how Dlk1 can alter gene transcription. Also, Dlk1 intracellular segment, has a weak NLS and due to its small size and strong interaction with NFATc4 it can possibly enter the nucleus too where it can act as co-regulator of NFATc4. Therefore, it will be interesting to study if Dlk1 interaction with NFATs alters or modifies or even adds to the regulation of customary targets of NFATs.

6.6 Inhibition of NFAT Induces Hyperexcitability in MNs During Chick Spinal Cord Development

The electrophysiological recordings of chick MNs overexpressing the NFAT-dn construct which inhibits all isoforms of NFATs show that inhibition of NFAT induces hyperexcitability in MNs i.e. MNs start firing at very low thresholds (rheobase) and reach a peak firing frequency very easily (Fig. 5.12). Hyperexcitability is a property observed due to closing/reduction of voltage-gated potassium channels. Since NFATs are known to upregulate the transcription of potassium channels (Zhang and Shapiro 2012), hyperexcitability observed due to inhibition of NFAT is consistent with literature and our hypothesis that inhibition of NFAT will inhibit the transcription of voltage gate potassium channels like Kv7 and Kv4 (Yao, Zhao et al. 2016). The lowering of firing frequency at twice rheobase observed due to inhibition of NFAT is also consistent with our hypothesis as one of the component of voltage gate potassium channels have been shown to increase the firing frequency of MNs (Muller, Cherukuri et al. 2014). This lowering of frequency could also indicate a slow MN property but an increased peak firing frequency creates ambiguity. This ambiguity still needs to be confirmed in mouse models. Altogether, the significant lowering of AHP1/2 width and AHP1/2 due to inhibition of NFAT combined with the significant reduction in rheobase indicate that inhibition of NFAT induces hyperexcitability in MNs.

This observation suggests a vital role of NFATs during MN development, since hyperexcitability of MNs indicates an unhealthy state of MNs as observed in motor neurone diseases (MNDs). In case of Spinal Muscular Atrophy (SMA) for example, it has been shown that MNs derived from SMA patients show hyper-excitable electrophysiology (Liu, Lu et al. 2015) while similar hyperexcitability exists in hippocampal cortical neurons and spinal MNs in (Amyotrophic Lateral Sclerosis) ALS patients (Benedetti, Ghilardi et al. 2016, Geevasinga, Menon et al. 2016). Not only that NFATc4 is known to promote neuronal survival (Benedito, Lehtinen et al. 2005, Vashishta, Habas et al. 2009, Mojsa, Mora et al. 2015) but NFATs also regulate transcriptional status of MNs based on its firing activities (Zhang and Shapiro 2012).

Altogether, NFAT appears to play a crucial role in directing and maintaining the firing properties of MNs during its functional diversification by regulating the transcription of ion channels although the effector ion-channels of NFAT regulation may vary with its binding

partners. In context of present study, it appears that Dlk1 is the binding partner of NFAT during *KCNG4* transcriptional regulation.

6.7 Does Dlk1 Function Mediate via Activation of NFAT?

There remains a missing link in this study i.e. what happens when Dlk1 interacts with NFAT (Fig. 5.9). Although a direct evidence is still missing, in the light of current literature, it will not be an over-speculation to hypothesize that Dlk1 might activate NFATc4 signalling. On one hand a voltage gated potassium channel *KCNG4* is mentioned as target of Dlk1 signalling (Muller, Cherukuri et al. 2014), on the other NFAT binds to *KCNG4* cis-regulatory module (Fig.5.10). Moreover, several reports already exist that NFAT signalling upregulates transcription of voltage gated potassium channels (Yao, Zhao et al. 2016). Combining this information with the current observation that Dlk1 interacts robustly with NFATc4, it is intuitive to claim that Dlk1 activates NFATc4 signalling to upregulate *KCNG4* transcription in MNs which in turn will decrease the excitability and increase the firing frequency of MNs to promote a fast MN phenotype.

6.8 A Model for the Novel Notch-Dlk1- NFATc4 Signalling Pathway

Based on the present study together with the state of the art literature, an outline of novel signalling pathway (Fig. 6) shows how Dlk1 alters the electrophysiological properties of MNs at molecular level. Dlk1, located at the membrane, inhibits Notch receptor activation via cis-interaction thus forcing the MN progenitor cells to exit cell-cycle. Dlk1 is further cleaved intracellularly by an unidentified molecule, and a soluble intracellular segment of Dlk1 (Dlk1-ICD) is released in the cytoplasm. The Dlk1-ICD then interacts with phosphorylated NFATc4 in cytoplasm and activates NFAT signalling. Activation of NFAT signalling leads to upregulated *KCNG4* transcription which modifies the associated voltage gated potassium channels. Thus the newly differentiating MN is constituted with increased number of voltage-gated potassium channels which keep the MN in more hyperpolarised state and dampen the excitability of the neuron. Inhibition of Dlk1-NFATc4 signalling due to presence of dominant negative NFAT (NFAT-dn) therefore increases the excitability of MNs by inhibiting the transcription of *KCNG4* or other additional channels (Fig.6.8).

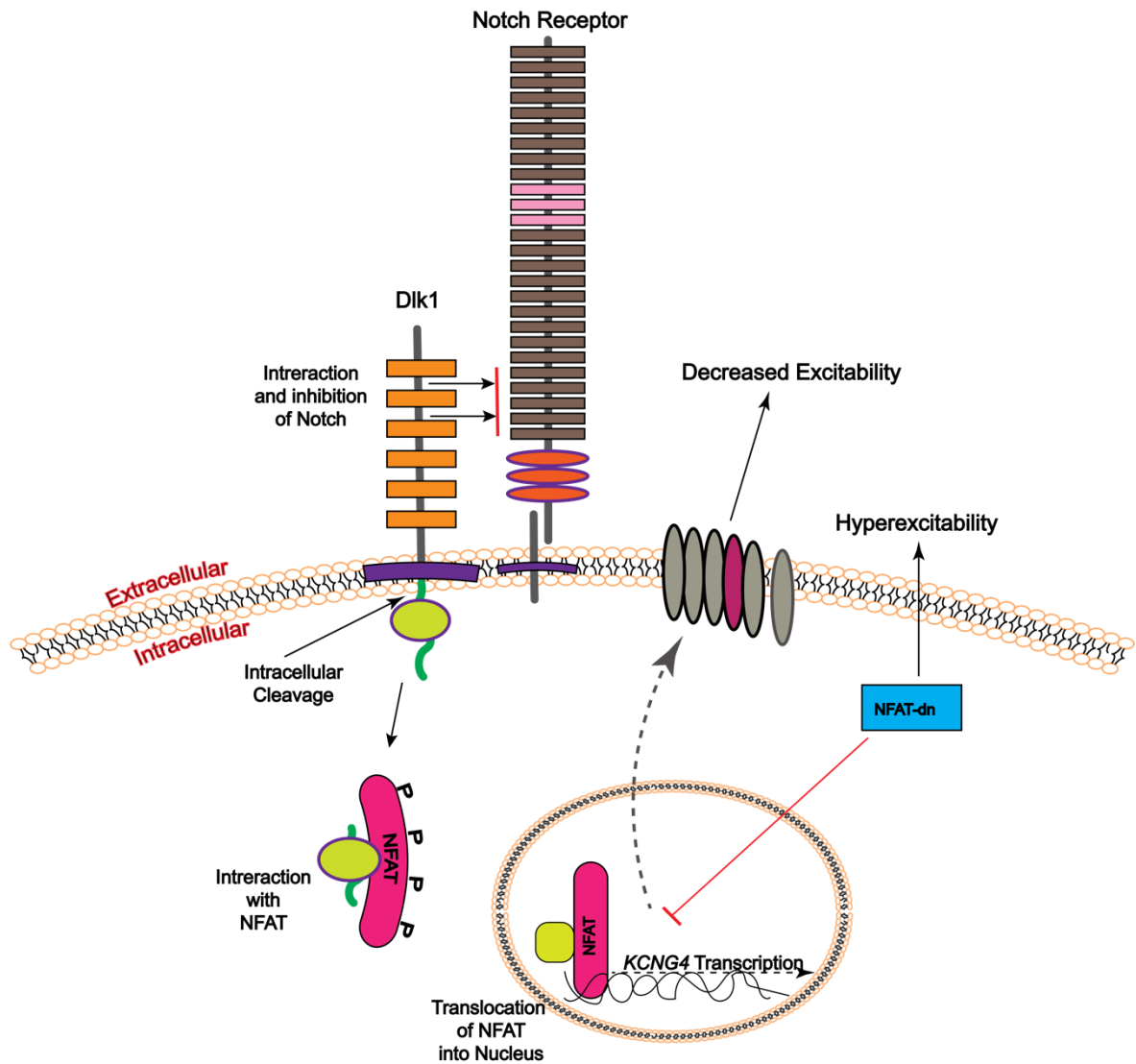


Fig.6.8 The Novel Notch-Dlk-NFATc4 Signalling Pathway

A preliminary outline of the events taking place in a motor neuron with reference to Dlk1. Dlk1, which is a type1 transmembrane protein, interacts with Notch in cis-configuration and inhibits Notch signalling. Further, Dlk1 is cleave at an intracellular position which generates a soluble form of Dlk1 intracellular segment (Dlk1-ICD). Dlk1-ICD interacts with NFATc4 after which via NFAT signalling *KCNG4* transcription is upregulated. Upregulation of *KCNG4* decreases the excitability of MNs while inhibition of NFAT signalling increases it.

6.9 Impact of Cis-inhibition of Notch by Dlk1 on the MN Diversification Process

Emerging experimental evidences support that the cis-interactions (cis-activation and cis-inhibition) can also trigger a cell-autonomous Notch signal, whose potential effects on cell fate decisions and patterning remain poorly understood. Although, concrete experimental evidences are missing, mathematically and computationally it had been shown that cis-inhibition and not cis-activation facilitates patterning, by enabling additional periodic patterns like stripes and by allowing localized patterning highly sensitive to the precursor state and cell-autonomous bistability (Formosa-Jordan and Ibanes 2014). In the mathematical model it was shown that when multiple ligands compete for the same receptor like Notch, but have different signalling efficiencies then they result in a regulatory switch from activation to inhibition or vice-versa. It was argued in the mathematical model that cis-inhibition of Notch signalling creates a positive intracellular feedback loop facilitating patterning and that cis-inhibition accelerates spontaneous diversification from very small initial variability between the precursor cells.

Applying this mathematical model to the current Delta-Notch-Dlk1 signalling where both Delta (trans-activating) and Dlk1 (cis-inhibiting) bind to the same receptor Notch, it appears that Dlk1, the cis-inhibitor, will hold the capacity to drive the diversification of MN progenitor cells into the wide range of cells produced from pMN domain.

Hence, while role of the canonical ligands of Notch like Delta and Jagged have been widely studied, similar amount of studies on cis-inhibitory ligands like Dlk1 will solve more questions of patterning during development like that of MN functional diversification.

6.10 Dlk1-NFATc4 a Novel Interaction or Different Flavour of NFAT Signalling

NFATc transcription factors bind DNA as monomers (at GGAA sites), as dimers (at κ B-like response elements) and as co-operative complexes (NFAT-AP1-Fos-Jun) (Hogan, Chen et al. 2003). The DNA-binding domain (RHD) of NFAT contains two distinct domains, N-terminal specificity domain (N-RHD) and C-terminal dimerization domain (C-RHD). The DNA-binding interactions involving N-RHD are conserved while those involving C-RHD is highly variable. This variability in DNA binding is due to the fact that NFATc proteins are not obligate dimers but can exist in multiple conformations depending on the interaction partners. This extra-ordinary flexibility of NFAT in DNA-binding modulates recruitment of specific transcriptional co-regulators in contexts of different promoters (Lefstin and Yamamoto 1998). Examples of the many interaction partners of NFAT include bZIP family members (AP-1, Maf, ICER and p21SNFT), zinc finger proteins (GATA and EGR), the helix-turn-helix domain proteins (Oct, HNF3 and IRF-4), the MADS-box protein (MEF2) and the nuclear receptor PPAR- γ . Hence interaction of Dlk1 with NFATc4 appears to be one of the many transcriptional co-regulators involved in NFATc4 signalling and this time in context of *KCNG4* regulation in motor neurons.

6.11 Transcriptional Regulation by NFAT Signalling

NFAT contributes to diverse cellular functions and is expressed in various cell types. The cellular context, time and source of Ca^{+} signal and the resulting NFAT-complex formation with context-dependent partners, all contribute significantly to the NFAT-mediated transcriptional regulation. The gene expression is fundamentally regulated at the proximate promoter but the distal regulatory elements also have thorough consequences on the expression of most of the genes. These distal regulatory elements (enhancers or cis-regulatory modules) are the medium of NFAT-dependent gene regulation in all the NFAT-target genes. The NFAT binding sites are often located in non-coding regions of the gene which can be 5' of the proximal promoter, within introns or 3' of the gene.

Because the source of Ca^{+} signal, the binding partners and even the distal regulatory elements change from cell to cell and are different at various points of differentiation process of a cell, the NFAT signalling has diverse function in wide range of cells. On one hand, NFAT regulates gene transcription in differentiated T cells and muscle fibres (Peng, Gerth et al. 2001, Kubis, Scheibe et al. 2002), on the other it also affects differentiation of T cells and osteoclasts. In the light of known roles of NFAT signalling in T-cell differentiation, osteoclast differentiation and cardiac valve development, it appears that NFAT typically takes part in developmental processes. Therefore, it does not come as a surprise that NFAT also regulates *KCNG4* transcription via the non-coding intronic region detected in this study. In context of MN diversification, *Dlk1* seems to deploy the extraordinary diverse signalling mechanism of NFATs to indirectly regulate gene transcription in the favour of fast MNs.

VII Summary

During my study of a signalling mechanism promoting MN diversification, I was able to provide evidence that, firstly Dlk1, a determinant of MN functional diversification, directly interacts with Notch and completely inhibits canonical Notch signalling via its extracellular segment. Secondly, Dlk1 is cleaved intracellularly and the intracellular segment engages in a robust interaction with NFATc4 as observed by Co-IP and western blots. A reporter assay revealed that NFAT directly binds to non-coding intronic region of the Dlk1 target gene, *KCNG4* suggesting Dlk1 regulates *KCNG4* expression through interacting with the NFAT. Also dominant negative NFAT, which inhibits the nuclear localization of all NFATs, induces hyperexcitability in MNs together with a reduction in firing frequency. These electrophysiological properties are in contrast to the increased firing frequency and decreased excitability observed when *KCNG4* is overexpressed. This suggests that Dlk1-NFAT heterodimer promote fast alpha MN specific gene expression including upregulation of *KCNG4*. Taken together the present study provides a putative pathway of how Dlk1 affects its effectors. The present study suggests that Dlk1 might operate by coupling neurogenesis to MN functional diversification by physically linking the Notch and NFAT signalling pathways. In MN progenitor cells, Dlk1 inhibits Notch to promote cell cycle exit and neurogenesis while the eventual release of Dlk1 intracellular segment engages with NFAT signalling which upregulates expression of the modulators delayed-rectifier potassium channels (*KCNG4*) to implement fast alpha MN properties (Fig.7)

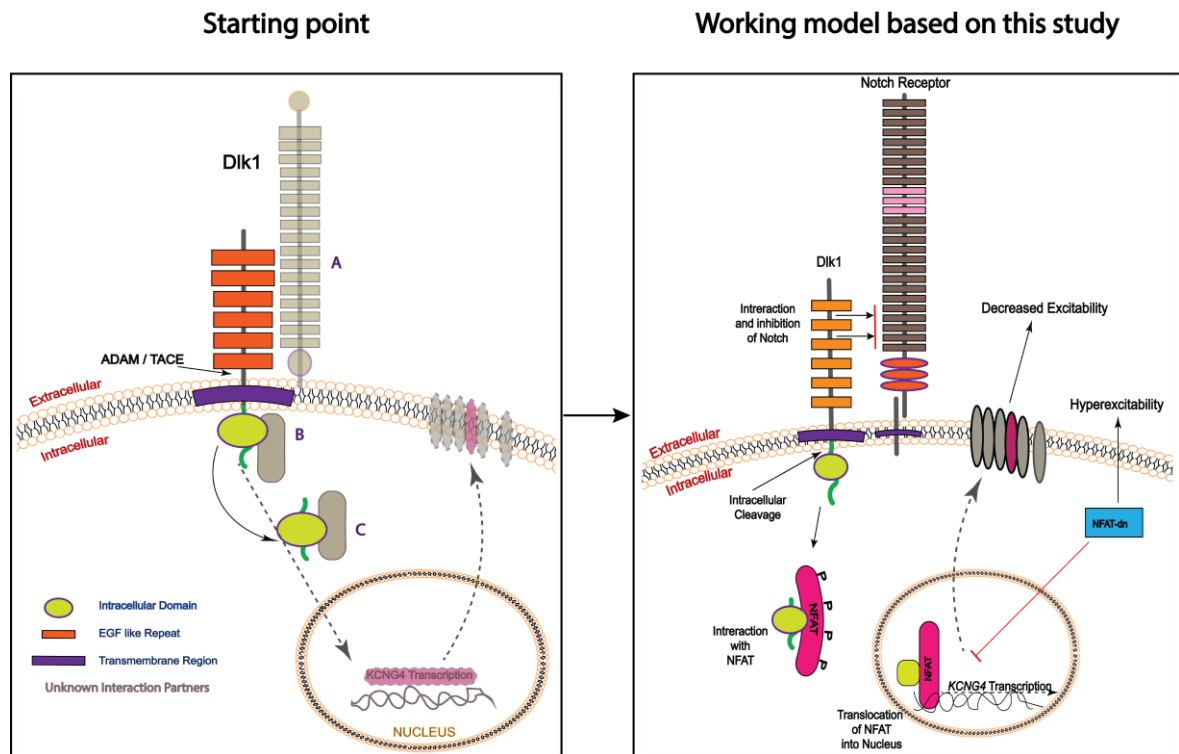


Fig.7 A Summary of the Study

After the present study, I was able to establish the unknown interaction partners of Dik1. Dik1 interaction with Notch and its inhibition was confirmed. Interaction of Dik1 with NFAT was revealed in this study while translocation of NFAT after dephosphorylation was already known. A preliminary reporter assay also indicated regulation of *KCNG4* by NFAT. Inhibition of NFAT mediated gene regulation leads to hyperexcitability was validate in this study while decreased excitability due to *KCNG4* overexpression was shown previously by our group.

VIII Outlook

The beauty and the inconvenience of science lies in the fact that the more we investigate, the more investigation it begins to aspire for. That my study also raises many further questions is inevitable. Since I chose to study the step by step mechanism of Dlk1 signalling during MN diversification, I faced new scientific questions at every step. First of the many questions unresolved in this study is how Dlk1 is able to inhibit Notch? Since in my study a possibility of sole competitive inhibition was ruled out, it will be really interesting to test exactly which binding interface contributes to achieve this inhibition – and in which respect this binding differs from canonical Notch ligands. Second question: what is the importance of Notch inhibition? Although it was shown that Notch inhibition was a prerequisite for Dlk1 activity, it remains elusive whether Notch inhibition is sufficient to promote fast MN properties. The third question came into picture when I recognized the intracellular cleavage of Dlk1 and i.e. what leads to the cleavage of Dlk1? The enzyme responsible for this cleavage is yet to be identified and it needs to be confirmed if the cleavage is important for Dlk1 activity. The fourth missing evidence regards the significance of the confirmed Dlk1 and NFAT interaction for Dlk1 activity and MN functional diversification. For instance, can NFAT alter the expression of same genes in motor neurons in absence of Dlk1? And how does this interaction affect NFAT activity? Would this involve additional factors and/or would this alter the dependence of NFAT nuclear translocation on Ca^{2+} /Calcineurin mediated dephosphorylation? The fifth dispute which still remains to be clarified whether Dlk1 and NFAT would specifically alter MN subtype dependent properties or complete MN identity? To address this question, we also need to identify the intermediate factors through which both Dlk1 and NFAT control biophysical properties. In my study, I had generated a mouse line that allows selective silencing of NFAT signalling in MNs that may ultimately help resolving at least some of these questions. Finally, it will be interesting to study whether Notch-Dlk1-NFAT signalling or similar mechanisms operate throughout the nervous system to establish functional diversity in otherwise relatively homogenous neuronal population.

IX References

- (2006). "Mowiol mounting medium." Cold Spring Harbor Protocols **2006**(1): pdb.rec10255.
- Abdul, H. M., J. L. Furman, M. A. Sama, D. M. Mathis and C. M. Norris (2010). "NFATs and Alzheimer's Disease." Mol Cell Pharmacol **2**(1): 7-14.
- Abdul, H. M., M. A. Sama, J. L. Furman, D. M. Mathis, T. L. Beckett, A. M. Weidner, E. S. Patel, I. Baig, M. P. Murphy, H. LeVine, 3rd, S. D. Kraner and C. M. Norris (2009). "Cognitive decline in Alzheimer's disease is associated with selective changes in calcineurin/NFAT signaling." J Neurosci **29**(41): 12957-12969.
- Appel, B., L. A. Givan and J. S. Eisen (2001). "Delta-Notch signaling and lateral inhibition in zebrafish spinal cord development." BMC Dev Biol **1**: 13.
- Ashrafi, S., M. Lalancette-Hebert, A. Friese, M. Sigrist, S. Arber, N. A. Shneider and J. A. Kaltschmidt (2012). "Wnt7A identifies embryonic gamma-motor neurons and reveals early postnatal dependence of gamma-motor neurons on a muscle spindle-derived signal." J Neurosci **32**(25): 8725-8731.
- Bai, S. and T. K. Kerppola (2011). "Opposing roles of FoxP1 and Nfat3 in transcriptional control of cardiomyocyte hypertrophy." Mol Cell Biol **31**(14): 3068-3080.
- Baladron, V., M. J. Ruiz-Hidalgo, M. L. Nueda, M. J. Diaz-Guerra, J. J. Garcia-Ramirez, E. Bonvini, E. Gubina and J. Laborda (2005). "dlk acts as a negative regulator of Notch1 activation through interactions with specific EGF-like repeats." Exp Cell Res **303**(2): 343-359.
- Becam, I., U. M. Fiuza, A. M. Arias and M. Milan (2010). "A role of receptor Notch in ligand cis-inhibition in Drosophila." Curr Biol **20**(6): 554-560.
- Benedetti, L., A. Ghilardi, E. Rottoli, M. De Maglie, L. Prosperi, C. Perego, M. Baruscotti, A. Bucci, L. Del Giacco and M. Francolini (2016). "INaP selective inhibition reverts precocious inter- and motoneurons hyperexcitability in the Sod1-G93R zebrafish ALS model." Sci Rep **6**: 24515.

Benedito, A. B., M. Lehtinen, R. Massol, U. G. Lopes, T. Kirchhausen, A. Rao and A. Bonni (2005). "The transcription factor NFAT3 mediates neuronal survival." J Biol Chem **280**(4): 2818-2825.

Birnboim, H. C. and J. Doly (1979). "A rapid alkaline extraction procedure for screening recombinant plasmid DNA." Nucleic Acids Res **7**(6): 1513-1523.

Blaumueller, C. M., H. Qi, P. Zagouras and S. Artavanis-Tsakonas (1997). "Intracellular cleavage of Notch leads to a heterodimeric receptor on the plasma membrane." Cell **90**(2): 281-291.

Boom, R., C. J. Sol, M. M. Salimans, C. L. Jansen, P. M. Wertheim-van Dillen and J. van der Noordaa (1990). "Rapid and simple method for purification of nucleic acids." J Clin Microbiol **28**(3): 495-503.

Bray, S. J., S. Takada, E. Harrison, S. C. Shen and A. C. Ferguson-Smith (2008). "The atypical mammalian ligand Delta-like homologue 1 (Dlk1) can regulate Notch signalling in Drosophila." BMC Dev Biol **8**: 11.

Briscoe, J., A. Pierani, T. M. Jessell and J. Ericson (2000). "A homeodomain protein code specifies progenitor cell identity and neuronal fate in the ventral neural tube." Cell **101**(4): 435-445.

Briscoe, J., L. Sussel, P. Serup, D. Hartigan-O'Connor, T. M. Jessell, J. L. Rubenstein and J. Ericson (1999). "Homeobox gene Nkx2.2 and specification of neuronal identity by graded Sonic hedgehog signalling." Nature **398**(6728): 622-627.

Buescher, M., S. L. Yeo, G. Udolph, M. Zavortink, X. Yang, G. Tear and W. Chia (1998). "Binary sibling neuronal cell fate decisions in the Drosophila embryonic central nervous system are nonstochastic and require inscuteable-mediated asymmetry of ganglion mother cells." Genes Dev **12**(12): 1858-1870.

Burke, R. E., D. N. Levine, P. Tsairis and F. E. Zajac, 3rd (1973). "Physiological types and histochemical profiles in motor units of the cat gastrocnemius." J Physiol **234**(3): 723-748.

Calabria, E., S. Ciciliot, I. Moretti, M. Garcia, A. Picard, K. A. Dyar, G. Pallafacchina, J. Tothova, S. Schiaffino and M. Murgia (2009). "NFAT isoforms control activity-dependent muscle fiber type specification." Proc Natl Acad Sci U S A **106**(32): 13335-13340.

Chang, Q. and L. J. Martin (2016). "Voltage-gated calcium channels are abnormal in cultured spinal motoneurons in the G93A-SOD1 transgenic mouse model of ALS." Neurobiol Dis **93**: 78-95.

Charlier, C., K. Segers, L. Karim, T. Shay, G. Gyapay, N. Cockett and M. Georges (2001). "The callipyge mutation enhances the expression of coregulated imprinted genes in cis without affecting their imprinting status." Nat Genet **27**(4): 367-369.

Cheng, S., S. L. Zhao, B. Nelson, C. Kesavan, X. Qin, J. Wergedal, S. Mohan and W. Xing (2012). "Targeted disruption of ephrin B1 in cells of myeloid lineage increases osteoclast differentiation and bone resorption in mice." PLoS One **7**(3): e32887.

Chin, E. R., E. N. Olson, J. A. Richardson, Q. Yang, C. Humphries, J. M. Shelton, H. Wu, W. Zhu, R. Bassel-Duby and R. S. Williams (1998). "A calcineurin-dependent transcriptional pathway controls skeletal muscle fiber type." Genes Dev **12**(16): 2499-2509.

Chomczynski, P. and N. Sacchi (1987). "Single-step method of RNA isolation by acid guanidinium thiocyanate-phenol-chloroform extraction." Anal Biochem **162**(1): 156-159.

Chow, C. W., M. Rincon and R. J. Davis (1999). "Requirement for transcription factor NFAT in interleukin-2 expression." Mol Cell Biol **19**(3): 2300-2307.

Cordle, J., S. Johnson, J. Z. Tay, P. Roversi, M. B. Wilkin, B. H. de Madrid, H. Shimizu, S. Jensen, P. Whiteman, B. Jin, C. Redfield, M. Baron, S. M. Lea and P. A. Handford (2008). "A conserved face of the Jagged/Serrate DSL domain is involved in Notch trans-activation and cis-inhibition." Nat Struct Mol Biol **15**(8): 849-857.

Crawford, T. Q. and H. Roelink (2007). "The Notch response inhibitor DAPT enhances neuronal differentiation in embryonic stem cell-derived embryoid bodies independently of sonic hedgehog signaling." Dev Dyn **236**(3): 886-892.

- D'Souza, B., L. Meloty-Kapella and G. Weinmaster (2010). "Canonical and non-canonical Notch ligands." Curr Top Dev Biol **92**: 73-129.
- Dasen, J. S., B. C. Tice, S. Brenner-Morton and T. M. Jessell (2005). "A Hox regulatory network establishes motor neuron pool identity and target-muscle connectivity." Cell **123**(3): 477-491.
- de Celis, J. F. and S. Bray (1997). "Feed-back mechanisms affecting Notch activation at the dorsoventral boundary in the Drosophila wing." Development **124**(17): 3241-3251.
- de Celis, J. F. and S. J. Bray (2000). "The Abruptex domain of Notch regulates negative interactions between Notch, its ligands and Fringe." Development **127**(6): 1291-1302.
- Dobretsov, M., S. L. Hastings, T. J. Sims, J. R. Stimers and D. Romanovsky (2003). "Stretch receptor-associated expression of alpha 3 isoform of the Na⁺, K⁺-ATPase in rat peripheral nervous system." Neuroscience **116**(4): 1069-1080.
- Durston, A. J., J. van der Wees, W. W. Pijnappel and S. F. Godsave (1998). "Retinoids and related signals in early development of the vertebrate central nervous system." Curr Top Dev Biol **40**: 111-175.
- Falix, F. A., D. C. Aronson, W. H. Lamers and I. C. Gaemers (2012). "Possible roles of DLK1 in the Notch pathway during development and disease." Biochim Biophys Acta **1822**(6): 988-995.
- Ferrari, D., C. Stroh and K. Schulze-Osthoff (1999). "P2X7/P2Z purinoreceptor-mediated activation of transcription factor NFAT in microglial cells." J Biol Chem **274**(19): 13205-13210.
- Ferron, S. R., M. Charalambous, E. Radford, K. McEwen, H. Wildner, E. Hind, J. M. Morante-Redolat, J. Laborda, F. Guillemot, S. R. Bauer, I. Farinas and A. C. Ferguson-Smith (2011). "Postnatal loss of Dlk1 imprinting in stem cells and niche astrocytes regulates neurogenesis." Nature **475**(7356): 381-385.
- Formosa-Jordan, P. and M. Ibanes (2014). "Competition in Notch Signaling with Cis Enriches Cell Fate Decisions." Plos One **9**(4).

- Francisovich, A. L., A. D. Mortimer, A. A. Freeman, J. Gu and S. Sanyal (2008). "Overexpression screen in Drosophila identifies neuronal roles of GSK-3 beta/shaggy as a regulator of AP-1-dependent developmental plasticity." Genetics **180**(4): 2057-2071.
- Freeman, A., A. Francisovich, M. Bowers, D. J. Sandstrom and S. Sanyal (2011). "NFAT regulates pre-synaptic development and activity-dependent plasticity in Drosophila." Mol Cell Neurosci **46**(2): 535-547.
- Friese, A., J. A. Kaltschmidt, D. R. Ladle, M. Sigrist, T. M. Jessell and S. Arber (2009). "Gamma and alpha motor neurons distinguished by expression of transcription factor Err3." Proc Natl Acad Sci U S A **106**(32): 13588-13593.
- Frise, E., J. A. Knoblich, S. Younger-Shepherd, L. Y. Jan and Y. N. Jan (1996). "The Drosophila Numb protein inhibits signaling of the Notch receptor during cell-cell interaction in sensory organ lineage." Proc Natl Acad Sci U S A **93**(21): 11925-11932.
- Geevasinga, N., P. Menon, K. Ng, M. Van Den Bos, K. Byth, M. C. Kiernan and S. Vucic (2016). "Riluzole exerts transient modulating effects on cortical and axonal hyperexcitability in ALS." Amyotroph Lateral Scler Frontotemporal Degener: 1-9.
- Genazzani, A. A., E. Carafoli and D. Guerini (1999). "Calcineurin controls inositol 1,4,5-trisphosphate type 1 receptor expression in neurons." Proc Natl Acad Sci U S A **96**(10): 5797-5801.
- Gerhart, J. (1999). "1998 Warkany lecture: signaling pathways in development." Teratology **60**(4): 226-239
- Gomez-Sintes, R. and J. J. Lucas (2010). "NFAT/Fas signaling mediates the neuronal apoptosis and motor side effects of GSK-3 inhibition in a mouse model of lithium therapy." J Clin Invest **120**(7): 2432-2445.
- Gong, N., I. Bodi, C. Zobel, A. Schwartz, J. D. Molkentin and P. H. Backx (2006). "Calcineurin increases cardiac transient outward K⁺ currents via transcriptional up-regulation of Kv4.2 channel subunits." J Biol Chem **281**(50): 38498-38506.

Graef, I. A., F. Chen, L. Chen, A. Kuo and G. R. Crabtree (2001). "Signals transduced by Ca(2+)/calcineurin and NFATc3/c4 pattern the developing vasculature." Cell **105**(7): 863-875.

Graef, I. A., F. Chen and G. R. Crabtree (2001). "NFAT signaling in vertebrate development." Curr Opin Genet Dev **11**(5): 505-512.

Graef, I. A., J. M. Gastier, U. Francke and G. R. Crabtree (2001). "Evolutionary relationships among Rel domains indicate functional diversification by recombination." Proc Natl Acad Sci U S A **98**(10): 5740-5745.

Graef, I. A., P. G. Mermelstein, K. Stankunas, J. R. Neilson, K. Deisseroth, R. W. Tsien and G. R. Crabtree (1999). "L-type calcium channels and GSK-3 regulate the activity of NF-ATc4 in hippocampal neurons." Nature **401**(6754): 703-708.

Graef, I. A., F. Wang, F. Charron, L. Chen, J. Neilson, M. Tessier-Lavigne and G. R. Crabtree (2003). "Neurotrophins and netrins require calcineurin/NFAT signaling to stimulate outgrowth of embryonic axons." Cell **113**(5): 657-670.

Grandbarbe, L., J. Bouissac, M. Rand, M. Hrabe de Angelis, S. Artavanis-Tsakonas and E. Mohier (2003). "Delta-Notch signaling controls the generation of neurons/glia from neural stem cells in a stepwise process." Development **130**(7): 1391-1402.

Hayflick, L. and P. S. Moorhead (1961). "The serial cultivation of human diploid cell strains." Exp Cell Res **25**: 585-621.

Hernandez, G. L., O. V. Volpert, M. A. Iniguez, E. Lorenzo, S. Martinez-Martinez, R. Grau, M. Fresno and J. M. Redondo (2001). "Selective inhibition of vascular endothelial growth factor-mediated angiogenesis by cyclosporin A: roles of the nuclear factor of activated T cells and cyclooxygenase 2." J Exp Med **193**(5): 607-620.

Hill-Eubanks, D. C., M. F. Gomez, A. S. Stevenson and M. T. Nelson (2003). "NFAT regulation in smooth muscle." Trends Cardiovasc Med **13**(2): 56-62.

Ho, A. M., J. Jain, A. Rao and P. G. Hogan (1994). "Expression of the transcription factor NFATp in a neuronal cell line and in the murine nervous system." J Biol Chem **269**(45): 28181-28186.

Ho, I. C., J. H. Kim, J. W. Rooney, B. M. Spiegelman and L. H. Glimcher (1998). "A potential role for the nuclear factor of activated T cells family of transcriptional regulatory proteins in adipogenesis." Proc Natl Acad Sci U S A **95**(26): 15537-15541.

Hoess, R. H., M. Ziese and N. Sternberg (1982). "P1 site-specific recombination: nucleotide sequence of the recombining sites." Proc Natl Acad Sci U S A **79**(11): 3398-3402.

Hogan, P. G., L. Chen, J. Nardone and A. Rao (2003). "Transcriptional regulation by calcium, calcineurin, and NFAT." Genes Dev **17**(18): 2205-2232.

Hudry, E., H. Y. Wu, M. Arbel-Ornath, T. Hashimoto, R. Matsouaka, Z. Fan, T. L. Spires-Jones, R. A. Betensky, B. J. Bacskai and B. T. Hyman (2012). "Inhibition of the NFAT pathway alleviates amyloid beta neurotoxicity in a mouse model of Alzheimer's disease." J Neurosci **32**(9): 3176-3192.

Inoue, H., H. Nojima and H. Okayama (1990). "High efficiency transformation of Escherichia coli with plasmids." Gene **96**(1): 23-28.

Jensen, C. H., M. Meyer, H. D. Schroder, A. Kliem, J. Zimmer and B. Teisner (2001). "Neurons in the monoaminergic nuclei of the rat and human central nervous system express FA1/dlk." Neuroreport **12**(18): 3959-3963.

Jessell, T. M. (2000). "Neuronal specification in the spinal cord: inductive signals and transcriptional codes." Nat Rev Genet **1**(1): 20-29.

Jung, H., J. Lacombe, E. O. Mazzoni, K. F. Liem, Jr., J. Grinstein, S. Mahony, D. Mukhopadhyay, D. K. Gifford, R. A. Young, K. V. Anderson, H. Wichterle and J. S. Dasen (2010). "Global control of motor neuron topography mediated by the repressive actions of a single hox gene." Neuron **67**(5): 781-796.

Kao, S. C., H. Wu, J. Xie, C. P. Chang, J. A. Ranish, I. A. Graef and G. R. Crabtree (2009). "Calcineurin/NFAT signaling is required for neuregulin-regulated Schwann cell differentiation." Science **323**(5914): 651-654.

Kawakami, K. and A. Shima (1999). "Identification of the Tol2 transposase of the medaka fish *Oryzias latipes* that catalyzes excision of a nonautonomous Tol2 element in zebrafish *Danio rerio*." Gene **240**(1): 239-244.

- Kawakami, T., T. Chano, K. Minami, H. Okabe, Y. Okada and K. Okamoto (2006). "Imprinted DLK1 is a putative tumor suppressor gene and inactivated by epimutation at the region upstream of GTL2 in human renal cell carcinoma." Hum Mol Genet **15**(6): 821-830.
- Keyser, P., K. Borge-Renberg and D. Hultmark (2007). "The Drosophila NFAT homolog is involved in salt stress tolerance." Insect Biochem Mol Biol **37**(4): 356-362.
- Kopan, R. and M. X. Ilagan (2009). "The canonical Notch signaling pathway: unfolding the activation mechanism." Cell **137**(2): 216-233.
- Kubis, H. P., R. J. Scheibe, J. D. Meissner, G. Hornung and G. Gros (2002). "Fast-to-slow transformation and nuclear import/export kinetics of the transcription factor NFATc1 during electrostimulation of rabbit muscle cells in culture." J Physiol **541**(Pt 3): 835-847.
- Lee, S. K., L. W. Jurata, J. Funahashi, E. C. Ruiz and S. L. Pfaff (2004). "Analysis of embryonic motoneuron gene regulation: derepression of general activators function in concert with enhancer factors." Development **131**(14): 3295-3306.
- Lee, S. K., B. Lee, E. C. Ruiz and S. L. Pfaff (2005). "Olig2 and Ngn2 function in opposition to modulate gene expression in motor neuron progenitor cells." Genes Dev **19**(2): 282-294.
- Lefstin, J. A. and K. R. Yamamoto (1998). "Allosteric effects of DNA on transcriptional regulators." Nature **392**(6679): 885-888.
- Li, L., S. J. Forman and R. Bhatia (2005). "Expression of DLK1 in hematopoietic cells results in inhibition of differentiation and proliferation." Oncogene **24**(27): 4472-4476.
- Li, L., J. Tan, Y. Zhang, N. Han, X. Di, T. Xiao, S. Cheng, Y. Gao and Y. Liu (2014). "DLK1 promotes lung cancer cell invasion through upregulation of MMP9 expression depending on Notch signaling." PLoS One **9**(3): e91509.
- Liem, K. F., Jr., T. M. Jessell and J. Briscoe (2000). "Regulation of the neural patterning activity of sonic hedgehog by secreted BMP inhibitors expressed by notochord and somites." Development **127**(22): 4855-4866.

- Liu, H., J. Lu, H. Chen, Z. Du, X. J. Li and S. C. Zhang (2015). "Spinal muscular atrophy patient-derived motor neurons exhibit hyperexcitability." Sci Rep **5**: 12189.
- Lu, Q. R., T. Sun, Z. Zhu, N. Ma, M. Garcia, C. D. Stiles and D. H. Rowitch (2002). "Common developmental requirement for Olig function indicates a motor neuron/oligodendrocyte connection." Cell **109**(1): 75-86.
- Lu, S., C. S. Shashikant and F. H. Ruddle (1996). "Separate cis-acting elements determine the expression of mouse Dbx gene in multiple spatial domains of the central nervous system." Mech Dev **58**(1-2): 193-202.
- Luo, J., L. Sun, X. Lin, G. Liu, J. Yu, L. Parisiadou, C. Xie, J. Ding and H. Cai (2014). "A calcineurin- and NFAT-dependent pathway is involved in alpha-synuclein-induced degeneration of midbrain dopaminergic neurons." Hum Mol Genet **23**(24): 6567-6574.
- Machado, C. B., K. C. Kanning, P. Kreis, D. Stevenson, M. Crossley, M. Nowak, M. Iacovino, M. Kyba, D. Chambers, E. Blanc and I. Lieberam (2014). "Reconstruction of phrenic neuron identity in embryonic stem cell-derived motor neurons." Development **141**(4): 784-794.
- Macian, F. (2005). "NFAT proteins: key regulators of T-cell development and function." Nat Rev Immunol **5**(6): 472-484.
- Mansouri, A. and P. Gruss (1998). "Pax3 and Pax7 are expressed in commissural neurons and restrict ventral neuronal identity in the spinal cord." Mech Dev **78**(1-2): 171-178.
- Manuel, M. and D. Zytynicki (2011). "Alpha, beta and gamma motoneurons: functional diversity in the motor system's final pathway." J Integr Neurosci **10**(3): 243-276.
- Marambaud, P., U. Dreses-Werringloer and V. Vingtdeux (2009). "Calcium signaling in neurodegeneration." Mol Neurodegener **4**: 20.
- Marquardt, T. and S. L. Pfaff (2001). "Cracking the transcriptional code for cell specification in the neural tube." Cell **106**(6): 651-654.

- Mastick, G. S., N. M. Davis, G. L. Andrew and S. S. Easter, Jr. (1997). "Pax-6 functions in boundary formation and axon guidance in the embryonic mouse forebrain." Development **124**(10): 1985-1997.
- McCullagh, K. J., E. Calabria, G. Pallafacchina, S. Ciciliot, A. L. Serrano, C. Argentini, J. M. Kalhovde, T. Lomo and S. Schiaffino (2004). "NFAT is a nerve activity sensor in skeletal muscle and controls activity-dependent myosin switching." Proc Natl Acad Sci U S A **101**(29): 10590-10595.
- Mei, Z., P. Yan, X. Tan, S. Zheng and B. Situ (2015). "Transcriptional regulation of BACE1 by NFAT3 leads to enhanced amyloidogenic processing." Neurochem Res **40**(4): 829-836.
- Micchelli, C. A., E. J. Rulifson and S. S. Blair (1997). "The function and regulation of cut expression on the wing margin of *Drosophila*: Notch, Wingless and a dominant negative role for Delta and Serrate." Development **124**(8): 1485-1495.
- Miller, A. C., E. L. Lyons and T. G. Herman (2009). "cis-Inhibition of Notch by endogenous Delta biases the outcome of lateral inhibition." Curr Biol **19**(16): 1378-1383.
- Misawa, H., M. Hara, S. Tanabe, M. Niikura, Y. Moriwaki and T. Okuda (2012). "Osteopontin is an alpha motor neuron marker in the mouse spinal cord." J Neurosci Res **90**(4): 732-742.
- Mognol, G. P., F. R. Carneiro, B. K. Robbs, D. V. Faget and J. P. Viola (2016). "Cell cycle and apoptosis regulation by NFAT transcription factors: new roles for an old player." Cell Death Dis **7**: e2199.
- Mojsa, B., S. Mora, J. P. Bossowski, I. Lassot and S. Desagher (2015). "Control of neuronal apoptosis by reciprocal regulation of NFATc3 and Trim17." Cell Death Differ **22**(2): 274-286.
- Molkentin, J. D., J. R. Lu, C. L. Antos, B. Markham, J. Richardson, J. Robbins, S. R. Grant and E. N. Olson (1998). "A calcineurin-dependent transcriptional pathway for cardiac hypertrophy." Cell **93**(2): 215-228.

Muhr, J., E. Graziano, S. Wilson, T. M. Jessell and T. Edlund (1999). "Convergent inductive signals specify midbrain, hindbrain, and spinal cord identity in gastrula stage chick embryos." Neuron **23**(4): 689-702.

Muller, D., P. Cherukuri, K. Henningfeld, C. H. Poh, L. Wittler, P. Grote, O. Schluter, J. Schmidt, J. Laborda, S. R. Bauer, R. M. Brownstone and T. Marquardt (2014). "Dlk1 promotes a fast motor neuron biophysical signature required for peak force execution." Science **343**(6176): 1264-1266.

Nelson, B. R., B. H. Hartman, S. A. Georgi, M. S. Lan and T. A. Reh (2007). "Transient inactivation of Notch signaling synchronizes differentiation of neural progenitor cells." Dev Biol **304**(2): 479-498.

Nilsson, L. M., J. Nilsson-Ohman, A. V. Zetterqvist and M. F. Gomez (2008). "Nuclear factor of activated T-cells transcription factors in the vasculature: the good guys or the bad guys?" Curr Opin Lipidol **19**(5): 483-490.

Noto, Y., K. Shibuya, S. Vucic and M. C. Kiernan (2016). "Novel therapies in development that inhibit motor neuron hyperexcitability in amyotrophic lateral sclerosis." Expert Rev Neurother **16**(10): 1147-1154.

Novitch, B. G., A. I. Chen and T. M. Jessell (2001). "Coordinate regulation of motor neuron subtype identity and pan-neuronal properties by the bHLH repressor Olig2." Neuron **31**(5): 773-789.

Nueda, M. L., V. Baladron, B. Sanchez-Solana, M. A. Ballesteros and J. Laborda (2007). "The EGF-like protein dlk1 inhibits Notch signaling and potentiates adipogenesis of mesenchymal cells." J Mol Biol **367**(5): 1281-1293.

Park, H. C. and B. Appel (2003). "Delta-Notch signaling regulates oligodendrocyte specification." Development **130**(16): 3747-3755.

Patten, I. and M. Placzek (2000). "The role of Sonic hedgehog in neural tube patterning." Cell Mol Life Sci **57**(12): 1695-1708.

Pei, Z. and N. E. Baker (2008). "Competition between Delta and the Abruptex domain of Notch." BMC Dev Biol **8**: 4.

Peng, C. Y., H. Yajima, C. E. Burns, L. I. Zon, S. S. Sisodia, S. L. Pfaff and K. Sharma (2007). "Notch and MAML signaling drives Scl-dependent interneuron diversity in the spinal cord." Neuron **53**(6): 813-827.

Peng, S. L., A. J. Gerth, A. M. Ranger and L. H. Glimcher (2001). "NFATc1 and NFATc2 together control both T and B cell activation and differentiation." Immunity **14**(1): 13-20.

Pierani, A., S. Brenner-Morton, C. Chiang and T. M. Jessell (1999). "A sonic hedgehog-independent, retinoid-activated pathway of neurogenesis in the ventral spinal cord." Cell **97**(7): 903-915.

Pierani, A., L. Moran-Rivard, M. J. Sunshine, D. R. Littman, M. Goulding and T. M. Jessell (2001). "Control of interneuron fate in the developing spinal cord by the progenitor homeodomain protein Dbx1." Neuron **29**(2): 367-384.

Placzek, M. (1995). "The role of the notochord and floor plate in inductive interactions." Curr Opin Genet Dev **5**(4): 499-506.

Raghunandan, R., M. Ruiz-Hidalgo, Y. Jia, R. Ettinger, E. Rudikoff, P. Riggins, R. Farnsworth, A. Tesfaye, J. Laborda and S. R. Bauer (2008). "Dlk1 influences differentiation and function of B lymphocytes." Stem Cells Dev **17**(3): 495-507.

Rao, A. and O. Avni (2000). "Molecular aspects of T-cell differentiation." Br Med Bull **56**(4): 969-984.

Rebay, I., R. G. Fehon and S. Artavanis-Tsakonas (1993). "Specific truncations of Drosophila Notch define dominant activated and dominant negative forms of the receptor." Cell **74**(2): 319-329.

Rebay, I., R. J. Fleming, R. G. Fehon, L. Cherbas, P. Cherbas and S. Artavanis-Tsakonas (1991). "Specific EGF repeats of Notch mediate interactions with Delta and Serrate: implications for Notch as a multifunctional receptor." Cell **67**(4): 687-699.

Richardson, W. D., H. K. Smith, T. Sun, N. P. Pringle, A. Hall and R. Woodruff (2000). "Oligodendrocyte lineage and the motor neuron connection." Glia **29**(2): 136-142.

Riegel, J. S., E. R. Richie and J. P. Allison (1990). "Nuclear events after activation of CD4+8+ thymocytes." J Immunol **144**(9): 3611-3618.

Rodriguez, P., M. A. Higuera, A. Gonzalez-Rajal, A. Alfranca, M. Fierro-Fernandez, R. A. Garcia-Fernandez, M. J. Ruiz-Hidalgo, M. Monsalve, F. Rodriguez-Pascual, J. M. Redondo, J. L. de la Pompa, J. Laborda and S. Lamas (2012). "The non-canonical NOTCH ligand DLK1 exhibits a novel vascular role as a strong inhibitor of angiogenesis." Cardiovasc Res **93**(2): 232-241.

Rojanathammanee, L., A. M. Floden, G. D. Manocha and C. K. Combs (2015). "Attenuation of microglial activation in a mouse model of Alzheimer's disease via NFAT inhibition." J Neuroinflammation **12**: 42.

Rossi, J., N. Balthasar, D. Olson, M. Scott, E. Berglund, C. E. Lee, M. J. Choi, D. Lauzon, B. B. Lowell and J. K. Elmquist (2011). "Melanocortin-4 receptors expressed by cholinergic neurons regulate energy balance and glucose homeostasis." Cell Metab **13**(2): 195-204.

Sabharwal, P., C. Lee, S. Park, M. Rao and S. Sockanathan (2011). "GDE2 regulates subtype-specific motor neuron generation through inhibition of Notch signaling." Neuron **71**(6): 1058-1070.

Sanchez-Solana, B., M. L. Nueda, M. D. Ruvira, M. J. Ruiz-Hidalgo, E. M. Monsalve, S. Rivero, J. J. Garcia-Ramirez, M. J. Diaz-Guerra, V. Baladron and J. Laborda (2011). "The EGF-like proteins DLK1 and DLK2 function as inhibitory non-canonical ligands of NOTCH1 receptor that modulate each other's activities." Biochim Biophys Acta **1813**(6): 1153-1164.

Sander, M., S. Paydar, J. Ericson, J. Briscoe, E. Berber, M. German, T. M. Jessell and J. L. Rubenstein (2000). "Ventral neural patterning by Nkx homeobox genes: Nkx6.1 controls somatic motor neuron and ventral interneuron fates." Genes Dev **14**(17): 2134-2139.

Sato, Y., T. Kasai, S. Nakagawa, K. Tanabe, T. Watanabe, K. Kawakami and Y. Takahashi (2007). "Stable integration and conditional expression of electroporated transgenes in chicken embryos." Dev Biol **305**(2): 616-624.

- Schulz, R. A. and K. E. Yutzey (2004). "Calcineurin signaling and NFAT activation in cardiovascular and skeletal muscle development." Dev Biol **266**(1): 1-16.
- Schwartz, N., A. Schohl and E. S. Ruthazer (2009). "Neural activity regulates synaptic properties and dendritic structure in vivo through calcineurin/NFAT signaling." Neuron **62**(5): 655-669.
- Shaw, J. P., P. J. Utz, D. B. Durand, J. J. Toole, E. A. Emmel and G. R. Crabtree (1988). "Identification of a putative regulator of early T cell activation genes." Science **241**(4862): 202-205.
- Shneider, N. A., M. N. Brown, C. A. Smith, J. Pickel and F. J. Alvarez (2009). "Gamma motor neurons express distinct genetic markers at birth and require muscle spindle-derived GDNF for postnatal survival." Neural Dev **4**: 42.
- Shoji, H., T. Ito, Y. Wakamatsu, N. Hayasaka, K. Ohsaki, M. Oyanagi, R. Kominami, H. Kondoh and N. Takahashi (1996). "Regionalized expression of the Dbx family homeobox genes in the embryonic CNS of the mouse." Mech Dev **56**(1-2): 25-39.
- Smas, C. M., L. Chen and H. S. Sul (1997). "Cleavage of membrane-associated pref-1 generates a soluble inhibitor of adipocyte differentiation." Mol Cell Biol **17**(2): 977-988.
- Smas, C. M. and H. S. Sul (1993). "Pref-1, a protein containing EGF-like repeats, inhibits adipocyte differentiation." Cell **73**(4): 725-734.
- Spana, E. P. and C. Q. Doe (1996). "Numb antagonizes Notch signaling to specify sibling neuron cell fates." Neuron **17**(1): 21-26.
- Stern, C. D. (2005). "Neural induction: old problem, new findings, yet more questions." Development **132**(9): 2007-2021.
- Takahashi, M., T. Ogino and K. Baba (1969). "Estimation of relative molecular length of DNA by electrophoresis in agarose gel." Biochim Biophys Acta **174**(1): 183-187.
- Tan, G. C., E. O. Mazzoni and H. Wichterle (2016). "Iterative Role of Notch Signaling in Spinal Motor Neuron Diversification." Cell Rep **16**(4): 907-916.

Tanabe, Y., C. William and T. M. Jessell (1998). "Specification of motor neuron identity by the MNR2 homeodomain protein." Cell **95**(1): 67-80.

Tian, Y., I. Voineagu, S. P. Pasca, H. Won, V. Chandran, S. Horvath, R. E. Dolmetsch and D. H. Geschwind (2014). "Alteration in basal and depolarization induced transcriptional network in iPSC derived neurons from Timothy syndrome." Genome Med **6**(10): 75.

Traustadottir, G. A., C. H. Jensen, M. Thomassen, H. C. Beck, S. B. Mortensen, J. Laborda, V. Baladron, S. P. Sheikh and D. C. Andersen (2016). "Evidence of non-canonical NOTCH signaling: Delta-like 1 homolog (DLK1) directly interacts with the NOTCH1 receptor in mammals." Cell Signal **28**(4): 246-254.

Vashishta, A., A. Habas, P. Pruunsild, J. J. Zheng, T. Timmusk and M. Hetman (2009). "Nuclear factor of activated T-cells isoform c4 (NFATc4/NFAT3) as a mediator of antiapoptotic transcription in NMDA receptor-stimulated cortical neurons." J Neurosci **29**(48): 15331-15340.

Vogelstein, B. (1987). "Rapid purification of DNA from agarose gels by centrifugation through a disposable plastic column." Anal Biochem **160**(1): 115-118.

Vogelstein, B. and D. Gillespie (1979). "Preparative and analytical purification of DNA from agarose." Proc Natl Acad Sci U S A **76**(2): 615-619.

Waddell, J. N., P. Zhang, Y. Wen, S. K. Gupta, A. Yevtodiynko, J. V. Schmidt, C. A. Bidwell, A. Kumar and S. Kuang (2010). "Dlk1 is necessary for proper skeletal muscle development and regeneration." PLoS One **5**(11): e15055.

Wang, Y. and H. S. Sul (2006). "Ectodomain shedding of preadipocyte factor 1 (Pref-1) by tumor necrosis factor alpha converting enzyme (TACE) and inhibition of adipocyte differentiation." Mol Cell Biol **26**(14): 5421-5435.

Wang, Y., L. Zhao, C. Smas and H. S. Sul (2010). "Pref-1 interacts with fibronectin to inhibit adipocyte differentiation." Mol Cell Biol **30**(14): 3480-3492.

Yang, J., B. Rothermel, R. B. Vega, N. Frey, T. A. McKinsey, E. N. Olson, R. Bassel-Duby and R. S. Williams (2000). "Independent signals control expression of the

calcineurin inhibitory proteins MCIP1 and MCIP2 in striated muscles." Circ Res **87**(12): E61-68.

Yao, J. J., Q. R. Zhao, D. D. Liu, C. W. Chow and Y. A. Mei (2016). "Neuritin Up-regulates Kv4.2 alpha-Subunit of Potassium Channel Expression and Affects Neuronal Excitability by Regulating the Calcium-Calcineurin-NFATc4 Signaling Pathway." J Biol Chem **291**(33): 17369-17381.

Yoon, K. and N. Gaiano (2005). "Notch signaling in the mammalian central nervous system: insights from mouse mutants." Nat Neurosci **8**(6): 709-715.

Zawadzka, M., L. E. Rivers, S. P. Fancy, C. Zhao, R. Tripathi, F. Jamen, K. Young, A. Goncharevich, H. Pohl, M. Rizzi, D. H. Rowitch, N. Kessaris, U. Suter, W. D. Richardson and R. J. Franklin (2010). "CNS-resident glial progenitor/stem cells produce Schwann cells as well as oligodendrocytes during repair of CNS demyelination." Cell Stem Cell **6**(6): 578-590.

Zengel, J. E., S. A. Reid, G. W. Sybert and J. B. Munson (1985). "Membrane electrical properties and prediction of motor-unit type of medial gastrocnemius motoneurons in the cat." J Neurophysiol **53**(5): 1323-1344.

Zhang, J. and M. S. Shapiro (2012). "Activity-dependent transcriptional regulation of M-Type (Kv7) K(+) channels by AKAP79/150-mediated NFAT actions." Neuron **76**(6): 1133-1146.

Zhao, C., N. Irie, Y. Takada, K. Shimoda, T. Miyamoto, T. Nishiwaki, T. Suda and K. Matsuo (2006). "Bidirectional ephrinB2-EphB4 signaling controls bone homeostasis." Cell Metab **4**(2): 111-121.

Zhou, B., R. Q. Cron, B. Wu, A. Genin, Z. Wang, S. Liu, P. Robson and H. S. Baldwin (2002). "Regulation of the murine Nfatc1 gene by NFATc2." J Biol Chem **277**(12): 10704-10711.

Zhou, Q. and D. J. Anderson (2002). "The bHLH transcription factors OLIG2 and OLIG1 couple neuronal and glial subtype specification." Cell **109**(1): 61-73

mousespinal.brain-map.org.

Curriculum vitae

Nidhi subhashini

Date of Birth : 05.05.1987

Nationality : Indian

nidhi.subhashini@gmail.com

<https://de.linkedin.com/in/nidhi-subhashini-49873222>

OBJECTIVE

To work in a premier organization where knowledge, hard work and innovation are valued and encouraged. To give sincere and devoted efforts towards any work assigned to me by using my learned and earned skills together with analytical and reasoning abilities to the best of my potential.

EDUCATION

September 2011-November 2016: IMPRS Neuroscience MSc-PhD, Göttingen, Germany

August 2009-May 2011 : M.Sc. Life Sciences, JNU, New Delhi, India

July 2006-May 2009 : B.Sc. Chemistry (Hons.), BHU, Varanasi, India

STIPENDS AND AWARDS

Stipend of the Excellence Foundation for the Promotion of the Max Planck Society 2011

Joint CSIR-UGC Test and NET Junior Research Fellowship December 2010 with All India Rank 52

Selected for fully government funded residential masters' studies in JNU (2009)

All India Rank 45 for fully government funded residential undergraduate studies in BHU (2006)

LAB EXPERIENCE

PhD thesis (October 2012- September 2016): Lab. of Developmental Neurobiology, ENI, Göttingen under supervision of Prof. Till Marquardt

Master's Thesis (June 2010- May 2011): REM Sleep Lab., SLS, JNU, New Delhi, supervision of Prof. B.N. Mallick

Bachelor's Thesis (March 2008-February 2009): Lab. of Plant Molecular Biology, BHU, Varanasi, supervision of Dr. Shashi Pandey

PUBLICATION

Involvement of the $\alpha 1$ -adrenoceptor in sleep-waking and sleep loss-induced anxiety behaviour in zebrafish. Singh A, Subhashini N, Sharma S, Mallick BN

